REVIEWS OF

MODERN PHYSICS

VOLUME 35, NUMBER 4 OCTOBER 1963

Determination of Pion–Nucleon Parameters and Phase Shifts by Dispersion Relations*

J. HAMILTON

Department of Physics, University College, Gower Street, London, W. C. 1

AND

W. S. WOOLCOCK

Department of Mathematics, University of Queensland, Brisbane, Australia

CONTENTS

1. INTRODUCTION AND NOTATION

THE purpose of this article is to give an account of the application of single variable dispersion relations to calculate the main parameters of low-energy pion–nucleon scattering and the low-energy

* This work has been partially supported by the U. S. Air Office of Scientific Research, OAR (European Office, Aerospace Research, U. S. Air Force).

phase shifts. The input data consist of fairly compete information about the total cross sections and the dominant resonances of the π–N system. Our aim is to give precise numerical values of the parameters and low-energy phase shifts, since these quantities are required for a variety of purposes in other investigations. We do not attempt here to give any physical discussion of low-energy pion–nucleon scattering.[1] Also, it should be emphasized that this article only discusses those topics with which one or both of the authors have been directly involved. We do not claim any completeness for the topics discussed or for the references.

(i) Summary of the Topics Discussed

In Sec. 1(ii) we give the relativistic notation for the pion–nucleon scattering amplitudes which was used by Chew, Goldberger, Low, and Nambu (to be referred to as CGLN).[2] This notation is used throughout. In the same section we give the charge notation, the appropriate partial wave analysis, and the basic dispersion relations themselves.

In applying dispersion relations, the questions of high-energy behavior and the subtractions are of considerable importance. In Sec. 2 we discuss their mathematical and physical features for both forward and fixed momentum-transfer pion–nucleon scattering. This involves some account of Pomeranchuk's theorem and the Regge pole method.

Physical measurements of pion–nucleon scattering are conveniently expressed in terms of partial wave amplitudes and phase shifts, but the dispersion relations which are useful for our purposes refer to scattering amplitudes. The relation between these quantities is given by the Legendre series for the expansion of scattering amplitudes. The rate of convergence of this series and of its inverse is a matter of basic importance in any attempt to predict low-energy pion–nucleon phase shifts by dispersion relations. In Sec. 3 these convergence problems are examined. We use both the domains of convergence given by Lehmann's theorems, and the larger domains of convergence which follow from the Mandelstam representation. (In this article the Mandelstam representation has only been used to give these domains of convergence of the Legendre series and of its inverse. Moreover the results of the calculations of partial wave amplitudes appear to give strong support to the validity of the larger domains of convergence which are obtained from the Mandelstam representation.)

In Sec. 4 we give an account of Woolcock's calculations,[3] and other determinations, of the parameters of low-energy pion–nucleon physics. Various improvements are made in the original calculations. The parameters are the coupling constant f^2, the s-wave scattering lengths a_1, a_3, the p-wave scattering lengths $a_{2T,2J}$, and the curvature constants in the parametric form for the low-energy s-wave phase shifts. The calculations are based mainly on the use of forward and fixed momentum-transfer dispersion relations for various pion–nucleon scattering amplitudes (these are really sum rules). The dispersion relations are evaluated by using the considerable amount of accurate experimental data which is available on the total $\pi^{\pm}$–p cross sections, and the reliable information which we have about the resonances of the π–N system. An effort has been made to give a careful assessment of the errors in these determinations of the parameters.

In Sec. 5 the fixed momentum-transfer dispersion relations are used to predict the s-wave and p-wave pion–nucleon phase shifts at low energies. The method is an improved form of the CGLN calculations[2]; all recoil and relativistic effects are included; and only the f waves (and higher) are ignored. Again the original calculations[3] are improved in various ways and a careful assessment of the errors is included. The input data is the same information about the total cross sections and resonances that is used in Sec. 4.

The main limitation on the method is the convergence of the inverse of the Legendre series which, as was mentioned above, is needed to deduce the partial wave amplitudes from the calculated scattering amplitudes and their derivatives with respect to momentum transfer. As the energy increases, the domain of convergence becomes smaller, and the rate of convergence of the inverse series deteriorates rapidly. In practice this means that the corrections due to f-wave, g-wave, . . . terms, which we ignore, become large, and further, errors in the results due to inaccuracies in the d-wave subtraction term (in one of the $A^{(+)}$ relations) can be troublesome. A complete and (we believe) accurate prediction of the s-wave and p-wave phase shifts is possible up to about 120 MeV (lab) energy, and the results are in good agreement with the accurate experimental

[1] For a physical discussion of the dominant (3/2, 3/2) state, see G. F. Chew and F. E. Low, Phys. Rev. **101**, 1570 (1956). For the remaining p-wave states and the s-wave states, see, for example, J. Hamilton, P. Menotti, G. C. Oades, and L. L. J. Vick, Phys. Rev. **128**, 1881 (1962).

[2] G. F. Chew, M. L. Goldberger, F. E. Low, and Y. Nambu, Phys. Rev. **106**, 1337 (1957).

[3] W. S. Woolcock, Ph.D. thesis, Cambridge University (1961) (unpublished).

values which are available. Above 120 MeV we can only predict certain special combinations of the scattering amplitudes. It is expected that the rate of convergence of the inverse series in the $(-)$ charge combination is good up to around 300 MeV, and the corresponding partial wave amplitudes turn out to agree well with experiment in the p-wave case. For the s waves the results in the $(-)$ case up to 300 MeV should be reasonably reliable. Another special case is the $f_2^{(+)}$ amplitude which again avoids the difficulties just discussed, up to around 220 MeV. The relation between these two special cases and our knowledge of the pion–pion interactions is discussed fully.

(ii) Kinematic Invariants and Invariant Amplitudes

We shall use the notation of CGLN.[2] The S-matrix elements for elastic π–N scattering can be written

$$S = \delta_{fi} - (2\pi)^4 i\delta^{(4)}(p_2 + q_2 - p_1 - q_1) \times (M^2/4E_1E_2\omega_1\omega_2)^{\frac{1}{2}}\, \bar{u}_2 T u_1 , \quad (1.1)$$

where $\delta_{fi} = 0$ unless there is no scattering (then $\delta_{fi} = 1$). E_1, E_2 are the initial and final nucleon energies, and p_1, p_2 are the corresponding 4-vector energy momenta. ω_1, ω_2 and q_1, q_2 are the same quantities for the initial and final pions. u_1 and u_2 are the initial and final spinors for the nucleon, normalized so that (for nucleons) $\bar{u}_1 u_1 = \bar{u}_2 u_2 = 1$. M is the nucleon mass, and μ is the pion mass.

The 4×4 matrix T is a Lorentz invariant.[4] It can be expressed as a function of the kinematic invariants, which in turn are formed from the three independent 4 vectors associated with the scattering. These are

$$P_\mu = \tfrac{1}{2}(p_1 + p_2)_\mu , \quad Q_\mu = \tfrac{1}{2}(q_1 + q_2)_\mu ,$$
$$\Delta_\mu = \tfrac{1}{2}(q_1 - q_2)_\mu .$$

Two independent invariants (apart from the masses) can be formed, and it is convenient to take

$$\nu = -P\cdot Q/M , \quad t = -4\Delta^2 . \quad (1.2)$$

We can write T in the form

$$T = -A + i\gamma\cdot QB , \quad (1.3)$$

where $\gamma\cdot Q = \gamma^\mu Q_\mu$ and A, B are scalar functions of the kinematic invariants ν,t. The quantities ν and t between them specify the energy and the scattering angle. It is easy to deduce from (1.2) that

$$t = -2q^2(1 - \cos\theta)$$
$$\nu = \omega_L + t/4M , \quad (1.4)$$

where ω_L is the total energy of the incident pion in the lab system, q^2 is the square of the momentum of either particle in the c.m. system, and θ is the scattering angle in the c.m. system.

It is sometimes convenient to use the pair of kinematic invariants

$$s = -(p_1 + q_1)^2 , \quad t = -(q_1 - q_2)^2 .$$

Evaluating s in the lab system we find

$$s = M^2 + \mu^2 + 2M\omega_L = M^2 + \mu^2 + 2M\nu - \tfrac{1}{2}t . \quad (1.5)$$

The variables s and t are used in the Mandelstam representation,[5] and it is often convenient to use also a third invariant u defined by

$$s + t + u = 2M^2 + 2\mu^2 , \quad (1.6)$$

so that

$$u = M^2 + \mu^2 - 2M\nu - \tfrac{1}{2}t . \quad (1.6a)$$

(iii) Charge Properties

It is customary, but not necessary, to assume charge independence in analyzing the amplitudes. A and B are then 3×3 matrices $(A_{\beta\alpha})$, $(B_{\beta\alpha})$, where $\alpha, \beta = 1, 2, 3$ are the pion-charge indices. By charge independence we can write

$$A_{\beta\alpha} = A^{(+)}\delta_{\beta\alpha} + A^{(-)}\tfrac{1}{2}[\tau_\beta,\tau_\alpha] ,$$
$$B_{\beta\alpha} = B^{(+)}\delta_{\beta\alpha} + B^{(-)}\tfrac{1}{2}[\tau_\beta,\tau_\alpha] . \quad (1.7)$$

where τ_α ($\alpha = 1, 2, 3$) are the 2×2 isotopic spin matrices for the nucleons. Clearly $A^{(+)}$, $B^{(+)}$ refer to the parts of $(A_{\beta\alpha})$, $(B_{\beta\alpha})$ which are symmetric in the charge indices (α, β), and $A^{(-)}$, $B^{(-)}$ to the antisymmetric part. No transfer of charge between pion and nucleon occurs in the $A^{(+)}$, $B^{(+)}$ parts, so they do not require any τ matrices.

The amplitudes $A^{(T)}$, $B^{(T)}$ for π–N scattering in isotopic spin eigenstates $T = \frac{1}{2}, \frac{3}{2}$ are related to $A^{(\pm)}$, $B^{(\pm)}$ by

$$A^{(+)} = \tfrac{1}{3}A^{(\frac{1}{2})} + \tfrac{2}{3}A^{(\frac{3}{2})} ; \; A^{(\frac{1}{2})} = A^{(+)} + 2A^{(-)} ,$$
$$A^{(-)} = \tfrac{1}{3}(A^{(\frac{1}{2})} - A^{(\frac{3}{2})}) ; \; A^{(\frac{3}{2})} = A^{(+)} - A^{(-)} . \quad (1.8)$$

Identical relations hold for the B amplitudes.

We can avoid relying on charge independence [cf. Sec. 4(iv)] if we define $A^{(\pm)}$, $B^{(\pm)}$ in terms of the amplitudes A_+, B_+ and A_-, B_- which describe the elastic scattering processes $\pi^+ + p \to \pi^+ + p$ and $\pi^- + p \to \pi^- + p$, respectively.

[4] Strictly it is $\bar{u}_2 T u_1$ which is invariant.

[5] S. Mandelstam, Phys. Rev. **112**, 1344 (1958); **115**, 1741, 1752 (1959).

It is easy to deduce from (1.9) that

$$A^{(+)} = \tfrac{1}{2}(A_+ + A_-)\,, \quad A^{(-)} = \tfrac{1}{2}(A_- - A_+)\,,$$
$$B^{(+)} = \tfrac{1}{2}(B_+ + B_-)\,, \quad B^{(-)} = \tfrac{1}{2}(B_- - B_+)\,. \quad (1.9)$$

If we do not wish to assume charge independence we take (1.9) as the *definition* of $A^{(\pm)}$, $B^{(\pm)}$. This indeed corresponds to what happens mostly in practice, since for elastic π–N scattering in general we only use experimental results on $\pi^+ + p \to \pi^+ + p$ and $\pi^- + p \to \pi^- + p$ scattering.

(iv) Crossing Symmetry

Let the scattering amplitude for the process in Eq. (1.1) be written

$$\langle p_2,q_2,\beta|T|p_1,q_1,\alpha\rangle\,.$$

Then Low's expression for this quantity in terms of Heisenberg operators and real state vectors shows the symmetry property[6]

$$\langle p_2,q_2,\beta|T|p_1,q_1,\alpha\rangle = \langle p_2,-q_1,\alpha|T|p_1,-q_2,\beta\rangle\,. \quad (1.10)$$

This replacement $q_1 \leftrightarrow -q_2$, $\alpha \leftrightarrow \beta$ leaves P_μ and Δ_μ unaltered and reverses Q_μ ($Q_\mu \to -Q_\mu$). Thus, it gives

$$\nu \to -\nu\,, \quad t \to t\,, \quad (1.11)$$

and by (1.5) and (1.6a)

$$s \to u\,, \quad t \to t\,, \quad u \to s\,. \quad (1.12)$$

Remembering that $A^{(+)}$ is the symmetric part of $(A_{\beta\alpha})$ we get [from (1.10) and (1.3) and $\gamma Q \to -\gamma Q$]

$$A^{(+)}(-\nu,t) = A^{(+)}(\nu,t)\,, \quad B^{(+)}(-\nu,t) = -B^{(+)}(\nu,t)\,,$$
$$A^{(-)}(-\nu,t) = -A^{(-)}(\nu,t)\,, \quad B^{(-)}(-\nu,t) = B^{(-)}(\nu,t)\,. \quad (1.13)$$

Again, we can, if we wish, derive the crossing relations (1.13) without using charge independence. From Eq. (1.3) and definition (1.9) we have

$$T^{(+)} = \tfrac{1}{2}(T_+ + T_-)\,, \quad T^{(-)} = \tfrac{1}{2}(T_- - T_+)\,, \quad (1.14)$$

where T_+ and T_- are the amplitudes for $\pi^+ + p \to \pi^+ + p$ and $\pi^- + p \to \pi^- + p$, respectively. The crossing property follows directly from Low's relation. It relates physical $\pi^+ + p$ scattering to unphysical $\pi^- + p$ scattering and vice versa. We have,

$$\langle p_2,q_2|T_+|p_1,q_1\rangle = \langle p_2,-q_1|T_-|p_1,-q_2\rangle\,,$$
$$\langle p_2,q_2|T_-|p_1,q_1\rangle = \langle p_2,-q_1|T_+|p_1,-q_2\rangle\,. \quad (1.15)$$

[6] See for example, J. Hamilton, *Theory of Elementary Particles* (Oxford University Press, New York, 1959), Chap. VI, paragraph 5.

Thus, by (14)

$$T^{(+)}(-\nu,t) = T^{(+)}(\nu,t)\,, \quad T^{(-)}(-\nu,t) = -T^{(-)}(\nu,t)\,.$$

Now using (1.3) we obtain (1.13).

(v) The Dispersion Relations for A and B

We are here only interested in dispersion relations for fixed momentum transfer t. The positions of the singularities are easiest expressed in terms of the invariants s and u [Eqs. (1.5) and (1.6)]. There is the single nucleon pole at $s = M^2$ (the Born term), and the corresponding crossed pole at $u = M^2$. There is the physical cut $s \geqslant (M+\mu)^2$ and the crossed cut $u \geqslant (M+\mu)^2$. By (1.5) and (1.6a) we express the positions of these singularities in terms of ν. Using Cauchy's theorem and Eq. (1.13) in the way indicated in Sec. 2(i) below and Fig. 1, and ignoring for the moment any questions about convergence, we get the dispersion relations for fixed momentum transfer t.

These equations, which were first written down by CGLN[2] are

$$\mathrm{Re}\,A^{(\pm)}(\nu,t) = \frac{1}{\pi}P\int_{\mu+t/4M}^{\infty} d\nu'\,\mathrm{Im}\,A^{(\pm)}(\nu',t) \times\left(\frac{1}{\nu'-\nu} \pm \frac{1}{\nu'+\nu}\right)\,, \quad (1.16)$$

$$\mathrm{Re}\,B^{(\pm)}(\nu,t) = \frac{G_r^2}{2M}\left(\frac{1}{\nu_B-\nu} \mp \frac{1}{\nu_B+\nu}\right) + \frac{1}{\pi}P\int_{\mu+t/4M}^{\infty} d\nu'\,\mathrm{Im}\,B^{(\pm)}(\nu',t)\left(\frac{1}{\nu'-\nu} \mp \frac{1}{\nu'+\nu}\right)\,. \quad (1.17)$$

Here, $\nu_B = -\mu^2/2M + t/4M$ is the position of the nucleon pole, and G_r^2 is the rationalized renormalized (Watson–Lepore) pseudoscalar coupling constant.

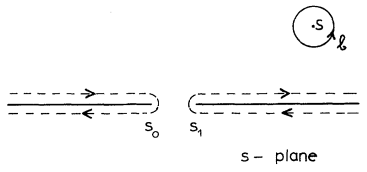

FIG. 1. The contour C and the contours around the cuts of $f(s)$ used in deriving Eqs. (1.16), (1.17), and (2.1).

The Born terms in (1.7) are calculated by second-order perturbation theory. The reason why they appear in the $B^{(\pm)}$ equations but not in the $A^{(\pm)}$ equations is that at low energies the pseudoscalar π–N interaction is equivalent to a pseudovector π–N interaction. This latter type of interaction must involve the nucleon spin $\boldsymbol{\sigma}$, so it can contribute to the $\gamma\cdot Q$ term in (1.3) (i.e., to B), but not to A.

It has been proved[7] (assuming microscopic causality and the usual asymptotic axioms of field theory) that for fixed t, such that

$$0 \leqslant -t \leqslant \frac{32}{3}\cdot\frac{2M+\mu}{2M-\mu}\cdot\mu^2 \simeq 12\mu^2 ,$$

the above enumerated singularities are the only singularities of $A^{(\pm)}(\nu,t)$, $B^{(\pm)}(\nu,t)$. To establish the dispersion relations (1.16) and (1.17) (or subtracted versions of them) for these values of t, it is only necessary to examine their convergence properties; this will be done in Sec. 2.

(vi) Partial Wave Analysis

We now set down the relations between the invariant A and B amplitudes and the usual partial wave amplitudes. From (1.1) it follows that the differential cross section in the c.m. system is

$$d\sigma/d\Omega = (M/4\pi W)^2\Sigma|\bar{u}_2 T u_1|^2 , \qquad (1.18)$$

where Σ denotes the sum over final spin states and the average over the initial spin states. Also,

$$W = (M^2+q^2)^{\frac{1}{2}} + (\mu^2+q^2)^{\frac{1}{2}} \qquad (1.19)$$

is the total energy in the c.m. system. Clearly $W^2 = s$.

We can also write the differential cross section in the c.m. system in the form

$$d\sigma/d\Omega = \Sigma|\langle f|M|i\rangle|^2 , \qquad (1.20)$$

where $|i\rangle$ and $|f\rangle$ are the Pauli spinors for the initial and final nucleon states. M is commonly written in the form

$$M = f(\theta) + (\boldsymbol{\sigma}\cdot\mathbf{n})g(\theta) , \qquad (1.21)$$

where θ is the c.m. scattering angle and $\mathbf{n} = \mathbf{q}_2 \times \mathbf{q}_1/|\mathbf{q}_2 \times \mathbf{q}_1|$ is the normal to the plane of scattering. $f(\theta)$ and $g(\theta)$ are the no-flip and spin-flip amplitudes, respectively. A more convenient form is

$$M = f_1(\theta) + \frac{(\boldsymbol{\sigma}\cdot\mathbf{q}_2)(\boldsymbol{\sigma}\cdot\mathbf{q}_1)}{q_1 q_2} f_2(\theta) . \qquad (1.22)$$

The relation between (1.21) and (1.22) is

$$\begin{aligned} f(\theta) &= f_1(\theta) + \cos\theta f_2(\theta) , \\ ig(\theta) &= \sin\theta f_2(\theta) . \end{aligned} \qquad (1.23)$$

The form (1.22) connects directly with the helicity amplitudes.[8] Denoting the nucleon's helicity by subscripts $+$ or $-$, we have

$$M_{++} = \langle f_+|i_+\rangle(f_1+f_2) , \quad M_{-+} = \langle f_-|i_+\rangle(f_1-f_2) , \quad \text{etc}\cdots , \qquad (1.23a)$$

where the subscripts $\pm$ denote the helicity, and $|i_\pm\rangle$, $|f_\pm\rangle$ are the spin-state vectors. Using

$$|f\rangle = \exp(-i\sigma_z\varphi/2)\exp(i\sigma_y\theta/2)\exp(i\sigma_z\varphi/2)|i\rangle$$

gives

$$\begin{aligned} &\langle f_+|i_+\rangle = \langle f_-|i_-\rangle = \cos(\theta/2) , \\ &\langle f_-|i_+\rangle = -e^{-i\phi}\sin(\theta/2) , \\ &\langle f_+|i_-\rangle = e^{i\phi}\sin(\theta/2) . \end{aligned} \qquad (1.23b)$$

From (1.18) and (1.20) we relate M to T in the c.m. system by the convention

$$\langle f|M|i\rangle = -(M/4\pi W)\bar{u}_2 T u_1 . \qquad (1.24)$$

Using the representation in which

$$\boldsymbol{\alpha} = \begin{pmatrix} 0, & \boldsymbol{\sigma} \\ \boldsymbol{\sigma}, & 0 \end{pmatrix} , \quad \gamma^4 = \beta = \begin{pmatrix} 1, & 0 \\ 0, & -1 \end{pmatrix} ,$$

$$\boldsymbol{\gamma} = -i\beta\boldsymbol{\alpha} = \begin{pmatrix} 0, & i\boldsymbol{\sigma} \\ -i\boldsymbol{\sigma}, & 0 \end{pmatrix} ,$$

the Dirac (4-component) spinors u_1, $\bar{u}_2$ can be expressed in terms of the Pauli (2-component) spinors $|i\rangle$, $|f\rangle$ by

$$\begin{aligned} u_1 &= \frac{(M - i\gamma p_1)}{(2M(E_1+M))^{\frac{1}{2}}}\begin{pmatrix} |i\rangle \\ 0 \end{pmatrix} , \\ \bar{u}_2 &= (\langle f|,0)\gamma^4\frac{(M - i\gamma p_2)}{(2M(E_2+M))^{\frac{1}{2}}} . \end{aligned} \qquad (1.25)$$

Substituting (1.25) in (1.24) we relate M [Eq. (1.22)] to T [Eq. (1.3)]. A little elementary manipulation gives

$$\begin{aligned} f_1 &= \frac{E+M}{8\pi W}[A + (W-M)B] , \\ f_2 &= \frac{E-M}{8\pi W}[-A + (W+M)B] . \end{aligned} \qquad (1.26)$$

Here, $E = (M^2+q^2)^{\frac{1}{2}}$ is the energy of the nucleon in the c.m. system. In connection with (1.26) it is useful to notice that

$$E \pm M = [(W \pm M)^2 - \mu^2]/2W . \qquad (1.27)$$

Substituting (1.27) in (1.26) and using (1.5) (and $W^2 = s$) we can express f_1 and f_2 in terms of the invariants s and t, or ν and t.

The conventional partial wave expansions are

$$\begin{aligned} f(\theta) &= \sum_{l=0}^{\infty}\{(l+1)f_{l+} + lf_{l-}\}P_l(\mu) , \\ g(\theta) &= i\sum_{l=1}^{\infty}\{f_{l+} - f_{l-}\}P_l^{(1)}(\mu) , \end{aligned} \qquad (1.28)$$

[7] H. J. Bremermann, R. Oehme, and J. G. Taylor, Phys. Rev. **109**, 2178 (1958); H. Lehmann, Nuovo Cimento **10**, 579 (1958).

[8] M. Jacob and G. C. Wick, Ann. Phys. **7**, 404 (1959).

where $\mu = \cos\theta$ and $P_l(\mu)$, $P_l^{(1)}(\mu)$ are ordinary and associated Legendre polynomials. $f_{l\pm}$ are the partial wave amplitudes,[9] and in the elastic region $f_{l\pm} = \exp(i\delta_{l\pm})\sin(\delta_{l\pm})/q$. Using the relations $P_l^{(1)}(\mu) = \sin\theta P_l'(\mu)$ and

$$(l+1)P_l(\mu) = P_{l+1}'(\mu) - \mu P_l'(\mu)\,,$$
$$lP_l(\mu) = \mu P_l'(\mu) - P_{l-1}'(\mu)\,, \quad (1.29)$$

Eqs. (1.28) and (1.23) give

$$f_1(\theta) = \sum_{l=0}^{\infty}[f_{l+}P_{l+1}'(\mu) - f_{l-}P_{l-1}'(\mu)]\,,$$
$$f_2(\theta) = \sum_{l=1}^{\infty}[f_{l-} - f_{l+}]P_l'(\mu)\,. \quad (1.30)$$

The orthogonality relations associated with (1.30) are

$$\int_{-1}^{1} d\mu P_j'(\mu)[P_{l+1}(\mu) - P_{l-1}(\mu)] = \delta_{jl}\,.$$

They give

$$f_{l\pm} = \tfrac{1}{2}\int_{-1}^{1} d\mu[P_l(\mu)f_1 + P_{l\pm1}(\mu)f_2]\,.$$

(vii) Laboratory System Relations

We use q and q_L for the c.m. and incident lab pion momenta. We always use E and W to denote the nucleon energy and the total energy in the c.m. system. The (total) lab energy of the incident pion is ω_L.

Then we have

$$q_L/q = W/M \quad (1.31)$$

and

$$\omega_L = (EW/M) - M\,. \quad (1.32)$$

The forward-scattering amplitudes $f_L(q_L,0)$, $f(q,0)$ in the lab and c.m. system are related by

$$f_L(q_L,0)/q_L = f(q,0)/q\,. \quad (1.33)$$

The forward amplitude in the c.m. system is deduced from (1.23), (1.26), and (1.32). It is

$$f(q,0) = (M/4\pi W)(A + \omega_L B)\,. \quad (1.34)$$

By (1.31) and (1.33)

$$f_L(q_L,0) = (1/4\pi)(A + \omega_L B)\,. \quad (1.35)$$

For the real part of the forward-scattering amplitude we shall use the notation

$$D(\omega_L) = \mathrm{Re}\,f_L(q_L,0)\,,$$
$$D_B(\omega) = \mathrm{Re}\,f(q,0)\,. \quad (1.36)$$

[9] $f_{l\pm}$ and $\delta_{l\pm}$ are the partial wave amplitudes and phase shifts for the states with orbital angular momentum and total angular momentum $j = l \pm 1/2$, respectively.

As a special case of (1.33), the threshold values of the scattering amplitudes $D_\pm(\omega_L)$ for $\pi^\pm - p$ scattering are given by

$$D_+(\mu) = (1 + \mu/M)a_3\,,$$
$$D_-(\mu) = (1 + \mu/M)\tfrac{1}{3}(2a_1 + a_3)\,, \quad (1.37)$$

where a_1 and a_3 are the s-wave scattering lengths in the isotopic states $T = \frac{1}{2}$ and $\frac{3}{2}$. Finally, the optical theorem can be written in two forms

$$\mathrm{Im}\,f_L(q_L,0) = (q_L/4\pi)\sigma_{\mathrm{tot}}\,;\ \mathrm{Im}\,f(q,0) = (q/4\pi)\sigma_{\mathrm{tot}}\,. \quad (1.38)$$

2. SUBTRACTIONS, HIGH-ENERGY BEHAVIOR AND THE SUM RULE

From our knowledge of the positions of the singularities of a scattering amplitude as a function of the energy we can, as in Eqs. (1.16) and (1.17), set up a dispersion relation merely by using Cauchy's theorem. However, this relation will not be valid unless certain high-energy convergence conditions are obeyed. If these conditions are not satisfied, one or more subtractions must be made in order to obtain a valid dispersion relation. Since it is particularly necessary in making numerical applications that we are sure that we are using valid dispersion relations, we shall examine carefully the problem of the number of subtractions which is required.

In order to apply these general ideas in any particular case it is necessary to know the high-energy behavior of the various terms in the dispersion relation. This presents us with two somewhat difficult problems: (a) the mathematical question of determining the limiting behavior of principal value integrals, and (b) the physical question of conjecturing the asymptotic behavior of scattering amplitudes.

In the first half of this chapter [Secs. 2(i)–2(v)] we discuss these problems with particular reference to forward $\pi^\pm$–p scattering. It is convenient to do this because of the considerable amount of information which is available about forward $\pi^\pm$–p scattering. We include some discussion of two interesting features which are associated with the high-energy behavior: Pomeranchuk's theorem, and the sum rule. In the second half of the chapter [Secs. 2(vi)–2(ix)] we examine the high-energy behavior of the amplitudes $A(s,t)$, $B(s,t)$ and the question of what subtractions are needed in the dispersion relations (1.16) and (1.17).

The reader who finds these discussions of subtractions and high-energy behavior to be tedious can ignore this chapter [except for Sec. 2(iv) on the sum rule]. All the dispersion relations used in Secs. 4 and 5 have the correct number of subtractions!

(i) Additive Polynomials and Subtractions

When the integral in a dispersion relation [like (1.16) or (1.17)] does not converge, the usual procedure is to subtract, i.e., extra factors are inserted in the denominator of the integral until convergence is achieved. This automatically produces an extra polynomial—the additive polynomial—on the right-hand side of the dispersion relation, as can be seen from Eq. (2.3) below. Strictly speaking there are two distinct features here. In a dispersion relation of the usual type like (1.16) or (1.17) the number of subtractions is determined by the behavior of the imaginary, or absorptive, part of the scattering amplitude at high energy, whereas the degree of the additive polynomial can also depend on the behavior of the real, or dispersive, part of the scattering amplitude at high energy.

Let $f(s)$ be a scattering amplitude, where s is the energy or a function of the energy: $f(s)$ can be the forward scattering amplitude, or it can be any linear combination of the amplitudes $A^{(\pm)}(s,t)$, $B^{(\pm)}(s,t)$ (for fixed-momentum transfer t) defined in Sec. 1. We know that $f(s)$ as a function of s has cuts along $-\infty \leq s \leq s_0$, $s_1 \leq s \leq \infty$, and we derive a dispersion relation for $f(s)$ by writing

$$f(s) = \frac{1}{2\pi i}\int_C \frac{f(s')}{s'-s}\,ds', \tag{2.1}$$

where C is the small circle about s shown in Fig. 1.

Next we blow up the contour C until it is replaced by contours around the cuts as shown in Fig. 1 plus C_∞, the circle at infinity in the complex s plane. The integral around the infinite circle

$$\frac{1}{2\pi i}\int_{C_\infty} \frac{f(s')}{s'-s}\,ds'$$

may not converge, and if this is so, we have to replace it by an additive polynomial.

Suppose[10] that for

$$|s| \to \infty\,, \quad |f(s)| < |s|^{N-\epsilon}\,,$$

where N is a positive integer and ϵ is a small positive number. Define the function $g(s)$ by

$$g(s) = f(s) \Big/ \prod_{j=0}^{N-1} (s - s_j)\,,$$

where s_j $(j = 0,1,\cdots N-1)$ are real constants. Starting from the Cauchy integral

$$g(s) = \frac{1}{2\pi i}\int_C \frac{g(s')}{s'-s}\,ds'\,,$$

we get the dispersion relation

$$g(s) = \frac{1}{2\pi i}\int_{(\text{cuts})} \frac{\Delta g(s')}{s'-s}\,ds' + \sum_{j=0}^{N-1} \frac{\alpha_j}{s-s_j}\,, \tag{2.2}$$

where $\Delta g(s')$ is the *discontinuity* in $g(s')$ across the cut at s'. The terms $\alpha_j/(s-s_j)$ arise from the poles at $s = s_j$ which we introduced in the definition of $g(s)$. There is no contribution to (2.2) from the infinite circle C_∞, since $|g(s)|$ goes to zero faster than $|s|^{-\epsilon}$ (where $\epsilon > 0$) as $|s| \to \infty$. The numbers α_j $(j = 0,\ 1,\cdots N-1)$ (which are independent of s) are not determined by the dispersion relation itself; they represent physical information (scattering lengths, etc.) which we must insert before we can evaluate the dispersion relation.

From (2.2) we get the dispersion relation

$$f(s) = A_0 + A_1 s + \cdots + A_{N-1}s^{N-1} + \frac{1}{2\pi i}\prod_{j=0}^{N-1}(s-s_j) \times \int_{(\text{cuts})} ds' \frac{\Delta f(s')}{(s'-s)\prod_{j=0}^{N-1}(s'-s_j)}\,, \tag{2.3}$$

where $\Delta f(s')$ is the discontinuity in $f(s')$ across the cut at s', and A_0, $A_1 \cdots A_N$ are arbitrary constants (they will in general be functions of the momentum transfer t). If $N = 1$ the polynomial on the right of (2.3) reduces to the constant $f(s_0)$.

We assumed above that the complete amplitude $f(s)$ obeys the inequality

$$|f(s)| < |s|^{N-\epsilon} \quad \text{as} \quad |s| \to \infty$$

for real or complex s. It may happen that on the real axis $\Delta f(s)$ (which is in general the imaginary part of $f(s)$) obeys the stronger inequality

$$|\Delta f(s)| < s^{N'-\epsilon} \quad \text{as}^{11} \quad s \to \pm\,\infty\,,$$

where $\epsilon > 0$, and N' is zero or a positive integer, with $N' < N$. In that case we get a different dispersion relation. By successive use of the relations

$$\frac{1}{s'-s}\cdot\frac{s-s_j}{s'-s_j} = \frac{1}{s'-s} - \frac{1}{s'-s_j}\,,$$

Eq. (2.3) can be written in the form

$$f(s) = A_0' + A_1' s + \cdots + A_{N-1}' s^{N-1} + \frac{1}{2\pi i}\prod_{j=0}^{N'-1}(s-s_j) \times \int_{(\text{cuts})} ds' \frac{\Delta f(s')}{(s'-s)\prod_{j=0}^{N'-1}(s'-s_j)}\,, \tag{2.4}$$

[10] A similar argument was used by J. Hamilton, T. D. Spearman, and W. S. Woolcock, Ann. Phys. **17**, 1 (1962) [see Sec. V(B)].

[11] The notation $s \to \pm\,\infty$ always implies that s goes to infinity along the real axis.

where $A_0', A_1' \cdots A_{N-1}'$ are arbitrary constants. If $N' = 0$, we must replace

$$\prod_{j=0}^{N'-1}(s - s_j) \text{ and } \prod_{j=0}^{N'-1}(s' - s_j)$$

by unity. Letting s tend to the upper side of the physical cut[12] gives the dispersion relation

$$\begin{aligned}\mathrm{Re}\, f(s) &= A_0' + A_1's + \cdots + A_{N-1}'s^{N-1} \\ &\quad + \frac{1}{2\pi i}\prod_{j=0}^{N'-1}(s - s_j)P\int_{(\text{cuts})} ds' \\ &\quad \times \frac{\Delta f(s')}{(s' - s)\prod_{j=0}^{N'-1}(s' - s_j)}. \end{aligned} \tag{2.5}$$

The number N' of subtractions which are required in the integral in (2.5) is determined by the experimentally known behavior of $\Delta f(s)$ (i.e., of $\mathrm{Im}\, f(s)$) as $s \to \pm\infty$. The number N is given by the behavior of $|f(s)|$ as $|s| \to \infty$. However, N can be found in practice as follows. We find the asymptotic behavior of the integral in (2.5) as $s \to \pm\infty$. Using Eq. (2.5) and the known experimental behavior of $\mathrm{Re}\, f(s)$ as $s \to \pm\infty$ now determines the integer N. There appears in general to be no *a priori* reason to assume that $N = N'$.

We shall show in the following sections how this method is applied in various practical cases. A somewhat awkward feature is the determination of the asymptotic form of the dispersion integral as $s \to \pm\infty$, and we shall quote several theorems which are of value for this purpose.

(ii) Theorems Relating to Forward $\pi^{\pm} - p$ Scattering

We first show how the problem of subtractions and high-energy behavior can be treated for forward scattering. Let $D_{\pm}(\omega_L)$ be the real part of the lab system forward scattering amplitude for $\pi^{\pm} + p$ at lab (kinetic) energy $(\omega_L - \mu)$. From Eqs. (1.35), (1.16), and (1.17) we can write down the once subtracted dispersion relations

$$\begin{aligned}D_{\pm}(\omega_L) &= \tfrac{1}{2}\left(1 + \frac{\omega_L}{\mu}\right)D_{\pm}(\mu) + \tfrac{1}{2}\left(1 - \frac{\omega_L}{\mu}\right)D_{\mp}(\mu) \\ &\quad \pm 2\frac{f^2}{\mu^2}\frac{q_L^2}{\omega_L \mp \mu^2/2M}\frac{1}{1 - \mu^2/4M^2} \\ &\quad + \frac{q_L^2}{4\pi^2}P\int_{\mu}^{\infty}\frac{d\omega'}{q'}\left[\frac{\sigma_{\pm}(\omega')}{\omega' - \omega_L} + \frac{\sigma_{\mp}(\omega')}{\omega' + \omega_L}\right]. \end{aligned} \tag{2.6}$$

Here, $\sigma_{\pm}(\omega')$ are the total cross sections for $\pi^{\pm} + p$ at lab (kinetic) energy $(\omega' - \mu)$, and $q' = (\omega'^2 - \mu^2)^{\frac{1}{2}}$ is the corresponding lab momentum. Also $q_L = (\omega_L^2 - \mu^2)^{\frac{1}{2}}$, and $f = G\mu/2M$ is the equivalent pseudovector coupling constant. Up to Sec. 2(v) we frequently use ω_L, ω, ω', and in these sections they always denote the lab pion energy.

We shall now show that the single subtraction and the first-degree polynomial in Eq. (2.6) are sufficient. For this we must know the high-energy behavior of $\sigma_{\pm}(\omega)$ and $D_{\pm}(\omega)/\omega$ and the asymptotic behavior of the integral in (2.6) as $\omega \to \infty$. The mathematical techniques which are required are neither trivial, nor are they particularly well known, and we shall state the most useful general theorems. The same methods are necessary for discussing the $A^{(\pm)}$ and $B^{(\pm)}$ dispersion relations in Sec. 2(vi) and (vii).

We can obtain a rough idea of how the principal value integrals in Eq. (2.6) behave as $\omega_L \to \infty$ by using a basic theorem on Hilbert transforms. Let $L^p(-\infty, \infty)$ denote the class of real functions $f(x)$ such that

$$\int_{-\infty}^{\infty} dx |f(x)|^p \quad (p > 0)$$

exists. Then we have[13]

Theorem A. If $f(x)$ belongs to $L^p(-\infty, \infty)$, where $p > 1$, then the formula

$$g(x) = \frac{1}{\pi}P\int_{-\infty}^{\infty}\frac{f(y)}{y - x}dy \tag{2.7}$$

almost everywhere defines a function $g(x)$, and $g(x)$ also belongs to $L^p(-\infty, \infty)$. Further, $g(x)$ and $f(x)$ are Hilbert transforms of each other.

We apply this theorem to the integrals

$$g_{\pm}(\omega_L) = \frac{1}{\pi}P\int_{\mu}^{\infty}\frac{d\omega'}{q'}\frac{\sigma(\omega')}{\omega' \pm \omega_L}, \tag{2.8}$$

where $\sigma(\omega')$ represents either of $\sigma_{\pm}(\omega')$. So in the g_+ case we take

$$f(\omega') = \begin{cases} -\sigma(-\omega')/q', & \omega' \leqslant -\mu; \\ 0, & \omega' > -\mu, \end{cases}$$

and in the g_- case

$$f(\omega') = \begin{cases} \sigma(\omega')/q', & \omega' \geqslant \mu; \\ 0, & \omega' < \mu. \end{cases}$$

Restrictions on the Cross Sections $\sigma_{\pm}(\omega)$. The cross sections $\sigma_{\pm}(\omega)$ are continuous functions of ω, and we shall also assume that they have *bounded* derivatives with respect to ω. This means that the words "almost

[12] The physical value of an amplitude is always defined by its value as s moves in to the upper side of the physical cut.

[13] E. C. Titchmarsh, *Theory of Fourier Integrals* (Oxford University Press, New York, 1948), theorem 101.

everywhere" can be dropped from theorem A, i.e., $g_\pm(\omega_L)$ are everywhere finite. We also make the very plausible assumption that $\sigma_\pm(\omega)$ are bounded as $\omega \to \infty$.

With these assumptions, $f(\omega)$ is in $L^p(-\infty, \infty)$ with[14] $1 < p < 2$. Now, theorem A shows that $g_\pm(\omega_L)$ is in $L^p(-\infty, \infty)$. The consequences are important. First, it is necessary that $g_\pm(\omega_L) \to 0$ as $\omega_L \to \infty$. Next *suppose* that $|g(\omega_L)|$ behaves like $\omega_L{}^{-\lambda}(\ln \omega_L)^n$ as $\omega_L \to \infty$, where n is some integer. Because $g(\omega_L)$ is in L^p we must have $\lambda > 1/p$. Also p can take any value in $1 < p < 2$. Thus, $|g(\omega_L)|\omega_L{}^{1-\eta} \to 0$ as $\omega_L \to \infty$ where η is any small positive number. The functions $1/\omega_L$, $(\ln \omega_L)/\omega_L$, $(\ln \omega_L)^2/\omega_L$, etc., are therefore possible examples of the behavior of $g(\omega_L)$.

The restriction that $\sigma_\pm(\omega)$ should have *bounded* derivatives is convenient but is not necessary. We could include the case of cusps in $\sigma_\pm(\omega)$ by using Theorem 106 of Titchmarsh.[13] This states that $g(x)$, given by Eq. (2.7), exists for all x and belongs to $L^p(-\infty, \infty)$, provided $f(x)$ belongs to $L^p(-\infty, \infty)$ $(p > 1)$ and obeys a Lipschitz condition.

$$|f(x + h) - f(x)| < K|h|^\alpha$$

uniformly in x as $h \to \pm 0$. K is some constant. Also $g(x)$ obeys a Lipschitz condition with the same α. Taking $\alpha = \frac{1}{2}$ we can include any cusps[15] and we see that in this case $g_\pm(\omega_L)$ are continuous.

Asymptotic Behavior of Principal Value Integrals

We wish to be able to make more definite statements about the behavior of $g_\pm(\omega_L)$ [Eq. (2.8)] as $\omega_L \to \infty$. This can only be done by imposing further restrictions on the behavior of $\sigma_\pm(\omega)$ for large ω.

First consider $g(x)$ given by Eq. (2.7). It might be thought that, provided

$$\int_{-\infty}^{\infty} f(y)dy$$

converges, then

$$g(x) \to -\frac{1}{\pi x}\int_{-\infty}^{\infty} f(y)dy\,, \quad \text{as} \quad x \to \infty\,. \tag{2.9}$$

This is not true. To ensure (2.9) further conditions must be imposed on $f(y)$. Sufficient conditions are[16]:

(i) $\int^{\infty} |f(y)|dy$ and $\int_{-\infty} |f(y)|dy$ converge,

and

(ii) given $\epsilon > 0$, there exists a V such that

$$\left|\frac{yf(y) - xf(x)}{y - x}\right| < \frac{\epsilon}{x} \left(\text{or} < \frac{\epsilon}{(xy)^{\frac{1}{2}}}\right)$$

for all $y \geqslant x > V$.

These conditions are satisfied by simple forms of $f(y)$, such as $f(y) \sim y^{-1-\eta}$ as $y \to \infty$ where $\eta > 0$, but they are not satisfied by certain oscillatory forms of $f(y)$.

In fact Eq. (2.9) is not particularly useful here, and we use several other theorems to find the behavior of $g(x)$ as $x \to \infty$. Now we quote a standard theorem on the limiting form of a principal value integral with a finite range of integration. [We also need this theorem in another connection below. Cf. Sec. 4(iii).]

Theorem B.[17] Let

$$g(x) = \frac{1}{\pi}\int_{-1}^{1} \frac{f(y)}{y - x}\,dy\,,$$

where $f(y)$ is in $L^p(-1,1)$ $(p > 1)$, and suppose that near $y = 1$

$$f(y) = A(1 - y)^{-\alpha} + \psi(y)\,, \quad 0 \leqslant \alpha < 1\,,$$

where A is a constant. Also $\psi(y = 1) = 0$, and near $y = 1$, $\psi(y)$ obeys uniformly the Lipschitz (or Hölder) condition

$$|\psi(y) - \psi(y_0)| < K|y - y_0|^\epsilon$$

where K and ϵ are positive constants. Then as $x \to 1$,

$$g(x) \to -A \cos(\pi\alpha)(1 - x)^{-\alpha} + O(1)\,,$$

if $0 < \alpha < 1$;

and

$$g(x) \to (1/\pi)A \ln(1 - x) + O(1)\,, \quad \text{if } \alpha = 0\,.$$

Transforming one end point to infinity we have a theorem on the asymptotic behavior of Eq. (2.7).

Theorem C. Suppose that as $y \to \infty$

$$f(y) \to Ay^{-1+\alpha} + F(y)\,, \quad 0 \leqslant \alpha < 1\,,$$

where A is a constant and $yF(y) \to 0$ as $y \to \infty$. Also we require[18] that for any large y and y_0

[14] For $\omega' \simeq \mu$, $f(\omega') \sim \sigma\{2\mu(\omega' - \mu)\}^{-1/2}$, so $p \geq 2$ is not possible. If necessary the restriction $p < 2$ can be removed by writing $f(\omega') = [\sigma(\omega') - \sigma(\mu)]/q' + \sigma(\mu)/q'$. The second term can be evaluated explicitly, and for the first, $1 < p < \infty$.

[15] We assume that all cusps in $\sigma_\pm$ are of the square root type, hence the choice $\alpha = 1/2$.

[16] We are indebted to D. Atkinson, P. Menotti, G. C. Oades, and L. L. J. Vick (private communication) for this statement of sufficient conditions.

[17] F. G. Tricomi, *Integral Equations* (Interscience Publishers, Inc., New York, 1957), Chapter 4. See also N. I. Muskhelishvili, *Singular Integral Equations* (P. Noordhoff Ltd., Groningen, the Netherlands, 1953), Chapter 4.

[18] This is an adaptation of the Hölder condition which is in general required in some form to set bounds on a principal value integral.

$$|yF(y) - y_0F(y_0)| < K\left|\frac{1}{y} - \frac{1}{y_0}\right|^\epsilon$$

where K and ϵ are positive constants. Then as $x \to \infty$

$$g(x) \to -A \cot(\pi\alpha)x^{-1+\alpha} + B(x)/x\,, \quad \text{if } 0 < \alpha < 1\,,$$

and

$$g(x) \to -\frac{A}{\pi}\frac{\ln x}{x} + \frac{B(x)}{x}\,, \quad \text{if } \alpha = 0\,,$$

where $B(x)$ is a bounded function.[19]
The special case of $\alpha = \frac{1}{2}$ should be emphasized; it gives $g(x) \to B(x)/x$ as $x \to \infty$ (where $B(x)$ is bounded). Also note that in this case (as for all $\alpha \geqslant 0$), $\int^\infty f(y)dy$ does not exist.

Application to the $D_\pm(\omega_L)$ Dispersion Relations

We apply theorem C to the integral in Eq. (2.6) [or Eq. (2.8)]. We assume that $\sigma_+(\omega)$ and $\sigma_-(\omega)$ tend to limiting values σ_+ and σ_- as $\omega \to \infty$. Further, the Hölder condition requires that these limits are approached in such a way that

$$|\sigma_\pm(\omega) - \sigma_\pm(\omega_0)| < K\left|\frac{1}{\omega} - \frac{1}{\omega_0}\right|^\epsilon\,, \quad (2.10)$$

where K and ϵ are some positive constants, and ω, ω_0 take all large values. [We shall return shortly to discuss these limitations on $\sigma_\pm(\omega)$.] Now Eq. (2.6) is seen to have the asymptotic form[20]

$$D_\pm(\omega_L) \backsim \mp(1/4\pi^2)(\sigma_+ - \sigma_-)\omega_L \ln \omega_L\,, \quad \text{as } \omega_L \to \infty\,, \quad (2.11)$$

provided $\sigma_+ - \sigma_- \neq 0$. This result will be used in the derivation of Pomeranchuk's theorem in Sec. 2(iii) below.

Several comments should be made here. First, suppose that we are not allowed to assume that $\sigma_\pm(\omega_L)$ tend to limits as $\omega_L \to \infty$, but merely assume that $\sigma_\pm(\omega_L)$ are bounded as $\omega_L \to \infty$. Then theorem A applied to Eq. (2.8) enables us to infer that $g_\pm(\omega_L) \to 0$ as $\omega_L \to \infty$. It follows that the last term on the right of Eq. (2.6) cannot increase[21] as fast as ω_L^2 when $\omega_L \to \infty$.

Next, we look at the condition (2.10) which was required in applying theorem C. Letting $\omega_0 \to \infty$ we see that (2.10) requires that $\sigma_\pm(\omega)$ should approach the limit $\sigma_\pm$ at least as fast as some (fractional) power law, that is (writing σ for σ_+ or σ_-), $\sigma(\omega) - \sigma(\infty) \sim K\omega^{-\lambda}$ $(\lambda > 0)$, as $\omega \to \infty$.[22] However, this is not sufficient. We actually require that

$$\sigma(\omega) - \sigma(\infty) = [K + \gamma(\omega)]/\omega^\lambda\,, \quad \text{as } \omega \to \infty\,, \quad (2.12)$$

where $\gamma(\omega) \to 0$ as $\omega \to \infty$, and $\gamma(\omega)$ itself obeys (2.10) for some $\epsilon > 0$.

The estimates of high-energy behavior which are derived from the analogy with Regge poles are referred to in Sec. 2(iii) below. They suggest that[23]

$$\sigma(\omega) - \sigma(\infty) = \frac{K_1}{\omega^{\mu_1}} + \frac{K_2}{\omega^{\mu_2}} + \cdots + \frac{K_\mu}{\omega^{\mu_u}}\,, \quad \text{as } \omega \to \infty\,, \quad (2.13)$$

where $K_1, \cdots K_n$ are constants, and $\mu_1, \cdots \mu_n$ are positive constants which are less than unity. This high-energy behavior satisfied condition (2.10). In what follows we shall in general assume that $\sigma_\pm(\omega)$ do obey Eq. (2.10).

Behavior of $D_\pm(\omega_L)$ as $\omega_L \to \infty$

If the π–N interaction has a finite range R, then assuming that little scattering occurs for angular momentum values $l > q_{\text{c.m.}}R$ it follows [as in Sec. 2(vi) below] that $D_\pm(\omega_L)/\omega_L$ are bounded as $\omega_L \to \infty$. This is the final step which establishes the validity of the dispersion relations (2.6). The additive polynomial cannot contain a term in ω_L^2, because, as we have just seen, provided $\sigma_\pm(\omega)$ are bounded as $\omega \to \infty$, no other term in (2.6) can increase as fast as ω_L^2.

In fact there is good evidence for the much stronger statement $D_\pm(\omega_L)/\omega_L \to 0$, as $\omega_L \to \infty$. Cool, Piccioni, and Clark[24] found that the forward c.m. scattering amplitude $f_-(\omega_L,0)$ for π^-–p scattering obeyed the relation $|\text{Re } f_-(\omega_L,0)| \ll |\text{Im } f_-(\omega_L,0)|$ in the range 1 to 1.5 BeV. The result comes from comparing the differential cross section extrapolated to the forward direction,

$$\frac{d\sigma}{d\Omega}(\theta = 0) = |f_-(\omega_L,0)|^2$$

with the total cross section $\sigma_-(\omega_L)$ by using the optical theorem (1.37).

An experiment by Thomas[25] on $\pi^- - p$ scattering

---

[19] See also H. Lehmann, Hamburg University (1961) (to be published) on the asymptotic behavior of dispersion relations.

[20] It is easy to show by standard methods that

$$\int_1^\infty \frac{d\omega'}{q'}\frac{\sigma_\pm(\omega')}{\omega' + \omega_L} \sim \sigma_\pm\frac{(\ln\omega_L)}{\omega_L} \text{ as } \omega_L \to \infty\,.$$

[21] The same result is true under the much weaker condition that $\sigma_\pm(\omega_L)\omega_L^{-1+\eta} \to 0$ as $\omega_L \to \infty$, where $\eta > 0$. This follows from theorem A and the method indicated in footnote 14.

[22] Thus (2.10) is not satisfied if $\sigma(\omega)$ approaches $\sigma(\infty)$ as slowly as $(\ln \omega)^{-1}$.

[23] See for example B. M. Udgaonkar, Phys. Rev. Letters **8**, 142 (1962).

[24] R. Cool, O. Piccioni, and D. Clarke, Phys. Rev. **103**, 1082 (1956).

[25] R. G. Thomas. Phys. Rev. **120**, 1015 (1960).

at 5.17 BeV gives $(d\sigma/d\Omega)\ \theta = 0) = 29.8$ mb/sr. If we assume that $\mathrm{Re}\, f_-(\omega_L,0) = 0$ this gives $\sigma_-(5.17$ BeV$) = (29.1 \pm 3)$ mb, which is in good agreement with the direct measurements of $\sigma_-(\omega_L)$ (cf. Fig. 2). There is also experimental evidence at higher energies that $\mathrm{Re}\, f_-(\omega_L,0)$ is small.[26]

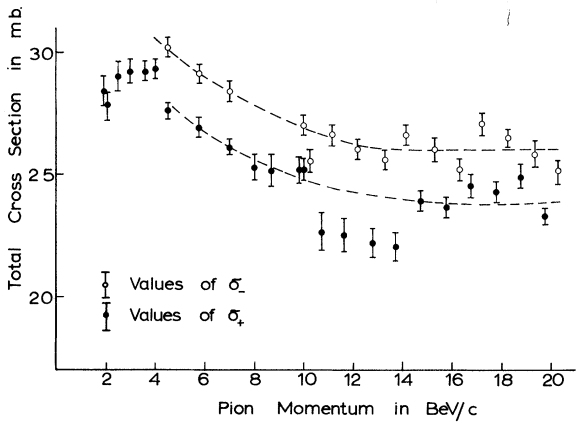

FIG. 2. Experimental values of the total $\pi^+ + p$ and $\pi^- + p$ cross sections σ_+ and σ_- at high energies. The broken lines are possible smooth fits to the data. The values used are based on the results of M. J. Longo, J. Helland, W. N. Hess, B. J. Moyer, and V. Perez-Mendez, Phys. Rev. Letters **3**, 568 (1959); G. von Dardel, R. Mermod, P. A. Piroué, M. Vivargent, G. Weber, and K. Winter, *ibid.* **7**, 127 (1961); S. J. Lindenbaum, W. A. Love, J. A. Niederer, S. Ozaki, J. J. Russell, and L. C. L. Yuan, *ibid.* **7**, 352 (1961).

We shall assume that

$$|\mathrm{Re}\, f_-(\omega_L,0)/\mathrm{Im}\, f_-(\omega_L,0)| \to 0\,, \quad \text{as } \omega_L \to \infty\,. \tag{2.14}$$

Assuming also that $\sigma_-(\omega_L)$ is bounded as $\omega_L \to \infty$, the optical theorem (1.38) now gives

$$D_-(\omega_L)/\omega_L \to 0\,, \quad \text{as } \omega_L \to \infty\,, \tag{2.15}$$

where $D_- \equiv \mathrm{Re}\ f_{L-}(\omega_L,0)$. The data on $\pi^+ - p$ differential cross sections is not at present so good, and we cannot directly deduce from experiment the relation analogous to (2.15).[27] However, it is shown in Sec. 2(iv) [Eq. (2.6)] that, from (2.15) and some general properties of the dispersion relations (2.6), we can deduce

$$D_+(\omega_L)/\omega_L \to 0\,, \quad \text{as } \omega_L \to \infty\,. \tag{2.16}$$

Further evidence in favor of (2.15) and (2.16) comes from evaluating the dispersion relations (2.6) at high energies. Our discussion above showed that the relations (2.6) are valid under very wide assumptions[28] about the high-energy behavior of $\sigma_\pm(\omega)$, and from now on we take them to be true. Inserting the known values of the scattering lengths and the cross sections $\sigma_\pm(\omega)$ in (2.6), the amplitudes $D_\pm(\omega_L)$ have been evaluated[29] up to about $\omega_L = 2.5$ BeV. The results indicate that $D_\pm(\omega_L)$ are almost constant above 1.8 BeV.

(iii) High-Energy Consequences of the Forward Dispersion Relations

Pomeranchuk's Theorem. We have seen that the dispersion relations (2.6) give the asymptotic form (2.11) for $D_\pm(\omega)$ provided $\sigma_\pm(\omega)$ have limiting values $\sigma_\pm$ as $\omega \to \infty$, and provided $\sigma_\pm(\omega)$ approach these limiting values so that condition (2.10) is satisfied. Now comparing (2.11) with (2.15) and (2.16) we must have

$$\sigma_+ = \sigma_-[=\sigma(\infty)]\,. \tag{2.17}$$

This important result is Pomeranchuk's theorem.[30] Towards the end of this section we shall derive it under less restrictive assumptions about $\sigma_\pm(\omega)$.

In Fig. 2 we show the experimental data on $\sigma_+(\omega)$ and $\sigma_-(\omega)$ in the range 2 BeV to 20 BeV. Two facts appear to be established: (a) the cross sections $\sigma_+(\omega)$ and $\sigma_-(\omega)$ have not reached their limiting values at the highest energies yet attained; and (b) the difference $\sigma_-(\omega) - \sigma_+(\omega)$ is decreasing very slowly with increasing ω in the energy range considered, and it is not zero at the highest energy attained.

The Rate of Decrease of $\sigma_-(\omega) - \sigma_+(\omega)$

We can try to use physical arguments to determine how fast $\sigma_-(\omega) - \sigma_+(\omega)$ goes to zero. First, there are the early arguments of Pomeranchuk[31] based on charge exchange processes. These state that above some energy ω_0 (which is of the order of a few BeV) the phase space for the charge exchange process $\pi^- + p \to \pi^0 + n$ is much smaller than the phase space for all other inelastic processes originating from $\pi^- + p$. Therefore, for $\omega > \omega_0$, the total cross section for $\pi^- + p \to \pi^0 + n$ within the forward diffraction cone, is a rapidly decreasing fraction of the total cross section $\sigma_-(\omega)$. Also the cross section for elastic scattering $\pi^- + p \to \pi^- + p$ within the forward diffraction cone is an appreciable fraction

[26] For details see *Proceedings of the International Conference on High-Energy Nuclear Physics, Geneva, 1962* (CERN Scientific Information Service, Geneva, Switzerland, 1962), edited by J. Prentk and A. Taylor.

[27] See however reference 26.

[28] Namely that $\sigma_\pm(\omega)$ do not increase faster than $\omega^{1-\eta}$ where $\eta > 0$, and that $|D_\pm(\omega)/\omega|$ do not increase as fast as ω.

[29] See, for example, J. W. Cronin, Phys. Rev. **118**, 824 (1960).

[30] I.Ia Pomeranchuk, Soviet Phys.—JETP **7**, 499 (1958).

[31] I. Ia. Pomeranchuk, Soviet Phys.—JETP **3**, 306, 307 (1956); also S. Z. Belenki, Soviet Phys.—JETP **6**, 960 (1958).

of $\sigma_-(\omega)$. Thus [in the notation of (1.14) and (1.23)] we expect

$$|f^{(-)}(q,\theta=0)|^2/|f^{(+)}(q,\theta=0)|^2 \to 0\,, \quad \text{as } q \to \infty\,. \tag{2.18}$$

In particular by (2.15), (2.16), and the optical theorem, we expect $|\sigma_-(\omega) - \sigma_+(\omega)|$ to fall to zero rapidly for $\omega > \omega_0$.

The Regge Pole Estimates

As we have seen, the rate of decrease of $|\sigma_-(\omega) - \sigma_+(\omega)|$ appears to be slower than this crude model would indicate. It has been suggested[32] that this is due to a considerable amount of coherence in the exchange processes involved in high-energy forward scattering, and that the difference $\sigma_-(\omega) - \sigma_+(\omega)$ is due to such effects associated with the ρ-meson isobar ($T = 1$, $J = 1$, 2π isobar). If, further, the Regge pole method is used, the rate of decrease of $|\sigma_-(\omega) - \sigma_+(\omega)|$ can be estimated. From Eqs. (35) and (36) of reference 33 we can find the effect of the exchange of a mesonic isobar of angular momentum J upon the amplitudes $A(\nu,t)$, $B(\nu,t)$ for small values of t and large ν. We have $|A(\nu,t)| \sim \nu^J, |B(\nu,t)| \sim \nu^{J-1}$. If the mesonic isobar is to be treated as a Regge pole, we replace its spin J in these relations by $\alpha(t)$ where $0 < \alpha(t) < J$. Thus, using Eq. (2.42), the differential cross section for $\pi^\pm + p \to \pi^\pm + p$ small-angle scattering at high energy obeys

$$d\sigma/d\Omega \backsim \nu^{2\alpha(t)-1} \quad \text{as } \nu \to \infty\,, \tag{2.19}$$

where $t(\leqslant 0)$ is small, and $\alpha(t)$ is a slowly varying function of t. Note that $\nu = \omega_L + t/4M$ and $d\Omega$ is the c.m. solid angle. By the optical theorem this gives the total cross sections

$$\sigma_{\text{tot}} \backsim \omega_L{}^{\alpha(0)-1}\,, \quad \text{as } \omega_L \to \infty\,. \tag{2.20}$$

It is proposed[32] that the high-energy behavior of the cross sections is given by the vacuum pole which has $\alpha(0) = 1$, plus other poles each having $0 < \alpha(0) < 1$, so that the cross sections are of the form shown in Eq. (2.13) (say, at energies above 2 BeV). The difference $\sigma_-(\omega) - \sigma_+(\omega)$ is given primarily by the ρ isobar pole, so that

$$\sigma_-(\omega_L) - \sigma_+(\omega_L) \backsim \omega_L{}^{-[1-\alpha_\rho(0)]}\,. \tag{2.21}$$

The experimental results (cf. Fig. 2) suggest[32] that $\alpha_\rho(o) \backsimeq 0.5$.

Evidence on $\sigma_-(\omega) - \sigma_+(\omega)$ from the Forward Dispersion Relations

Since the Regge pole considerations are as yet not firmly established,[33a] while taking their consequences as valuable indications, we shall examine what information can be obtained about $\sigma_-(\omega) - \sigma_+(\omega)$ from the forward dispersion relations, making as few assumptions as possible.

Following Amati *et al.*[34] we write one of Eqs. (2.6) in the form[35]

$$\begin{aligned}\frac{D_+(\omega_L)}{\omega_L} &= \tfrac{1}{2}\left(\frac{1}{\omega_L}+\frac{1}{\mu}\right)D_+(\mu) + \tfrac{1}{2}\left(\frac{1}{\omega_L}-\frac{1}{\mu}\right)\\ &\quad\times D_-(\mu) + \frac{2f^2}{\mu^2(1-\mu^2/4M^2)}\cdot\frac{\omega_L-\mu^2/\omega_L}{\omega_L-\mu^2/2M}\\ &\quad+\frac{1}{4\pi^2}\left(\omega_L-\frac{\mu^2}{\omega_L}\right)P\int_\mu^\infty\frac{d\omega'}{q'}\,\omega'\,\frac{\sigma_+(\omega')}{\omega'^2-\omega_L^2}\\ &\quad+\frac{1}{4\pi^2}\left(\omega_L-\frac{\mu^2}{\omega_L}\right)\int_\mu^\infty\frac{d\omega'}{q'}\,\sigma_-\frac{(\omega')-\sigma_+(\omega')}{\omega'+\omega_L}\,.\end{aligned} \tag{2.22}$$

If $\sigma_+(\omega)$ approaches the limiting value σ_+ as $\omega \to \infty$ in such a way that theorem C is applicable[36] to the first integral on the right of (2.22), then this integral behaves like ω_L^{-2} as $\omega_L \to \infty$. Therefore, using Eq. (2.16),

$$\omega_L\int_\mu^\infty\frac{d\omega'}{q'}\,\frac{\sigma_-(\omega')-\sigma_+(\omega')}{\omega'+\omega_L} \to K\,, \quad \text{as } \omega_L \to \infty\,, \tag{2.23}$$

where K is a constant. By a standard theorem[37] it follows from (2.23) that

$$\int_\mu^\infty\frac{d\omega'}{q'}\,[\sigma_-(\omega')-\sigma_+(\omega')] = K\,. \tag{2.24}$$

The importance of this result is that the integral in (2.24) must converge, and this provides some information about how fast $\Delta\sigma(\omega) \equiv \sigma_-(\omega) - \sigma_+(\omega)$ must go to zero. For example, if $\Delta\sigma(\omega)$ decreases mono-

[32] G. F. Chew and S. C. Frautschi, Phys. Rev. **7**, 394 (1961) and **8**, 41 (1962); B. M. Udgaonkar Phys. Rev. Letters **8**, 142 (1962). We are indebted to Dr. Udgaonkar for information about his results before they were published.

[33] J. Hamilton and T. D. Spearman, Ann. Phys. **12**, 172 (1961).

[33a] *Note added in proof.* If, as it now appears, the Regge pole ideas do not apply in any simple way to high-energy $\pi^\pm$–p scattering, Eq. (2.21) can still give a useful parameterization of $\sigma(\omega_L) - \sigma_+(\omega_L)$ as $\omega_L \to \infty$.

[34] D. Amati, M. Fiertz, and V. Glaser, Phys. Rev. Letters **4**, 59 (1960).

[35] This is done in order to make use of Tauberian theorems for Stieltjes integrals. We could equally well replace $\sigma_+(\omega')$ by $\sigma_-(\omega')$ in the first integral and in the subsequent arguments.

[36] Change variables by $x = \omega'^2$, and get the case $\alpha = \frac{1}{2}$ of theorem C. Here, the condition on $\sigma_+(\omega)$ is much more restrictive than Eq. (2.10).

[37] G. H. Hardy and D. E. Littlewood, Proc. Math. Soc. (London) **30**, 23 (1930), theorem 5; we must assume that either $\sigma_-(\omega) - \sigma_+(\omega) \geq -\,K'/\omega$, or that $\sigma_+(\omega) - \sigma_-(\omega) \geq -\,K'/\omega$, for all sufficiently large ω. K' is some positive constant.

tonically, then $\Delta\sigma(\omega)$ must go to zero faster[38] than $(\ln\omega)^{-1}$. Unfortunately the above derivation is open to some criticism. In particular theorem C is only applicable to the first integral on the right of (2.22) if $\sigma_+(\omega)$ approaches σ_+ faster than $\omega^{-1-\eta}$ $(\eta>0)$. We now outline a method which avoids this difficulty.

Consider the first integral on the right of (2.22). We apply to it the following useful theorem.

Theorem D.[39] Let

$$h(y)=P\int_1^\infty \frac{f(x)}{x^{\frac{1}{2}}(x-y)}\,dx$$

and suppose that:

(i) $\int_1^\infty \frac{f(x)}{x}\,dx$ exists,

(ii) $f(x)\ln x\to 0$ as $x\to\infty$,

(iii) $|f'(x)|\leqslant M$ (where M is a constant);

then

$$y^{\frac{1}{2}}h(y)\to 0 \text{ as } y\to\infty .$$

Now put $x=\omega'^2$, $y=\omega_L^2$, and $f(x)=\sigma_+(\omega')-\sigma_+$ in the first integral on the right of (2.22). The conditions for theorem D become:

(i) $\int_\mu^\infty \frac{\sigma_+(\omega')-\sigma_+}{\omega'}\,d\omega'$ exists,

(ii) $(\sigma_+(\omega)-\sigma_+)\ln\omega\to 0$ as $\omega\to\infty$,

(iii) $|\sigma_+'(\omega)|<M\omega$.

Then[40]

$$\omega_L P\int_\mu^\infty \frac{d\omega'}{q'}\,\omega'\,\frac{\sigma_+(\omega')}{\omega'^2-\omega_L^2}\to 0 \quad \text{as } \omega_L\to\infty .$$

In particular we note that the conditions (i) and (ii) are satisfied if $\sigma_+(\omega)\to\sigma_+$ as fast as, or faster than $(\ln\omega)^{-2}$. It follows as before that the integral (2.24) exists and [provided $\sigma_-(\omega)\to\sigma_-$ as $\omega\to\infty$] we have Pomeranchuk's theorem (17). This proof of (2.17) avoids the rather restrictive condition (2.10).

We can do even better if we assume that $\sigma_+(\omega)-\sigma_+$ decreases (or increases) steadily to zero. For example[41] with $f(x)=(\ln x)^{-1}$ or $f(x)=(\ln\ln x)^{-1}$ we still have $y^{\frac{1}{2}}h(y)\to 0$ as $y\to\infty$, and Eqs. (2.17) and (2.24) again follow. In all of this we have assumed that the cross sections $\sigma_\pm(\omega)$ have limiting values $\sigma_\pm$ (which may be zero) as $\omega\to\infty$. Various pathological types of behavior of $\sigma_\pm(\omega)$ as $\omega\to\infty$ have been discussed in the literature. For example, if $\sigma_+(\omega)\to\sigma_0+\sigma_1\sin(\omega^2)$ as $\omega\to\infty$, where σ_0 and σ_1 are constants (and $\sigma_1<\sigma_0$), then Eq. (2.23) is not true, and the integral (2.24) need not exist.[42]

The theorems we have just proved and quoted cover a wide variety of physically reasonable behavior of $\sigma_\pm(\omega)$. We shall in what follows assume that Pomeranchuk's theorem (17) is true, and that the integral (2.24) exists.

(iv) The Sum Rule

Dividing Eqs. (2.6) by ω_L and adding, we get for ω_L large,

$$\frac{1}{\omega_L}[D_+(\omega_L)+D_-(\omega_L)]\to\frac{2f^2}{M\omega_L}\left(1-\frac{\mu^2}{4M^2}\right)^{-1}+\frac{\omega_L}{2\pi^2}P\int_\mu^\infty\frac{d\omega'}{q'}\,(\sigma_+(\omega')+\sigma_-(\omega'))\,\frac{\omega'}{\omega'^2-\omega_L^2}\,. \tag{2.25}$$

Substituting $x=\omega'^2$, $y=\omega_L^2$ we can apply theorem D to the integral on the right under the conditions on $\sigma_+(\omega)$ and $\sigma_-(\omega)$ just discussed in the previous section. Then the last term on the right tends to zero as $\omega_L\to\infty$, so we have

$$[D_+(\omega_L)+D_-(\omega_L)]/\omega_L\to 0 \quad \text{as } \omega_L\to\infty . \tag{2.26}$$

Therefore Eq. (2.15) implies Eq. (2.16) and vice versa.

Now if we divide either of Eqs. (2.6) by ω_L, and let $\omega_L\to\infty$ we get the sum rule[43]

$$\frac{f^2}{\mu^2(1-\mu^2/4M^2)}+\frac{1}{4\pi}[D_+(\mu)-D_-(\mu)]=\frac{1}{8\pi^2}\int_\mu^\infty\frac{d\omega'}{q'}\,[\sigma_+(\omega')-\sigma_-(\omega')]\,. \tag{2.27}$$

The existence of this sum rule depends on (2.15) and (2.16) and the convergence of the integral (2.24). It gives a useful relation between the coupling constant f^2, the s-wave scattering lengths a_1, a_3, and the total cross sections $\sigma_\pm(\omega)$. Unfortunately, the slow convergence of the integral means that in practice

[38] If (2.24) is true, then

$$\int_\omega^{\omega^2}\frac{d\omega'}{q'}\,\Delta\sigma(\omega')\to 0 \text{ as } \omega\to\infty .$$

Therefore, $\Delta\sigma(\omega).\ln\omega\to 0$ as $\omega\to\infty$.

[39] The proof is given in Appendix A. Note that $f(x)$ can be positive, negative, or oscillatory.

[40] By explicit calculation or by theorem C,

$$\omega_L P\int_\mu^\infty\frac{d\omega'}{q'}\,\omega'\,\frac{\sigma_+}{\omega'^2-\omega_L^2}\to 0 \text{ as } \omega_L\to\infty .$$

[41] See Appendix A for details.

[42] S. Weinberg, Phys. Rev. **124**, 2049 (1961) has proved that the integral (2.24) exists if $D_\pm(\omega)/\omega$ and $\sigma_\pm(\omega)$ are bounded as $\omega\to\infty$, *provided* that $\sigma_-(\omega)-\sigma_+(\omega)$ does not change sign an infinite number of times. Our theorem D catches many of the cases of oscillatory behavior of $\sigma_-(\omega)-\sigma_+(\omega)$, which Weinberg's result misses.

[43] M. L. Goldberger, H. Miyazawa, and R. Oehme, Phys. Rev. **99**, 986 (1955).

this relation will not give results of high precision. Using the values[44] $a_1 = 0.178$, $a_3 = -0.087$, and the data on $\sigma_\pm(\omega)$ available in 1960, Spearman's calculation[45] gives $f^2 = 0.082 \pm 0.008$. Later information[46] on $\sigma_\pm(\omega)$, and in particular the values of $\sigma_-(\omega) - \sigma_+(\omega)$ above 2 BeV, will reduce the mean value of f^2 by around[47] 0.003. The good agreement, within the errors, of this value of f^2 with the values obtained by other methods in Sec. 4 below provides reasonably strong experimental evidence in favor of the sum rule.

(v) An Unsubtracted Dispersion Relation

The analysis of Secs. 1 and 2(i) shows that, if it existed, an unsubtracted dispersion relation for $f_{L-}(\omega_L,0) - f_{L+}(\omega_L,0)$ would have the form[48]

$$\frac{1}{\omega_L}(D_-(\omega_L) - D_+(\omega_L)) = C + \frac{4f^2}{\omega_L^2 - \mu^4/4M^2} + \frac{1}{2\pi^2} P\int_\mu^\infty \frac{q'd\omega'}{\omega'^2 - \omega_L^2}[\sigma_-(\omega') - \sigma_+(\omega')], \quad (2.28)$$

where C is an arbitrary additive constant (no other term of the additive polynomial can appear). The existence of the integral (2.24) ensures that the integral in (2.28) converges. We shall show that $C = 0$. For this purpose we use[49]

Theorem E.
Let

$$g(y) = P\int_1^\infty \frac{f(x)}{x - y}\,dx$$

and suppose that:

(i) $\int_1^\infty \frac{f(x)}{x}\,dx$ exists,

(ii) $f(x)\ln x \to 0$ as $x \to \infty$,

(iii) $|f'(x)| \leqslant M$ (a constant);

then $g(y) \to 0$ as $y \to \infty$.

Substituting $x = \omega'^2$, $y = \omega_L^2$, $f(x) = \sigma_-(\omega') - \sigma_+(\omega')$ we see that under a wide variety of types of behavior of $\sigma_-(\omega') - \sigma_+(\omega')$ the integral in (2.28) vanishes as $\omega_L \to \infty$. Therefore by (2.15) and (2.16) we must put $C = 0$, and the unsubtracted dispersion relation is established.

Substituting $\omega_L = \mu$ in (2.28) we now get the sum rule (2.27). Thus (2.28) with ($C = 0$) and (2.27) are consistent with each other. Equation (2.28) and similar relations are of value in various calculations given below.

(vi) Subtractions for the $A^{(+)}$ and $B^{(+)}$ Dispersion Relations

The partial wave amplitudes $f_{l\pm}$ of Eq. (1.28) obey the inequality

$$|f_{l\pm}| \leqslant 1/q, \quad (2.29)$$

where q is the c.m. momentum. With a finite range of interaction R, we expect scattering quickly to become negligible as the angular momentum l increases above the value $L = Rq$. Thus, the forward c.m. amplitude obeys

$$|f(q,0)| \lesssim \sum_{l=0}^{L}(2l+1)\cdot(1/q) \simeq qR^2. \quad (2.30)$$

Thus, we expect $|f(q,0)|/q$ and $|f_L(q_L,0)|/q_L$ to be bounded as $q \to \infty$.

Finn[50] and Singh and Udgaonkar[51] have extended this argument to obtain bounds for $A(\nu,t)$, $B(\nu,t)$ as $\nu \to \infty$. From (1.26) we get

$$\frac{1}{4\pi}A = \frac{W+M}{E+M}f_1 - \frac{W-M}{E-M}f_2,$$
$$\frac{1}{4\pi}B = \frac{1}{E+M}f_1 + \frac{1}{E-M}f_2. \quad (2.31)$$

Using (1.30) to express f_1 and f_2 in partial wave amplitudes, and letting $q \to \infty$ (q is always the c.m. momentum) we find that for fixed $t (t \leqslant 0)$

$$\frac{1}{8\pi}A \to \sum_{l=0}^{\infty}[f_{l+}(q) - f_{l+1,-}(q)][P'_{l+1}(\mu) + P'_l(\mu)]$$
$$\frac{1}{8\pi}B \to \frac{1}{2q}\sum_{l=0}^{\infty}[f_{l+}(q) + f_{l+1,-}(q)][P'_{l+1}(\mu) - P'_l(\mu)]. \quad (2.32)$$

Now $|P'_l(\mu)| \leq \frac{1}{2}l(l+1)$ if $-1 \leq \mu \leq 1$, and the equality holds at $\mu = \pm 1$. Also,

$$P'_{l+1}(\mu) - P'_l(\mu) = (l+1)P_{l+1}(\mu) + (1-\mu)P'_{l+1}(\mu). \quad (2.33)$$

The summations in (2.32) are terminated at $L = Rq$, and using (2.29) we get, for $-1 \leq \mu \leq 1$

$$\frac{1}{8\pi}|A| \leqslant \frac{2}{q}\sum_{l=0}^{L}(l+1)^2 \backsim \frac{2}{3q}L^3 = \tfrac{2}{3}R^3q^2.$$

[44] J. Hamilton and W. S. Woolcock, Phys. Rev. **118**, 291 (1960).
[45] T. D. Spearman, Nucl. Phys. **16**, 402 (1960).
[46] G. von Dardel, D. Dekkers, R. Mermod, M. Vivargent, G. Weber, and K. Winter, Phys. Rev. Letters **8**, 173 (1962).
[47] J. Hamilton, *Proceedings of the International Conference on Very High-Energy Physics, Geneva, 1961* (CERN Scientific Information Service, Geneva, Switzerland, 1961), p. 151.
[48] f_{L+} and f_{L-} are the laboratory forward scattering amplitudes for $\pi^+ + p$ and $\pi^- + p$, respectively.
[49] We are indebted to Professor E. C. Titchmarsh for supplying this theorem.
[50] A. C. Finn, Phys. Rev. **119**, 1786 (1960).
[51] V. Singh and B. M. Udgaonkar, Phys. Rev. **123**, 1487 (1961).

Thus for fixed $t \leq 0$

$$|A(\nu,t)|/\nu < K \quad \text{as } \nu \to \infty \,, \tag{2.34}$$

where K is a constant. Here, we have used

$$\nu \simeq \omega_L \simeq 2q^2/M \quad \text{as } \nu \to \infty \quad (t \text{ fixed}) \,,$$

which follows from (1.4), (1.5), and (1.19).

We find limits for $|B(\nu,t)|$ for fixed $t \leq 0$ by using (2.33). As $\nu \to \infty$, $\mu \to 1$ because $(-t) = 2q^2(1-\mu)$. Also

$$(1-\mu)P'_{l+1}(\mu) \to \frac{(-t)}{2q^2}\,\tfrac{1}{2}\,l(l+1) \leqslant \frac{(-t)}{4q^2}\,L(L+1)$$
$$\simeq -(t/4)R^2$$

Hence, as $\nu \to \infty$ the term $(l+1)P_{l+1}(\mu)$ predominates on the right of (2.33), and by (2.32)

$$\frac{1}{8\pi}\,|B(\nu,t)| \leqslant \frac{1}{2q}\,\frac{2}{q}\sum_{l=0}^{L}(l+1) \simeq \frac{1}{2q^2}\,L^2 = \tfrac{1}{2}\,R^2 \,.$$

Thus, for fixed $t \leq 0$

$$|B(\nu,t)| < K' \quad \text{as } \nu \to \infty \,, \tag{2.35}$$

where K' is a constant.

Now we examine the consequences for the dispersion relations (1.16) and (1.17). First consider $A^{(+)}$. If $\operatorname{Im} A^{(+)}(\nu,t) \backsim \nu$ as $\nu \to \infty$, the dispersion integral does not converge, and we require one subtraction giving

$$\operatorname{Re} A^{(+)}(\nu,t) = \operatorname{Re} A^{(+)}(\nu_0,t)$$
$$+ \frac{2}{\pi}\,(\nu^2 - \nu_0^2)P\int_{\mu+t/4M}^{\infty} d\nu'\,\frac{\nu' \operatorname{Im} A^{(+)}(\nu',t)}{(\nu'^2-\nu^2)(\nu'^2-\nu_0^2)} \,, \tag{2.36}$$

where ν_0 is a real constant. The dispersion integral now converges, and the second term on the right of (2.36) cannot increase as fast as ν^2 when $\nu \to \infty$. We examine whether an additive polynomial is required. Because $A^{(+)}(\nu,t)$ is an even function of ν [by (1.13)], such a polynomial would contain even powers of ν only. Since $\operatorname{Re} A^{(+)}(\nu,t)/\nu^2 \to 0$ as $\nu \to \infty$, the constant $\operatorname{Re} A^{(+)}(\nu_0,t)$ on the right of (2.36) is the only term required. We notice that the value of $\operatorname{Re} A^{(+)}(\nu_0,t)$ must be known before we can make use of the $A^{(+)}$ dispersion relation.

The $B^{(+)}$ relation is satisfactory as it stands in (1.17). Because $B^{(+)}(\nu,t)$ is bounded as $\nu \to \infty$, the last term on the right of (1.17) converges; also by theorem A of Sec. 2(ii) it cannot increase as fast as ν when $\nu \to \infty$. Any additive polynomial here has to be an odd function of ν, so even the lowest term $b_0\nu$ cannot occur.

(vii) Subtractions for the $A^{(-)}$ and $B^{(-)}$ Dispersion Relations[52]

Next consider the $A^{(-)}$ relation. Our considerations above show that $|A^{(-)}(\nu,t)|/\nu$ is bounded as $\nu \to \infty$. Therefore, one subtraction may be necessary in (1.16). This gives

$$\frac{1}{\nu}\operatorname{Re} A^{(-)}(\nu,t) = \frac{1}{\nu_0}\operatorname{Re} A^{(-)}(\nu_0,t) + \frac{2}{\pi}\,(\nu^2-\nu_0^2)P$$
$$\times \int_{\mu+t/4M}^{\infty} d\nu'\,\frac{\operatorname{Im} A^{(-)}(\nu',t)}{(\nu'^2-\nu^2)(\nu'^2-\nu_0^2)} \tag{2.37}$$

where ν_0 is the subtraction position and t is fixed. The integral in (2.37) converges, and by theorem A of Sec. 2(ii) the last term on the right of (2.37) certainly cannot increase as fast as ν^2 when $\nu \to \infty$. Since the additive polynomial in (2.37) must be an even function of ν, only the constant term can occur. This is in fact $\operatorname{Re} A^{(-)}(\nu_0,t)/\nu_0$.

Having established the dispersion relation (2.37), we now examine some of its consequences. By (2.34) $A^{(-)}(\nu,t)/\nu$ is bounded as $\nu \to \infty$. Suppose that $\operatorname{Im} A^{(-)}(\nu,t)/\nu$ tends to a limit $A^{(-)}(t)$ as $\nu \to \infty$, and suppose further that, as $\nu \to \infty$ $\operatorname{Im} A^{(-)}(\nu,t)/\nu$ obeys a condition like Eq. (2.10) so that theorem C of Sec. 2(ii) applies to the integral in (2.37). Substituting $x = \nu^2$, $y = \nu'^2$, $f(y) = \operatorname{Im} A^{(-)}(\nu',t)/\nu'^3$, we see that the last term on the right of (2.37) behaves like $(2/\pi)\,A^{(-)}(t)\ln\nu$ as $\nu \to \infty$. Since $\operatorname{Re} A^{(-)}(\nu,t)/\nu$ is bounded, this is impossible, and we must have $A^{(-)}(t) = 0$. Now, under the same conditions, the integral $\int^{\infty} d\nu' \operatorname{Im} A^{(-)}(\nu',t)/\nu'^2$ converges, and we can write down an unsubtracted dispersion relation [cf. (1.16)]

$$\frac{1}{\nu}\operatorname{Re} A^{(-)}(\nu,t) = a^{(-)}(t) + \frac{2}{\pi}\int_{\mu+t/4M}^{\infty} d\nu'\,\frac{\operatorname{Im} A^{(-)}(\nu',t)}{\nu'^2-\nu^2} \,, \tag{2.38}$$

where $a^{(-)}(t)$ is an arbitrary constant to be determined. [We shall see below in Sec. 2(ix) that $a^{(-)}(t) = 0$.]

The difficulty about this argument is that although $\operatorname{Im} A^{(-)}(\nu',t)/\nu'$ is bounded as $\nu' \to \infty$, it need not tend to a limit (or if it does, it need not do so sufficiently quickly). We therefore look for alternative justification for the relation (2.38). This comes either from Pomeranchuk's argument[31] on charge-exchange scattering, or the Regge pole argument, both of which were discussed in Sec. 2(iii) above. Pomeranchuk's argument implies that $|A^{(-)}(\nu,t)|/|A^{(+)}(\nu,t)|$

[52] This was first discussed by A. C. Finn (cf. reference 50).

and $|B^{(-)}(\nu,t)|/|B^{(+)}(\nu,t)|$ tend to zero steadily as ω_L increases beyond ω_0 (which is a few BeV), for small $t \leq 0$. The Regge pole argument suggests that these ratios fall off like $\nu^{-[1-\alpha_\rho(t)]}$, where $0 < \alpha_\rho(t) < 1$, and for small $t(t \leqslant 0)$, $\alpha_\rho(t)$ is not much different from 0.5. In either case we have reasonably strong support for the convergence of the integral in (2.38). We therefore assume that the unsubtracted relation (2.38) is valid, and we shall use it below for numerical calculations.

The situation for $B^{(-)}(\nu,t)$ is much the same as the $A^{(-)}(\nu,t)$ case. We infer by the same general arguments that Im $B^{(-)}(\nu,t) \to 0$ as $\nu \to \infty$, and that we can use the unsubtracted dispersion relation

$$\text{Im } B^{(-)}(\nu,t) = b^{(-)}(t) + \frac{G_r^2 \nu_B}{M(\nu_B^2 - \nu^2)} + \frac{2}{\pi} P \int_{\mu + t/4M}^{\infty} d\nu' \frac{\nu' \text{ Im } B^{(-)}(\nu',t)}{\nu'^2 - \nu^2} . \tag{2.39}$$

Here $b^{(-)}(t)$ is an arbitrary constant to be determined [we shall show in Sec. 2(ix) that $b^{(-)}(t) = 0$].

It should be emphasized that in view of the importance of the dispersion relations (2.38) and (2.39) (and for other general reasons) it would be valuable to check the assumptions which we have made about the rate of decrease of $A^{(-)}(\nu,t)$ and $B^{(-)}(\nu,t)$ as $\nu \to \infty$. It is very desirable to have an experimental investigation of the charge-exchange cross section $\pi^- + p \to \pi^0 + n$ over the diffraction peak region of angles at energies up to 20 BeV.

(viii) High-Energy Behavior of $A^{(+)}(\nu,t)$ and $B^{(+)}(\nu,t)$

In order to evaluate dispersion integrals for these functions it is necessary to know more about the high-energy behavior of Im $A^{(+)}(\nu,t)$ and Im $B^{(+)}(\nu,t)$ than is given by the bounds in (2.34) and (2.35).

First, we see from (2.32) and (2.33) that for large ν and fixed t $(t \leqslant 0)$, each term in the series for Im $B^{(+)}(\nu,t)$ is nonnegative.[53] We would therefore expect Im $B^{(+)}(\nu,t)$ to approach the bound (2.35), and we would not expect Im $B^{(+)}(\nu,t)$ to fall to zero as $\nu \to \infty$. The individual terms in the series (2.32) for Im $A^{(+)}(\nu,t)$ can be positive or negative, and we can make no simple statement about Im $A^{(+)}(\nu,t)$ except to note that it can be strongly affected by any appreciable difference between the amplitudes f_{l+} and the amplitudes f_{l-}, i.e., Im $A^{(+)}(\nu,t)$ will be strongly influenced by any force of spin-orbital type.

[53] This is because Im $f_{l\pm}^{(+)}(q) \geq 0$.

Consider the no-flip amplitude $f(\theta)$ [cf. (1.28)] near the forward direction. By (1.23) and (1.26), provided $E \gg (-t)/4M$ we have

$$f_1 + \cos\theta f_2 \simeq \frac{M}{4\pi W}\left[A(\nu,t) + \frac{EW}{M} B(\nu,t)\right] \tag{2.40}$$

where $E = (q^2 + M^2)^{\frac{1}{2}}$, $W = E + (q^2 + \mu^2)^{\frac{1}{2}}$, and q is the c.m. momentum. The helicity reversal amplitude [cf. Eq. (1.23a)] is given by

$$f_1 - f_2 = \frac{E}{4\pi W} A(\nu,t) + \frac{M}{4\pi}\left(1 - \frac{E}{W}\right) B(\nu,t) . \tag{2.41}$$

For ν large we have $E \simeq q$, $W \simeq 2q$, $\nu \simeq 2q^2/M$, and

$$f(\theta) = f_1 + \cos\theta f_2 \to \frac{1}{\pi}\left(\frac{M}{8\nu}\right)^{\frac{1}{2}} [A(\nu,t) + \nu B(\nu,t)]$$

$$f_1 - f_2 \to \frac{1}{8\pi}[A(\nu,t) + MB(\nu,t)] . \tag{2.42}$$

Now there appear to be two distinct types of high-energy behavior according to whether Im $A^{(+)}(\nu,t)$ does or does not reach the unitary limit given by (34).

The Ambiguity in Im $A^{(+)}$ as $\nu \to \infty$

Let Im $A^{(+)}(\nu,t) \sim C\nu$ and Im $B^{(+)}(\nu,t) \to C'$ as $\nu \to \infty$, where C and C' are constants, and $-t(\geqslant 0)$ is small. Then the helicity amplitudes $M_{++}(\nu,t)$ and $M_{-+}(\nu,t)$ given by (1.23a) have the asymptotic behavior

$$\left.\begin{aligned} &\text{Im } M_{++}(\nu,t) \backsim \frac{1}{\pi}(C + C')\left(\frac{M}{8}\right)^{\frac{1}{2}} \nu^{\frac{1}{2}} \\ &|\text{Im } M_{-+}(\nu,t)| \backsim \frac{C}{8\pi}\nu\left|\sin\frac{\theta}{2}\right| = \frac{C}{8\pi}\left(\frac{-t}{4M}\right)^{\frac{1}{2}} \nu^{\frac{1}{2}} \end{aligned}\right\} \text{as } \nu \to \infty \tag{2.43}$$

[by the optical theorem we require $(C + C') > 0$]. On the other hand if Im $A^{(+)}(\nu,t) \to 0$ and Im $B^{(+)}(\nu,t) \to C'$ as $\nu \to \infty$, we have[54]

$$\left.\begin{aligned} &\text{Im } M_{++}(\nu,t) \backsim \frac{C'}{\pi}\left(\frac{M}{8}\right)^{\frac{1}{2}} \nu^{\frac{1}{2}} \\ &|\text{Im } M_{-+}(\nu,t)|/\text{Im } M_{++}(\nu,t) \to 0 \end{aligned}\right\} \text{as } \nu \to \infty . \tag{2.44}$$

The behavior given by Eq. (2.44) is possible because there could be cancellations between the various partial wave amplitudes in Im $A^{(+)}(\nu,t)$ [Eq. (2.32)]. The Regge pole method does not resolve this ambi-

[54] The polarization of the recoil proton in the lab system for high-energy small-angle scattering is $(\nu p_2/M)$ Im $\{A^{(+)}(\nu,t)\, B(\nu,t)\}/|A(\nu,t) + \nu B(\nu,t)|^2$, where p_2 is the momentum of the recoiling proton. Because of Eqs. (2.48) this is expected to be undetectable even in the case Im $A^{(+)}(\nu,t) \sim C\nu$.

guity.[55] In his discussion[56] of high-energy elastic scattering Lovelace assumes that Im $A^{(+)}(\nu,t)$ is dominant for large ν, but it is clear that his analysis of the experimental differential cross sections could be carried out equally well by assuming that Im $B^{(+)}(\nu,t)$ is dominant.

Woolcock[3] in using the dispersion relations (1.17) and (2.36) assumed that the high-energy behavior of $A^{(+)}(\nu,t)$ and $B^{(+)}(\nu,t)$ is given by the partially opaque optical disk model. This model assumes $f_2(\theta) = 0$. [i.e., the spin-flip amplitude $g(\theta)$ is zero]. By (1.26) this gives

$$\frac{1}{4\pi}A^{(+)}(\nu,t) = \frac{W+M}{E+M}f(\theta)\,,$$
$$\frac{1}{4\pi}B^{(+)}(\nu,t) = \frac{1}{E+M}f(\theta)\,, \qquad (2.45)$$

where $f(\theta)$ is the no-flip amplitude as calculated from the optical model. This should give a reasonably good approximation for Im $B^{(+)}(\nu,t)$ in the forward direction and very close to it, for ν in the range 2 BeV–20 BeV. This is because Im $B^{(+)}(\nu,t)$ is the *sum* of partial wave absorptive parts, and the finer details, such as the differences between Im f_{l+} and Im f_{l-} should not matter much provided $(-t)$ is small. Also, the optical model gives a reasonably good fit to the experimental data very close to the forward direction. There are some corrections due to the narrowing of the diffraction peak with increasing ν which is expected on the Regge pole hypothesis.[57] In our account of the calculations, which is given in Secs. 4 and 5 below, these corrections are included where it is necessary. They are not large. (*Note added in proof.* If the narrowing does not occur, they can be ignored without appreciable error.) [Cf. Sec. 4(v) for an account of how the effect of the narrowing on the $(\partial/\partial t)\,A^{(-)}(\nu,t)$ and $(\partial/\partial t)\,B^{(-)}(\nu,t)$ dispersion relations is estimated.]

Clearly Eq. (2.45) may only give a rough estimate of Im $A^{(+)}(\nu,t)$ even at 2 BeV. On the other hand the integral in the subtracted dispersion relation (2.36) converges well at high energies and the effect of errors in Im $A^{(+)}(\nu,t)$ at, and above, 2 BeV is much reduced. There are other factors, such as the errors in the subtraction term [cf. Sec. 5(iii)(b)], and the Legendre series convergence problem [cf. Secs. 3(v), 5(iii), 5(iv)] which make the dispersion relations for $A^{(+)}(\nu,t)$ and its derivatives of much less value than the dispersion relations for the other scattering amplitudes.

(ix) Re $A^{(\pm)}(\nu,t)$ and Re $B^{(\pm)}(\nu,t)$ at High Energies

If, for high-energy forward scattering, we accept the optical model in the form given by Eq. (2.45) we get

$$\left.\begin{aligned}&(1/\nu)\,\mathrm{Re}\,A^{(+)}(\nu,0) \backsim \nu^{-1}\,\mathrm{Re}\,f^{(+)}(q,0)\\ &\mathrm{Re}\,B^{(+)}(\nu,0) \backsim \nu^{-\frac{1}{2}}\,\mathrm{Re}\,f^{(+)}(q\,0)\end{aligned}\right\}\text{as}\,\nu\to\infty\,, \qquad (2.46)$$

where Re $f^{(+)}(q,0)$ is the real part of the (c.m. system) forward-scattering amplitude. From Eqs. (2.15), (2.16) and the relation $\nu \simeq 2q^2/M$ we get

$$\left.\begin{aligned}&(1/\nu)\,\mathrm{Re}\,A^{(+)}(\nu,0)\to 0\\ &\mathrm{Re}\,B^{(+)}(\nu,0)\to 0\end{aligned}\right\}\quad\text{as}\,\nu\to\infty\,. \qquad (2.47)$$

The same result is given by the Regge pole treatment in the asymptotic high energy region.[58] The same result should also be true when t is small, as the variation is going from $A^{(+)}(\nu,0)$ to $A^{(+)}(\nu,t)$, $(t<0)$, should be smooth, and we are moving further away from the important strip of the double spectral region. Thus, we have

$$\left.\begin{aligned}&(1/\nu)\,\mathrm{Re}\,A^{(+)}(\nu,t)\to 0\\ &\mathrm{Re}\,B^{(+)}(\nu,t)\to 0\end{aligned}\right\}\text{as}\,\nu\to\infty\,\begin{pmatrix}\text{for small}\\ \text{negative}\,t\end{pmatrix}. \qquad (2.48)$$

The arguments given in Sec. 2(vii) above show that as $\nu\to\infty$ the $A^{(-)}(\nu,t)$ and $B^{(-)}(\nu,t)$ amplitudes tend to zero faster than the $A^{(+)}(\nu,t)$ and $B^{(+)}(\nu,t)$ amplitudes. This will also be true for the real parts of these amplitudes. Thus, (2.48) hold also for the $(-)$ amplitudes. [If we accept the Regge pole arguments $(1/\nu)$ Re $A^{(-)}(\nu,t)$ and Re $B^{(-)}(\nu,t)$ are directly seen[59] to obey (2.48).] It follows that the additive constants $a^{(-)}(t)$ and $b^{(-)}(t)$ in the unsubtracted dispersion relations (2.38) and (2.38) are to be equated to zero.

3. CONVERGENCE OF LEGENDRE POLYNOMIAL EXPANSIONS

In this chapter we examine the rate of convergence of the partial wave expansions of π–N scattering

[55] This method gives $|A^{(+)}(\nu,t)| \sim \nu^{\alpha(t)}$, $|B^{(+)}(\nu,t)| \sim \nu^{(\alpha(t)-1)}$ as $\nu\to\infty$ for $-t \geq 0$ and small. Here $\alpha(0)=1$ and $\alpha'(t)$ is positive and small. However, cancellations in $A^{(+)}(\nu,t)$ are not excluded without further assumptions, and $|A^{(+)}(\nu,t)|$ may not reach the unitary limit given by $\alpha(0)=1$. In the notation of S. C. Frautschi, M. Gell-Mann, and F. Zachariasen [Phys. Rev. **126**, 2204 (1962)] $A^{(+)}(\nu,t)$ does not reach the unitary limit if $b^{(1)}_{\pi\pi PNN}(0) = b^{(2)}_{\pi\pi PNN}(0)$, where $b^{(i)}_{\pi\pi PNN}(0)$ $(i=1,2)$ are the constants coupling the vacuum pole to the π-N system. In this case the spin-flip amplitude does not reach the unitary limit.

[56] C. Lovelace, Nuovo Cimento **25**, 730 (1962).

[57] This narrowing has been observed in N–N scattering in the region 2–20 BeV. See the report of G. Cocconi in *Proceedings of the International Conference on High-Energy Physics, Geneva, 1962* (CERN Scientific Information Service, Geneva, Switzerland, 1962).

[58] See the explicit forms for $A^{(+)}$ and $B^{(+)}$ given by S. C. Frautschi, M. Gell-Mann, and F. Zachariasen, Phys. Rev. **126**, 2204 (1962).

[59] Use footnote 55 and replace $\alpha(t)$ by $\alpha_\rho(t) \simeq \frac{1}{2}$ (for t small)

amplitudes. This is done by using either Lehmann's theorems or the Mandelstam representation. These give domains of convergence of the partial wave expansions, and enable us to estimate the rate of convergence. The results are applied to assess the errors in the practical evaluation of the absorptive parts of scattering amplitudes, and to find the limitations of the CGLN method for predicting partial wave amplitudes.

(i) Lehmann's Theorems

The basic theorems on the expansion of a scattering amplitude in a Legendre series are due to Lehmann.[60] He considers the amplitude $T(W, \cos\theta)$ for the scattering of pions on scalar nucleons. Here W, q, and θ are the total energy, pion momentum, and scattering angle in the c.m. system. The expansion can be written

$$T(W, \cos\theta) = \frac{1}{\pi^2}\frac{W}{q}\sum_{l=0}^{\infty}(2l+1)C_l(W)P_l(\cos\theta)\,, \tag{3.1}$$

where $C_l(W)$ are complex functions of W. It is convenient to consider the Legendre expansions for Re $T(W, \cos\theta)$ and Im $T(W, \cos\theta)$ which are obtained from (3.1) on replacing $C_l(W)$ on the right-hand side by Re $C_l(W)$ and Im $C_l(W)$, respectively. Now, we examine what happens to these Legendre expansions for Re $T(W, \cos\theta)$ and Im $T(W, \cos\theta)$ when W is kept in the physical range $W \geqslant (M+\mu)$, but $\cos\theta$ takes unphysical values such as $\cos\theta > 1$, or $\cos\theta < -1$, or becomes complex. From general field theoretic considerations plus microcausality[61] Lehmann proves the following two theorems:

Theorem 1. For physical values of W, Re $T(W, \cos\theta)$ is an analytic function of $\cos\theta$, which is regular inside an ellipse in the complex $\cos\theta$ plane centered on the origin with semi-axes along the real and imaginary axes having lengths x_0 and $(x_0^2-1)^{\frac{1}{2}}$, respectively. Here,

$$x_0(W) = \left[1 + \frac{8\mu^3(\mu+2M)}{q^2(W^2-(M-2\mu)^2)}\right]^{\frac{1}{2}}. \tag{3.2}$$

The Legendre expansion of Re $T(W, \cos\theta)$ converges uniformly inside this ellipse, and

$$\overline{\lim_{l\to\infty}}\,|\mathrm{Re}\,C_l(W)|^{1/l} \leqslant [x_0 + (x_0^2-1)^{\frac{1}{2}}]^{-1}\,. \tag{3.3}$$

(In Appendix B we give an analysis of the convergence of Legendre series which shows how relations of these forms can arise.)

Theorem 2. For physical values of W, Im $T(W, \cos\theta)$ is an analytic function of $\cos\theta$ which is regular inside a larger ellipse centered at the origin with semi-axes along the real and imaginary axes having lengths $(2x_0^2-1)$ and $2x_0(x_0^2-1)^{\frac{1}{2}}$, respectively. The Legendre expansion of Im $T(W, \cos\theta)$ converges uniformly inside this ellipse, and

$$\overline{\lim_{l\to\infty}}\,|\mathrm{Im}\,C_l(W)|^{1/l} \leqslant [x_0 + (x_0^2-1)^{\frac{1}{2}}]^{-2}\,. \tag{3.4}$$

An indication of the meaning of (3.3) and (3.4) can be seen as follows. Suppose that as $l\to\infty$ (for fixed W) Im $C_l(W) \simeq K\beta^l$, where K and β depend only on W. By (3.4)[62] $\beta \leqslant [x_0 + (x_0^2-1)^{\frac{1}{2}}]^{-2}$, and since $x_0 > 1$ we must have $\beta < 1$. Putting $\beta = 1-\eta$ where $\eta > 0$, it is easy to see that β^l tends to zero faster than $\exp(-l\eta)$ as $l\to\infty$.

Comparison with a Simple Model

It is interesting to compare (3.3) and (3.4) with the results of a simple model. Regard the nucleon as in distribution of matter in the form of a disk centered at the origin whose axis is along the pion beam. Let the density of matter at distance r from the axis be $\rho(r)$. The scattering amplitude for a pion of momentum q can be written in the form [cf. Eqs. (1.18) and (1.21)]

$$\frac{M}{4\pi W}T = f(\theta) = \sum_{l=0}^{\infty}(2l+1)f_l(q)P_l(\cos\theta)\,.$$

By the optical theorem

$$(2l+1)\,\mathrm{Im}\,f_l = \frac{q}{4\pi}\sigma_l\,,$$

where σ_l is the cross section for the lth partial wave. The impact parameter is $r = l/q$, and the lth partial component of the incident wave sweeps through an amount of matter approximately given by $2\pi r\,\Delta r\,\rho(r)$ where $\Delta r = 1/q$. For fixed q, large values of l give large values of r. It is reasonable to suppose that the outer part of the nucleon consists of one kind of matter (namely the pion cloud). We assume that the partial cross section σ_l cannot be greater than a fixed multiple of the amount of matter which the lth partial wave sweeps through. Therefore $\sigma_l \leqslant K'\,2\pi r\,\Delta r\,\rho(r)$, where K' is a constant. That is

$$\sigma_l \leqslant K'2\pi(l/q^2)\rho(l/q)\,.$$

It is reasonable to assume that the density of matter in the outer parts of the nucleon is given by $\rho(r) = \rho_0\exp(-r/R)$ where R is of the order of the

[60] H. Lehmann, Nuovo Cimento **10**, 579 (1958).

[61] Microcausality is the assumption that boson (fermion) field operates commute (anticommute) for space–time points whose separation is spacelike.

[62] Note that $\lim_{l\to\infty}|\mathrm{K}|^{1/l} = 1$.

Yukawa wavelength and ρ_0 is a constant. Thus

$$(0 \leqslant) \operatorname{Im} f_l(q) \leqslant (K''/q) \exp(-l/qR)$$

where K'' is a constant. Now for large l

$$(\operatorname{Im} f_l(q))^{1/l} \lesssim \exp(-1/qR), \tag{3.5}$$

Equation (3.5) is of the same general form as Eq. (3.4). Further they have in common that the right-hand sides increase monotonically towards unity as q increases. The actual dependence on q in the two cases is different, as might be expected from the very approximate nature of the model. From (3.5) we can also obtain a relation analogous to (3.3). By unitarity

$$(\operatorname{Re} f_l(q))^2 + (\operatorname{Im} f_l(q))^2 \leqslant 1/q \operatorname{Im} f_l(q)$$

so

$$|\operatorname{Re} f_l(q)| < q^{-\frac{1}{2}}(\operatorname{Im} f_l(q))^{\frac{1}{2}},$$

and by (3.5)

$$|\operatorname{Re} f_l(q)|^{1/l} \lesssim \exp(-1/2qR). \tag{3.6}$$

The similarity to (3.3) is obvious. It should be noted that the right-hand side of (3.6) is the square root of the right-hand side of (3.5). The same relation holds between (3.3) and (3.4).

(ii) Applications of Lehmann's Theorems

Lehmann's method can be applied to the scattering of pions by real (spin $\frac{1}{2}$) nucleons, and the real and imaginary parts of the scattering amplitudes are again found to be regular inside the ellipses of theorems 1 and 2 respectively. Further, the partial wave amplitudes f_{l+} and f_{l-} which were introduced in Eq. (1.28) obey the inequalities (3.3) and (3.4).

The first application[60] of theorem 2 is to the dispersion relations (1.16) and (1.17) for $A^{(\pm)}(\nu,t)$ and $B^{(\pm)}(\nu,t)$. In these relations the integration is over ν from $\mu + t/4M$ to ∞, and the invariant momentum transfer $t = -2q^2(1 - \cos\theta)$ is kept fixed. When $t < 0$ the bottom end of the range of integration lies outside the physical region. This can be seen as follows. For $q^2 \to \infty$, $\cos\theta \to 1$, and we have forward scattering. As q^2 decreases from ∞, $\cos\theta$ decreases, i.e., the scattering angle θ increases. When $q^2 = -t/4$ we have $\cos\theta = -1$. Values of q^2 in the range $0 \leqslant q^2 \leqslant -t/4$ correspond to $-\infty \leqslant \cos\theta \leqslant -1$, and are therefore outside the physical range. [$q^2 = 0$ gives $\nu = \mu + t/4M$ by (1.4).]

Continuation of Im $A^{(\pm)}(\nu,t)$ and Im $B^{(\pm)}(\nu,t)$ into the unphysical region $0 \leqslant q^2 \leqslant -t/4$ can be carried out by means of the Legendre expansion. For a typical amplitude we have, from (1),

$$\operatorname{Im} T(W, \cos\theta) = \frac{W}{\pi^2 q} \sum_{l=0}^{\infty} (2l+1) \operatorname{Im} C_l(W) P_l(\cos\theta). \tag{3.7}$$

Assuming that we know the phase shifts, the $C_l(W)$ are determined in the range $0 \leqslant q^2 \leqslant -t/4$. Now substitute $\cos\theta = 1 + t/2q^2$ in (3.7). Theorem 2 tells us that the series on the right of (3.7) converges provided

$$|1 + t/2q^2| \leqslant 2x_0^2 - 1. \tag{3.8}$$

It also tells us that, subject to (3.8), Eq. (3.7) gives the analytic continuation of Im $T(W, \cos\theta)$ from the physical region $|\cos\theta| \leqslant 1$, for any fixed q^2 in the range $0 \leqslant q^2 \leqslant -t/4$. This continuation gives the correct values of Im $A^{(\pm)}(\nu,t)$ and Im $B^{(\pm)}(\nu,t)$ for $0 \leqslant q^2 \leqslant -t/4$. From condition (3.8) it is easy to see that this continuation is possible for

$$(0 \leqslant) -t \leqslant \frac{32}{3} \frac{2M+\mu}{2M-\mu} \mu^2 \simeq 12\mu^2.$$

We saw in Sec. 1(v) that this is also the range of values of t for which the validity of the dispension relations (1.16) and (1.17) has been demonstrated mathematically.

Thus, theorem 2 completes the justification for using the dispersion relations (1.16) and (1.17) for small negative values of t. Below we report results obtained by using these relations and their derivatives with respect to t at $t = 0$.

(iii) Expansion of the Absorptive Parts of $A(\nu,t)$, $B(\nu,t)$ in Partial Waves

In evaluating the dispersion relations (1.16), (1.17) for Re $A(\nu,t=0)$, Re $B(\nu,t=0)$ and the derivative relations for

$$\frac{\partial}{\partial t} \operatorname{Re} A(\nu,t)_{|t=0}, \quad \frac{\partial}{\partial t} \operatorname{Re} B(\nu,t)|_{t=0}$$

etc., it is necessary to have good estimates of Im $A(\nu,0)$, Im $B(\nu,0)$, $(\partial/\partial t)$ Im $A(\nu,t)|_{t=0}$, $(\partial/\partial t)$ Im $B(\nu,t)|_{t=0}$ to insert in the dispersion integrals. Using Eqs. (2.31) and (1.30), these imaginary parts are expressed as infinite series of terms containing Im $f_{l\pm}$ where $f_{l\pm}(l = 0, 1, 2, \cdots)$ are the partial wave π–N amplitudes. In general it is to be expected that the integrals in these dispersion relations are dominated by one or several of the well-known π–N resonances, but we should examine the convergence of these partial wave expansions for Im $A(\nu,0)$ etc., in order to estimate the errors caused by ignoring partial waves with large l.

TABLE I. Values of $x_0(W)$ given by Eq. (3.2) for various pion energies. The last column gives $\rho(W)$ [Eq. (3.9)].

Lab energy ($\omega_L - \mu$)	Pion (c.m.) momentum ($\mu = 1$)	$s = W^2$	x_0	$2x_0^2 - 1$	$[x_0 + (x_0^2 - 1)^{\frac{1}{2}}]^{-1}$	$[x_0 + (x_0^2 - 1)^{\frac{1}{2}}]^{-2}$
$\ll$150 MeV	$\ll 1.4$	60–65	$1.75/q$	$6.14/q^2$	$0.29\,q$	$0.084q^2$
150 MeV	1.4	74	1.41	3.0	0.41	0.17
300 MeV	2.13	88	1.19	1.83	0.54	0.29
500 MeV	2.9	108	1.07	1.30	0.69	0.47
2 BeV	$\backsimeq M$	$5.6M^2$	1.011	1.02	0.90	0.81
$\gg$ 2 BeV	$\gg M$	$\gg 6M^2$	$1 + 2M/q^4$	$1 + 8M/q^4$	$1 - 2M^{\frac{1}{2}}/q^2$	$1 - 4M^{\frac{1}{2}}/q^2$

A rough measure of the rates of convergence is obtained as follows. We *assume* that the partial wave expansions for Im $A(\nu,0)$ and Im $B(\nu,0)$ will have approximately the same rate of convergence as the series $\sum_l[\rho(W)]^l$, and the partial wave expansions for $(\partial/\partial t)$ Im $A(\nu,t)|_{t=0}$ and $(\partial/\partial t)$ Im $B(\nu,t)|_{t=0}$ will have approximately the same rate of convergence as $\sum_l l(l+1)\,[\rho(W)]^l$ where

$$\rho(W) = [x_0 + (x_0^2 - 1)^{\frac{1}{2}}]^{-2}. \tag{3.9}$$

These estimates are based on using Eqs. (1.30), (2.31) and the experimental values of the small phase shifts at 310 MeV which are discussed in Sec. 3(v) below. Using the remainder of the series $\sum_l \rho^l$ for $l > L$, the fractional error in Im $A(\nu,0)$ and Im $B(\nu,0)$ due to ignoring partial waves with $l > L$ is ρ^{L+1}. Similarly using the series $\sum_l l(l+1)\rho^l$ the fractional error in $(\partial/\partial t)$ Im $A(\nu,t)|_{t=0}$ and $(\partial/\partial t)$ Im $B(\nu,t)|_{t=0}$ is estimated to be[63] $\rho^L[1 + \frac{1}{2}\,L(1-\rho)(3-\rho) + \frac{1}{2}\,L^2(1-\rho)^2]$.

In Sec. 3(iv) it will be seen that the values of $\rho(W)$ given by theorem 2 for Im A and Im B in the range 250 MeV–1 BeV (Table I) are almost the same as the values given by the Mandelstam representation (Table II). We shall therefore take over the arguments of this paragraph without change to the case of the Mandelstam representation. These estimates give the error in that part of Im $A(\nu,0)$ etc. which is not due to a dominant resonant amplitude. For example, at an energy for which the (3/2, 3/2) amplitude makes a large contribution to Im $A(\nu,0)$, the actual fractional error due to ignoring $f_{l\pm}$ for $l > L$ will be much less than ρ^{L+1}. This reduction in the error is easy to estimate in any particular case.

These formulas can be used with the help of Table I where x_0, $\rho(W)$ and various related quantities are given.

In evaluating the dispersion integrals in (1.16) and (1.17) and their derivative relations, partial waves with $l > 2$ have been ignored, except in the region of the $F_{\frac{5}{2}}$ resonance, where amplitudes with $l > 3$ have been ignored. The errors in Im $A(\nu,0)$ and Im $B(\nu,0)$ estimated by the above formula with $L = 2$ are 0.5% at 150 MeV, 3% at 300 MeV, 12% at 500 MeV. Taking $L = 3$ at 900 MeV gives 25% error. Similar estimates for $(\partial/\partial t)$ Im $A(\nu,t)|_{t=0}$ and $(\partial/\partial t)$ Im $B(\nu,t)|_{t=0}$ give relative errors of 14%, 30%, 60%, and 75% at 150, 300, 500, and 900 MeV, respectively.

In Fig. 8 following we show the values of $(\partial/\partial t)$ Im $A(\nu,t)|_{t=0}$ and $(\partial/\partial t)$ Im $B(\nu,t)|_{t=0}$ determined from the known phase shifts and cross sections. Clearly, below 1 BeV the predominant contributions are due to the resonances at 180 MeV, 600 MeV, and 900 MeV. The above estimated errors being percentages of the nonresonant parts, or background turn out to be unimportant except for energies above 1 BeV. For these higher energies other methods are used to estimate Im $A(\nu,0)$, Im $B(\nu,0)$ etc. [cf. Secs. 4(i) and 4(v) below].

(iv) Application of the Mandelstam Representation

According to the Mandelstam representation the amplitude $B^{(+)}(s,t)$ is of the form

$$\begin{aligned} B^{(+)}(s,t) = &-\frac{G_r^2}{s-M^2} + \frac{G_r^2}{u-M^2} \\ &+ \frac{1}{\pi^2}\int_{(M+\mu)^2}^{\infty} du' \int_{4\mu^2}^{\infty} dt' \frac{\rho_{12}(u',t')}{(u'-u)(t'-t)} \\ &+ \frac{1}{\pi^2}\int_{4\mu^2}^{\infty} dt' \int_{(M+\mu)^2}^{\infty} ds' \frac{\rho_{23}(t',s')}{(t'-t)(s'-s)} \\ &+ \frac{1}{\pi^2}\int_{(M+\mu)^2}^{\infty} ds' \int_{(M+\mu)^2}^{\infty} du' \frac{\rho_{31}(s',u')}{(s'-s)(u'-u)}, \end{aligned} \tag{3.10}$$

where the variables s, t, u were introduced in Eqs. (1.4)–(1.6a). G_r^2 is the rationalized π–N coupling constant and ρ_{12}, ρ_{23}, ρ_{31} are real weight (or spectral) functions. $B^{(-)}(s,t)$ obeys an equation similar to (3.10), while $A^{(\pm)}(s,t)$ obey relations like (3.10), except that the terms in G_r^2 (the Born terms) are missing.

For fixed energy, s (and q^2) are fixed, and u and t

[63] Errors in $(\partial^2/\partial t^2)$ Im $A(\nu,t)|_{t=0}$ etc. can be estimated in the same way.

are linear in cos θ. Equation (3.10) can be used to find the values of cos θ for which $B^{(+)}(s,t)$ becomes singular when cos θ is extended beyond the physical range $-1 \leqslant \cos\ \theta \leqslant 1$. Suppose that for given $s \geqslant (M+\mu)^2$ the smallest value of $|\cos\theta|$ for which (3.10) becomes singular is $y_0(s)$. Then $B^{(+)}(s,t)$ is a regular function of cos θ inside the circle $|\cos\theta| = y_0(s)$ in the complex cos θ plane. Within this circle $B^{(+)}(s,t)$ can be expanded in a power series in cos θ,

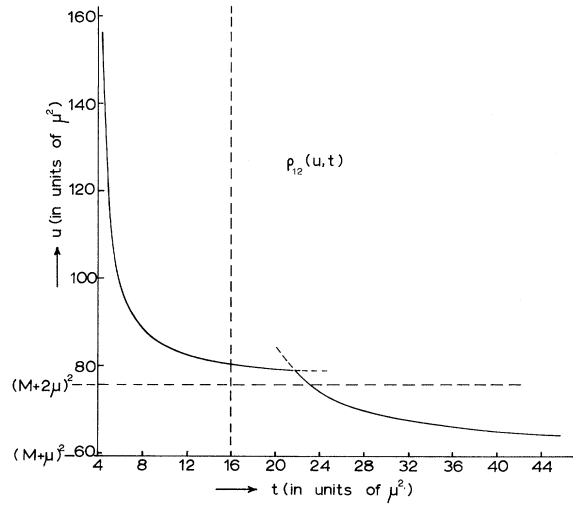

FIG. 3. The region to the right of the curve shows where the spectral function $\rho_{12}(u,t)$ is nonzero.

and this series can be rearranged into a series of Legendre polynomials $P_l(\cos\theta)$. We must find where the latter series converges.

In Appendix B it is shown that the Legendre series for $B^{(+)}(s,t)$ converges within an ellipse in the complex cos θ plane which has focuses at cos $\theta = \pm 1$ and semi-axes of lengths $y_0(s)$ $\{[y_0(s)]^2 - 1\}^{\frac{1}{2}}$ along the real and imaginary axes, respectively. The asymptotic behavior of the coefficients of the Legendre series is obtained on replacing Eq. (9) by $\rho(W) = \{y_0(s) + ([y_0(s)]^2 - 1)^{\frac{1}{2}}\}^{-1}$. It will be seen that there is one value of $y_0(s)$ for Re $B^{(+)}(s,t)$ and a larger value of $y_0(s)$ for Im $B^{(+)}(s,t)$. The real parts of all the amplitudes $A^{(\pm)}$, $B^{(\pm)}$ have the same $y_0(s)$, and the imaginary parts of all four amplitudes have the same (larger) value of $y_0(s)$. In general, the values of $y_0(s)$ exceed the corresponding quantities x_0, $2x_0^2 - 1$ given by theorems 1 and 2, respectively. This can be understood since the validity of the representation (3.10) is a stronger assumption than the concepts used in Lehmann's proof.

The fact that $y_0(s)$ is in general greater than x_0 [or $(2x_0^2 - 1)$] is expected to improve the convergence of the Legendre series. The estimated errors in the nonresonant part of any amplitude due to ignoring partial waves having $l > L$, are obtained by the method of the preceding section if we use for ρ the value given by Eq. (3.9) when x_0 is replaced by the appropriate value of $y_0(s)$. We now determine the values of $y_0(s)$ for the real and the imaginary parts of the amplitudes.

Values of $y_0(s)$ for the Real Parts of the Amplitudes

For physical π–N scattering the first three terms on the right of (3.10) contribute only to Re $B^{(+)}$. The nearest singularities of Re $B^{(+)}$ come from the Born pole $u = M^2$ and the cut $t \geqslant 4\mu^2$. The nearest singularities of Im $B^{(+)}$ come from the cuts $u \geqslant (M+\mu)^2$ and $t \geqslant 4\mu^2$.

The Born pole gives a singularity at

$$\cos\theta = 1 + (M^2 + 2\mu^2 - s)/2q^2 . \quad (3.11)$$

For $q/\mu \ll 1$ this gives $\cos\theta \simeq -(M/2\mu) - (M\mu/q^2)$. As q^2 increases, cos θ increases, and cos $\theta \to -1$ as $q^2 \to \infty$. Values of cos θ for various energies are given in column 4 of Table II.

The singularities due to the cuts are not found quite so easily. This is because the spectral functions

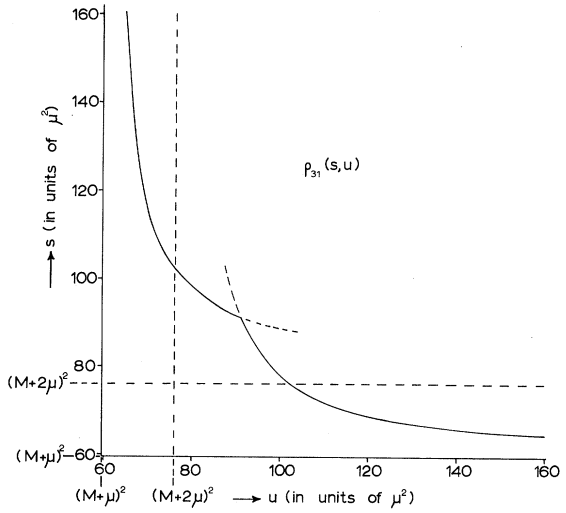

FIG. 4. The region to the right of the curve shows where the spectral function $\rho_{31}(s,u)$ is nonzero.

ρ_{ij} appearing in (3.10) in general vanish over a region adjacent to the thresholds $t' = 4\mu^2$, $s' = (M+\mu)^2$ $u' = (M+\mu)^2$. The region where $\rho_{12}(u',t')$ is nonzero is shown in Fig. 3. To obtain the region where $\rho_{23}(t',s')$ is nonzero we simply replace u' by s'. Figure 4 shows where $\rho_{31}(s',u')$ is nonzero.[64]

[64] The boundaries of these regions are given by W. R. Frazer and J. R. Fulco, Phys. Rev. **117**, 1063 (1960), Eqs. (4.10a), (4.10b), and (4.11).

TABLE II. Columns 3–6 give the values of $\cos\theta$ for which the real and the imaginary parts of the scattering amplitudes meet their first singularities in the $\cos\theta$ plane. In each case the $\pi-\pi$ term (i.e., the term in t) gives the nearest singularity and determines $y_0(s)$.

Lab energy ($\omega_L-\mu$)	Pion (c.m.) momentum ($\mu=1$)	Nearest singularities in $\cos\theta$ for the real parts.		Nearest singularities in $\cos\theta$ for the imaginary parts.	
		$\pi-\pi$ term [$y_0(s)$]	Crossed term	$\pi-\pi$ term [$y_0(s)$]	Crossed term
$\ll$150 MeV	$\ll$1.4	$1+2/q^2$	$-M/q^2$	$8/q^4$	$8M^2/[q^4(2M+1)]$
150 MeV	1.4	2.0	−6.25	7	−21.0
300 MeV	2.13	1.45	−3.4	1.9	− 8.6
500 MeV	2.9	1.24	−3.0	1.31	− 4.3
2 BeV	$\backsimeq M$	1.044	−1.43	1.048	− 1.64
$\gg$ 2 BeV	$\gg M$	$1+2/q^2$	$-1-M^2/2q^2$	$1+2/q^2$	$-1-(M+1)^2/2q^2$

Now consider the third term on the right of (3.10). Both terms in the denominator can give singularities. The term in the denominator containing u can only give singularities for $u \geqslant (M+\mu)^2$, and these correspond to values of $\cos\theta$ more negative than those given by Eq. (3.11), so they do not affect the value of $y_0(s)$. Using Fig. 3 and letting $u\to\infty$ we see that the term in t gives a singularity for $t=4\mu^2$, that is

$$\cos\theta = 1+2\mu^2/q^2 . \tag{3.12}$$

Column 3 of Table II gives these values of $\cos\theta$ for various energies. Clearly $\cos\theta\to+1$ as $q^2\to\infty$.

Values of $y_0(s)$ for the Imaginary Parts of the Amplitudes

From (3.10) we have for $s\geqslant(M+\mu)^2$

$$\operatorname{Im}B^{(+)}(s,t) = \frac{1}{\pi}\int_{4\mu^2}^{\infty}dt'\,\frac{\rho_{23}(t',s)}{t'-t} + \frac{1}{\pi}\int_{(M+\mu)^2}^{\infty}du'\,\frac{\rho_{31}(s,u')}{u'-u} . \tag{3.13}$$

For given s the nearest singularity is found by using Figs. 3 and 4 to determine the smallest values of t' and u' for which $\rho_{23}(t',s')$ and $\rho_{31}(s',u')$, respectively, are nonzero. Since these values of t' and u' are greater than $4\mu^2$ and $(M+\mu)^2$, respectively, the singularities in the imaginary parts are further away from the physical region $-1\leq\cos\theta\leq1$ than are the singularities in the real parts.

The data in columns 5 and 6 of Table II give the values of $y_0(s)$ for various energies. For $q/\mu\ll1$ the first term on the right of (3.13) gives a singularity at $\cos\theta\simeq 8\mu^4/q^4$, and the second term gives a singularity at $\cos\theta\simeq -8M^2\mu^2/[q^4\times(1+2M/\mu)]$. For q^2 very large the first term gives $\cos\theta=1+2\mu^2/q^2$, and the second gives $\cos\theta=-1-(M+\mu)^2/2q^2$ for the nearest singularities.

Comparing column 3 of Table II with the values of x_0 in Table I we see that the convergence of the series for the real parts of the amplitudes is appreciably better than would be inferred from Lehmann's theorem. The same is true for the imaginary parts of the amplitudes except for the range of energies 250 MeV to 1 BeV. Comparing column 5 of Table II and Table I, it is seen that $y_0(s)$ is very little greater than $(2x_0^2-1)$ at these energies. Thus the Mandelstam representation does not appreciably improve the convergence of the partial wave expansions for Im $A^{(\pm)}$ and Im $B^{(\pm)}$ in this energy range.

Assuming that the ellipse of convergence of the Legendre series is given by the Mandelstam representation, we can go somewhat further. Since the π–π term (i.e., the term in t) gives a singularity much closer to the physical region than the crossed term (i.e., the term in u), the rate at which the phase shifts fall off with increasing angular momentum is governed primarily by the π–π interactions. Information about these interactions is known directly from experiments,[65] and it appears that the $T=1$ π–π interaction, which is related to the $A^{(-)}$ and $B^{(-)}$ amplitudes (but not to $A^{(+)}$ and $B^{(+)}$), is only appreciable for $t\gtrsim16\mu^2$ (and possibly only for $t\gtrsim25\mu^2$).

For example if we ignore the π–π effects in the $T=1$ case for $t<15\mu^2$, the value of $y_0(s)$ for Im $A^{(-)}$ and Im $B^{(-)}$ is appreciably increased in the energy region 250 MeV to 500 MeV. At 300 MeV and 500 MeV we get $y_0(s)=2.7$ and 1.9, respectively, instead of the values 1.9 and 1.3 given in column 5 of Table II. This reduces the parameter $\rho=[y_0+(y_0^2-1)^{\frac{1}{2}}]^{-1}$ to about 2/3 of the previous values over this energy range, and appreciably improves the

[65] See, for example, A. R. Irwin, R. H. March, W. D. Walker, and E. West, *Proceedings of the International Conference on Elementary Particles, Aix-en-Provence, 1961* (C.E.N. Saclay, France, 1961), Vol. I, p. 249 for details of the experimental results. Also the review by G. Puppi, in *Proceedings of the International Conference on High-Energy Physics, Geneva, 1962*, edited by J. Prentke and A. Taylor (CERN Scientific Information Service, Geneva, Switzerland, 1962).

rate of convergence of Im $A^{(-)}$ and Im $B^{(-)}$. No such improvement is possible in the case of Im $A^{(+)}$ and Im $B^{(+)}$.

It should be emphasized that we aim to use dispersion relations like (1.16) and (1.17) in situations where the dispersion integrals are predominantly due to the contributions to Im $A(\nu,t)$ etc. from the known π–N resonances. The analysis just given is merely a way of estimating the errors due to neglecting higher partial waves: it does not include errors in the resonant amplitudes themselves.

(v) Deducing the Partial Waves; Validity of the CGLN Method

Having evaluated the dispersion relations for Re $A(\nu,t)$ Re $B(\nu,t)$ etc. we will wish to find the π–N partial wave amplitudes. This is done as follows.[2] Writing $\Delta^2 = -t/4 = \frac{1}{2}q^2(1-\cos\theta)$, Eqs. (1.30) give

$$\begin{aligned}
f_1 &= f_{0+} + 3\left(1-\frac{2\Delta^2}{q^2}\right)f_{1+} - f_{2-} \\
&\quad + \tfrac{1}{2}\left\{15\left(1-\frac{2\Delta^2}{q^2}\right)^2 - 3\right\}f_{2+} + \cdots, \\
f_2 &= (f_{1-} - f_{1+}) + 3\left(1-\frac{2\Delta^2}{q^2}\right)(f_{2-} - f_{2+}) + \cdots, \\
f_1' &= -\frac{6}{q^2}f_{1+} - \frac{30}{q^2}\left(1-\frac{2\Delta^2}{q^2}\right)f_{2+} + \cdots, \\
f_2' &= -\frac{6}{q^2}(f_{2-} - f_{2+}) + \cdots, \\
f_1'' &= \frac{60}{q^4}f_{2+} + \cdots,
\end{aligned} \tag{3.14}$$

where F and higher partial waves are ignored and $'$ denotes differentiation with respect to Δ^2. Solving (3.14) gives

$$\begin{aligned}
f_{0+} &= f_1(0) + \tfrac{1}{2}q^2f_1'(0) - \tfrac{1}{6}q^2f_2'(0) + \tfrac{1}{6}q^4f_1''(0) + \cdots, \\
f_{1-} &= f_2(0) - \tfrac{1}{6}q^2f_1'(0) + \tfrac{1}{2}q^2f_2'(0) - \tfrac{1}{12}q^4f_1''(0) \\
&\quad + \cdots, \\
f_{1+} &= -\tfrac{1}{6}q^2f_1'(0) - \tfrac{1}{12}q^4f_1''(0) + \cdots, \\
f_{2-} &= -\tfrac{1}{6}q^2f_2'(0) + \tfrac{1}{60}q^4f_1''(0) + \cdots, \\
f_{2+} &= \tfrac{1}{60}q^4f_1''(0) + \cdots.
\end{aligned} \tag{3.15}$$

Here, (0) indicates evaluation in the forward direction, $\Delta^2 = 0$.

It is necessary to assess how well the series in (3.15) converge. For this purpose, consider a typical partial wave $g_l(s)$. It is given by an expression like

$$g_l(s) = \int_{-1}^{1} dx T(s,x)P_l(x), \tag{3.16}$$

where $T(s,x)$ is some scattering amplitude (like A,B) and $x = \cos\theta$. Equations (3.15) are obtained essentially by substituting in (3.16) the expansion

$$\begin{aligned}
T(s,x) &= T(s,x=1) + (x-1)\left.\frac{\partial T}{\partial x}\right|_{x=1} \\
&\quad + \tfrac{1}{2}(x-1)^2\left.\frac{\partial^2 T}{\partial x^2}\right|_{x=1} + \cdots \\
&= T(s,\Delta^2=0) + \Delta^2\left.\frac{\partial T}{\partial \Delta^2}\right|_{\Delta^2=0} \\
&\quad + \frac{1}{2!}(\Delta^2)^2\left.\frac{\partial^2 T}{\partial(\Delta^2)^2}\right|_{\Delta^2=0} + \cdots.
\end{aligned} \tag{3.17}$$

This Maclaurin series must converge for the range of values of x used in (3.16), i.e., it must converge for $x - 1 = -2$. Thus the circle of convergence around $x = 1$ must have a radius of at least 2. This requires that the domain of regularity of $T(s,x)$ should extend to $x - 1 = +2$, i.e., $x = 3$ (or $y_0(s) = 3$).

We wish to use (3.16) for the real parts of the amplitudes, so Re $g_l(s)$ and Re $T(s,x)$ appear in (3.16). Equation (3.12) shows that by the Mandelstam representation the radius of the circle of convergence of the cosine series is $y_0 = 3$ for $q^2 = 1$, i.e., 80-MeV lab energy. Lehmann's results (theorem 1) give $x_0 = 3$ at 30 MeV. Thus assuming the Mandelstam representation, the method of extracting the partial wave amplitudes given in Eq. (3.15) should be satisfactory at least up to 80 MeV.

If the radius of convergence $\rho'(\rho' = y_0 - 1$ or $x_0 - 1)$ of Re $T(s,x)$ about the point $x = 1$ is at least 2 then the series for Re $g_l(s)$ which is obtained by substituting (3.17) in (3.16) will converge. Similarly the series in (3.15) will converge if the corresponding ρ' exceeds 2. It is also necessary to estimate the rate of convergence of this series, and for this purpose we again use (3.16) and (3.17). It is easy to show that if l is small (and fixed) and n is large then

$$I \equiv \int_{-1}^{1}(1-x)^n P_l(x)dx \simeq \frac{(-1)^l}{n}2^{n+1}. \tag{3.18}$$

Also by Cauchy's test applied to (3.17) we estimate (very roughly) that $(1/n!)(\partial^n T/\partial x^n)|_{x=1} \backsim (\rho')^{-n}$ when n is large. The rate of (absolute) convergence of the series obtained by substituting (3.17) in (3.16) is therefore similar to that of the series $\sum_n (2/\rho')^n$. From this we expect that the series in (3.15) will only converge well if ρ' is appreciably greater than 2. This behavior can also be seen in another way. At low energies $f_{l\pm} = a_{l\pm}q^{2l}$, where $a_\pm$ are roughly constant $(l > 1)$. Substituting in (3.14) and putting $\Delta^2 = 0$, it is obvious that the convergence of the series improves

rapidly as q^2 decreases.[66] The same applies to the series (3.15).

Examples of the Rate of Convergence of Eqs. (3.14) and (3.15)

In fact there is reason to believe that we have somewhat overstated the difficulty of using (3.15). We shall examine some numerical values at 80 MeV ($q^2 = 1$). We take an unfavorable case provided by a set of experimental phase shifts which give comparatively large D- and F-wave phase shifts at 310 MeV ($q^2 = 4.7$).[67] At this energy analysis of experiments suggests that some D-wave phase shifts *could* be as large as 12° and some F-wave phase shifts could be 2°.

From this we estimate $|f_{2\pm}| \simeq 0.006$ and $|f_{3\pm}| \simeq 0.0002$ at 80 MeV. For comparison we note that the smallest P-wave scattering length is of the order of 0.03. Thus at 80 MeV, or even at 120 MeV ($q^2 = 1.57$), the D-wave terms in the first three series in (3.14) are at the most no larger than the small P-wave terms. Further, using (1.30) we can find the F-wave contributions to (3.14). These extra terms are of order 0.002, 0.002, 0.02, 0.012, 0.10 in the Eqs. (3.14) for $f_1, f_2, f_1', f_2', f_1''$, respectively. In each case, except the equation for f_1'', these F-wave contributions are small compared with the small P-wave or D-wave terms. In the case of f_1'', the F-wave term gives a 30% contribution. Also, the situation is not appreciably worse at 100 MeV ($q^2 = 1.27$) than at 80 MeV.

These numerical values suggest that the series (3.14) and (3.15) are asymptotic approximations at energies somewhat above 80 MeV (say up to 120 MeV). This could be due to the fact that the series for $T(s,x)$ in (3.17) is only likely to be badly wrong for $-1 \leqslant x \leqslant 1 - \rho'$. Provided ρ' is not much less than 2 this should not be particularly important for the smaller[68] values of l. On the other hand the numerical values indicate that at 150 MeV ($q^2 = 2.0$) the series (3.14) may not even give a useful asymptotic approximation.

The $(-)$ Amplitudes

What has been said so far in this section applies to the $A^{(+)}$ and $B^{(+)}$ amplitudes. The $A^{(-)}$ and $B^{(-)}$ amplitudes are related to the $T = 1\,\pi + \pi \to N + \overline{N}$ channel. If, as we suggested in Sec. 3(iv) above, the $T = 1\,\pi - \pi$ effects can be ignored for $t \lesssim 15\mu^2$, instead of Eq. (3.12) we have

$$y_0(s) = 1 + 7.5/q^2 .$$

This gives a larger radius of convergence, and larger ρ' so $\rho' = 3.75$ at 150 MeV and $\rho' = 2$ at 260 MeV. Thus we expect that in the case of the $(-)$ charge combination the partial waves can be deduced accurately by the CGLN method up to 250 MeV, and tolerably accurately up to around 300 MeV. In practice this can be tested by estimating the D- (or F-) wave contributions to (14) and examining their relative importance. It will be seen in Sec. 5(v) below that the calculations in the $(-)$ case behave well up to 300 MeV.

(vi) The Subtraction Term in the $A^{(+)}$ Dispersion Relation

It has been suggested[69] that a difficulty arises in using the dispersion relation (2.36) for $A^{(+)}(\nu, \Delta^2)$ ($\Delta^2 \equiv -t/4$) in the CGLN analysis. A more detailed examination shows that this is not so.

We wish to evaluate the subtraction term $A^{(+)}(\nu_0, \Delta^2)$ at the threshold $q^2 = 0$ (i.e., $\nu_0 = \mu - \Delta^2/M$). For fixed $\Delta^2 > 0$ the physical region extends down to $q^2 = \Delta^2$ [cf. Sec. 3(ii)] and the segment $0 \leqslant q^2 \leqslant \Delta^2$ is unphysical. As was seen above, Lehmann's theorem 2 shows that for fixed $\Delta^2 > 0$, $\operatorname{Im} A^{(+)}(\nu, \Delta^2)$ can be continued analytically to the whole of the segment $0 \leqslant q^2 \leqslant \Delta^2$ provided $\Delta^2 \lesssim 3\mu^2$. However, theorem 1 does not allow us to continue $\operatorname{Re} A^{(+)}(\nu, \Delta^2)$ to the whole of $0 \leqslant q^2 \leqslant \Delta^2$ for fixed $\Delta^2 > 0$. On $0 \leqslant q^2 \leqslant \Delta^2$ we have $\cos\theta = 1 - 2\Delta^2/q^2$ and Eq. (3.12) shows that by the Mandelstam representation $\operatorname{Re} A^{(+)}(\nu, \Delta^2)$ can be continued for $|\cos\theta| \leqslant 1 + 2\mu^2/q^2$. Thus, the Mandelstam representation allows us to obtain $\operatorname{Re} A^{(+)}(\nu_0, \Delta^2)$ for all Δ^2, such that $|\Delta^2| \leqslant \mu^2$.

The situation is illustrated in Fig. 5 which shows the main features in the real (Δ^2, q^2) plane for $q^2 \ll \mu^2$. The Mandelstam representation allows us to evaluate the subtraction term $\operatorname{Re} A^{(+)}(\nu_0, \Delta^2)$ anywhere on the segment $-1 \leqslant \Delta^2 \leqslant 1$ of the line $q^2 = 0$. The expansion (3.17) can be made, and the radius of convergence ρ' of the power series in $(1 - x)$ is infinite for $q^2 = 0 (\rho' \simeq 2\mu^2/q^2)$.

However, we do not need to use the Mandelstam representation here. Theorem 1 allows us to continue $\operatorname{Re} A^{(+)}(\nu, \Delta^2)$ up to $|\cos\theta| \simeq 1.75(\mu/q)$ (of Table I), so the boundary of the region of continuation is $\Delta^2 \simeq 0.87q\mu$. This is shown in Fig. 5. Thus, by theorem 1, even for the backward direction, we can

[66] Notice that by Eq. (3.12) $(2/\rho') = 2/(y_0 - 1) = q^2$.

[67] J. H. Foote, O. Chamberlain, E. H. Rogers, and H. M. Steiner, Phys. Rev. 122, 959 (1961). We use here the phase shift set SPDF—II. The other sets given suggest a more rapid convergence of Eqs. (14) and (15). In Secs. 4 and 5 below, in the actual calculations, the phase shift set SPDF-I, which is considered more likely, is used.

[68] For moderate or large l, $P_l(x)$ varies rapidly towards $x = -1$, and the errors could be appreciable.

[69] A. C. Finn, Plays. Rev. 119, 1786 (1960).

find Re $A^{(+)}(\nu_0, \Delta^2)$. Further, the expansion (3.17) is quite satisfactory as $q^2 \to 0$, and the radius of convergence ρ' becomes infinite as $q^2 \to 0$ ($\rho' \simeq 1.75\mu/q$). Thus, the series (3.14) and (3.15) converge extremely well for q^2 small, and for $q^2 = 0$ only the first term remains in each of the series (3.14). This gives the very simple result that the appropriate scattering length gives the contribution of the subtraction term to the various partial wave amplitudes.

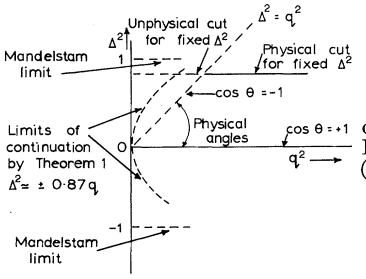

FIG. 5. The various continuation regions for Re $A^{(+)}(\nu,\Delta^2)$ in the real (Δ^2,q^2) plane.

(vii) Conclusions

For the (+) charge combination the Eqs. (3.15), which are essential in the CGLN method of deriving the small partial waves etc. are only expected to give reliable results up to about 100 MeV. This statement is based on the validity of the Mandelstam representation. Lehmann's method gives around 30 MeV as the upper energy limit. Inserting numerical (experimental) values of the higher angular momentum phase shifts in Eq. (3.14) confirms the deduction based on the Mandelstam representation.

For the (−) charge combination, if we assume in addition that the $T = 1$ π–π interaction is negligible for $t \lesssim 15\mu^2$, the CGLN method should work well up to about 250 MeV. The actual results in Sec. 5(v) below do confirm this.

Finally, we comment on a method which has been used by Hamilton *et al.*[70] to deduce the low-energy behavior of the $T = 0$ and $T = 1$ π–π interactions from low-energy π–N scattering. This method primarily depends on an accurate knowledge of the S-wave π–N phase shifts α_1 and α_3 up to about 120 MeV. The values of α_1 and α_3 which are used come partly from accurate experimental data, and partly from a semiphenomenological parameterization of this data.[71] This parametrization which is discussed in Sec. 4(ii) below can be justified by using certain forward dispersion relations, and it does not depend on the CGLN method.

Further, it has been shown[70] that P-wave π–N scattering in the region 0–100 MeV is reasonably consistent with the information on π–π interactions which is given by the S-wave π–N data. The P-wave data are partly based on the few accurate experimental results in this energy range and partly on the CGLN analysis as applied below. It has been shown above that the CGLN method should give accurate small P-wave π–N phase shifts up to about 100–120 MeV irrespective of any assumptions concerning the π–π interactions. The work on the π–π interactions[72] is therefore in no danger of being influenced by errors which are themselves caused by the π–π interactions.

4. THE PARAMETERS OF PION-NUCLEON PHYSICS

In this section it is shown that π–N dispersion relations for fixed momentum transfer can be used to give accurate information about the π–N coupling constant f^2, the S- and P-wave π–N scattering lengths and other parameters of low-energy pion physics. We also discuss the parametrization of the low-energy S-wave scattering. The general idea is to use dispersion relations in which the predominant contribution to the dispersion integrals comes from accurately known features of π–N scattering, such as the low- or moderate-energy resonances. Using the experimental data for these large contributions, we can get accurate values of the parameters. The errors in the values of the parameters found in this way depend partly on the experimental errors in the resonance data etc., and partly on the size of the small nonresonant terms which are either roughly estimated or ignored. We have to assess both of these errors.

It was first pointed out by Woolcock[73]: (i) that the B_+ relation [cf. Sec. 4(i)] gives a very good method of determining the coupling constant f^2; (ii) that the $C^{(\pm)}$ relations [cf. Sec. 4(iii)] can yield accurate information about the combinations $(2a_{33} + a_{31})$ and $(2a_{13} + a_{11})$ of the P-wave π–N scattering lengths $a_{2T,2J}$; and (iii) that the $B(\mu,0)$ relations [cf. Sec. 4(iv) below] can give accurate information about the combinations $(a_{33} - a_{31})$ and $(a_{13} - a_{11})$. Woolcock[73] also used the $f_1^{(-)\prime}(\mu,0)$ relation [cf. Sec. 4(v) below] to give information about $(a_{33} - a_{13})$. In the present article we shall allow for a larger error in the latter relation than that in Woolcock's original work.

[70] J. Hamilton, T. D. Spearman, and W. S. Woodcock, Ann. Phys. **17**, 1 (1962); J. Hamilton, P. Menotti, G. C. Oades, and L. L. J. Vick, Phys. Rev. **128**, 1881 (1962).

[71] J. Hamilton and W. S. Woolcock, Phys. Rev. **118**, 291 (1960).

[72] In the second paper in reference 70, $\pi - N$ data up to 200 MeV were used. However the deductions about the $\pi - \pi$ interactions were almost entirely dependent on the data for 0–100 MeV.

[73] W. S. Woolcock, Ph.D. thesis, University of Cambridge, 1961 (unpublished).

In this relation one term involves derivatives with respect to the momentum transfer and errors due to the nonresonant terms and other features will be larger here than in the other relations we have mentioned. It is important not to underestimate the size of these errors.

The numerical calculations reported here are mostly due to Woolcock.[73] Some improvements have been made, and we have taken account of more recent experimental data. Also we have used the Regge pole method to give better estimates of the contributions to the dispersion integrals from very high energies. For reasons of space we shall not give the full details, concentrating rather on the salient points. The calculation of f^2 and the study of the parameterization of the S-wave phase shifts are given in more detail than the remainder, because of the considerable importance of these results for numerous applications. Also, the Regge pole estimates are given in some detail.

(i) Determination of f^2

We define the equivalent pseudovector coupling constant by

$$f^2 = (\mu/2M)^2 G_r^2/4\pi\,, \tag{4.1}$$

where G is the rationalized pseudoscalar coupling constant used in Secs. 1, 2, and 3 above. The most promising method[74] for determining f^2 is to use the dispersion relations (1.17) for the B amplitudes in the forward direction ($t = 0$). It is convenient to use the amplitudes $B_\pm$ for the elastic scattering $\pi^\pm + p \to \pi^\pm + p$. By (1.9) $B_+ = B^{(+)} - B^{(-)}$, $B_- = B^{(+)} + B^{(-)}$. In the forward direction $\nu = \omega_L$ where ω_L is the (total) lab pion energy [Eq. (1.4)], and using Eq. (4.1), the relations (1.17) give the equations

$$\frac{1}{4\pi M}\,\mathrm{Re}\,B_+(\omega_L,0) = \frac{-4f^2/\mu^2}{\omega_L - \mu^2/2M} + \frac{1}{\pi}P\int_\mu^\infty \frac{d\omega'}{4\pi M}\left[\frac{\mathrm{Im}\,B_+(\omega',0)}{\omega' - \omega_L} - \frac{\mathrm{Im}\,B_-(\omega',0)}{\omega' + \omega_L}\right] \tag{4.2a}$$

$$\frac{1}{4\pi M}\,\mathrm{Re}\,B_-(\omega_L,0) = \frac{-4f^2/\mu^2}{\omega_L + \mu^2/2M} + \frac{1}{\pi}P\int_\mu^\infty \frac{d\omega'}{4\pi M}\left[\frac{\mathrm{Im}\,B_-(\omega',0)}{\omega' - \omega_L} - \frac{\mathrm{Im}\,B_+(\omega',0)}{\omega' + \omega_L}\right]. \tag{4.2b}$$

In the integrands ω' is the (total) lab pion energy.

Equations (4.2) are used by inserting known phase shifts on the left-hand side at low energies (up to 200 MeV). The integrals on the right are given by the absorptive parts of the partial waves, and the best accuracy is obtained by using the B_+ relation Eq. (4.2a) so that the major contribution to the term containing $(\omega' - \omega_L)^{-1}$ comes from the $(\frac{3}{2}, \frac{3}{2})$ resonance which is particularly well known. We find the difference between Re $B_+(\omega_L,0)/4\pi M$ and the integral for values of ω_L between 15 MeV and 185 MeV. This set of differences is fitted by the function $(\text{const})/(\omega_L - \mu^2/2M)$ and the best value of the constant yields the coupling constant f^2. Now we examine the evaluation of the various terms in (4.2a).

The basic formula, obtained from Eqs. (2.31) and (1.30) is

$$\begin{aligned}\frac{B(\omega_L,0)}{4\pi M} = {} & \frac{f_S}{M(E+M)} + \frac{f_{P_{\frac{1}{2}}}}{M(E-M)} \\ & - \frac{2}{q^2}\left(2 - \frac{E}{M}\right) f_{P_{\frac{3}{2}}} + \frac{2}{q^2}\left(2 + \frac{E}{M}\right) f_{D_{\frac{3}{2}}} \\ & - \frac{3}{q^2}\left(3 - \frac{E}{M}\right) f_{D_{\frac{5}{2}}} + \frac{3}{q^2}\left(3 + \frac{E}{M}\right) f_{F_{\frac{5}{2}}} \\ & - \frac{4}{q^2}\left(4 - \frac{E}{M}\right) f_{F_{\frac{7}{2}}} + \cdots\,,\end{aligned} \tag{4.3}$$

where $E = (M^2 + q^2)^{\frac{1}{2}}$. The subscript notation for the partial wave amplitudes $f_S, f_{P_{\frac{1}{2}}}, f_{P_{\frac{3}{2}}}, \cdots$ is obvious. The convergence of the series has been discussed in Secs. 3(iii) and (iv).

(a) *Evaluation of Re $B_+(\omega_L,0)$*

The dominant contribution to Re $B_+(\omega_L,0)$ over the range 15 MeV to 185 MeV is the $p_{\frac{3}{2}}$ term which is given by the α_{33} phase shift. This contribution varies from about -0.48 at 15 MeV to below -0.1 at 185 MeV. The remaining terms are small, and we consider them first.

The s-wave term is very small, due to the large denominator $[M(E+M)]^{-1}$. It is of order -0.001 at the lower energies, and is somewhat bigger near 185 MeV. It is quite sufficient to use the semi-phenomenological fit for α_3 given by Hamilton and Woolcock.[75] The $p_{\frac{1}{2}}$ term can be evaluated by using (and interpolating) the accurate results for α_{31} at 24.8, 31.5, and 41.5 MeV (Rochester),[76] 97 MeV (Liverpool)[77] and 310 MeV (Berkeley).[78] Several

[74] W. S. Woolcock, in *Proceedings of the Tenth International Conference on High-Energy Physics, Rochester*, edited by E. C. G. Sudarshan, J. H. Tinlot, and A. C. Melissinos (Interscience Publishers, Inc., New York, 1960), p. 302.

[75] J. Hamilton and W. S. Woolcock, Phys. Rev. **118**, 291 (1960). The solid curve for α_3 in Fig. 2 of that paper is used. This curve continues well to the 310 MeV value of α_3 given by J. H. Foote *et al.* (cf. reference 67).

[76] S. W. Barnes, B. Rose, G. Giacomelli, J. Ring, R. Miyake, and K. Kinsey, Phys. Rev. **117**, 116 and 238 (1960).

[77] D. N. Edwards and T. Massam (private communication). We are indebted to Dr. Edwards and Dr. Massam for these results.

[78] J. H. Foote *et al.* (cf. reference 67).

other (less accurate) values of α_{31} are used. The error in the $p_{\frac{3}{2}}$ contribution to Eq. (4.3) is 0.008 at 40 MeV and 0.004 at 200 MeV.

The contribution of the d-wave phase shifts to Re B_+ is not negligible. At 310 MeV Foote *et al.*[78] found $\delta_{33} = 3.1° \pm 2.6°$, $\delta_{35} = -4.9° \pm 2.2°$ (the SPDF–I fit). It is reasonable to assume that these phase shifts vary with energy as q^5 (this cannot introduce important errors). Errors or ambiguities in the d-wave phases do not cause as large errors in Re $B_+/4\pi M$ below 200 MeV as might be expected. This is because changes in δ_{33} and δ_{35} also alter the experimental values of α_{31} and α_{33} which we have used,[79] and the two effects act in opposite directions. The errors given for Re $B_+/4\pi M$ in Table V below include the effect of uncertainties in the d-wave analysis at 310 MeV, and they allow for the SPD or the SPDF–I sets[78] being possible.

As to f waves, even if the phase shifts are of order 0.5° at 310 MeV (the SPDF–I fit[78]) this only gives a contribution of around 0.008 to Re $B_+/4\pi M$ at 185 MeV, and much less at lower energies. Higher partial waves can certainly be ignored. In the notation of Sec. 3(iv) the radius of convergence of the series (4.3) for Re $B_+/4\pi M$ is $y_0 \simeq 2$ at 180 MeV, and (4.3) should still converge well at 180 MeV.

Finally we examine the $p_{\frac{3}{2}}$ term. There is much experimental data on α_{33} in the range 15–185 MeV. At the lower end of the energy range these values are used directly. Woolcock[73] found that for other energies the most accurate values could often be found by using the formula for the total cross section[80]

$$\sigma_+ = (4\pi/q^2)(\sin^2\alpha_3 + \sin^2\alpha_{31} + 2\sin^2\alpha_{33} + 2\sin^2\delta_{33} + 3\sin^2\delta_{35} + \cdots) . \quad (4.4)$$

The phase shifts α_3, α_{31}, δ_{33}, δ_{35} are not large. Even if some of them are not known very accurately, Eq. (4) will give accurate values for α_{33} whenever σ_+ is known accurately. The values of α_{33} which were used are given in Table III. The values of Re $B_+(\omega_L,0)/4\pi M$ are given in Table V.

(b) *Evaluation of Im $B_\pm(\omega_L,0)$ for 0–350 MeV*

In this energy range the dominant contribution to Im $B_+/4\pi M$ is given by α_{33}. The other phase shifts give much smaller contributions, and the information on these phase shifts which was discussed in the preceding paragraphs is quite sufficient and gives adequate accuracy for Im B_+. The α_{33} data in Table III are smoothed in order to evaluate the integral in (4.2a). Following Noyes and Edwards,[81] Woolcock[73] uses

$$q^3(\cot\alpha_{33})/\omega^* = m\omega^* + c \quad (4.5)$$

where $\omega^* + M = W$ is the total energy in the c.m. system and m and c are constants. These have the values $m = -3.813 \pm 0.071$, $c = 8.349 \pm 0.125$ (units $\hbar = c = \mu = 1$ as usual). The errors in m and c have a strong negative correlation, and the actual errors in cot α_{33} are very small. With these values Eq. (4.5) is a very good fit to all the α_{33} data up to 190 MeV.

TABLE III. The values of α_{33} used in computing Re $B_+(\omega_L,0)/4\pi M$. The asterisks denote those values obtained by using Eq. (4.4). The remainder are from direct phase shift analyses.

Lab energy (MeV)	α_{33} (degrees)	Lab energy (MeV)	α_{33} (degrees)
15	0.8 ± 0.2	113	27.5 ± 1.0*
25	1.9 ± 0.4	120	31.4 ± 2.0
35	2.8 ± 0.7		31.8 ± 1.6
37	3.1 ± 0.8	135	40.8 ± 0.8*
40	4.5 ± 1.0	143	45.7 ± 1.1*
41.5	4.3 ± 0.2*	144	48.2 ± 0.9*
45	4.4 ± 1.1	150	55.1 ± 2.0
58	7.5 ± 0.5*	170	69.5 ± 2.4*
78	13.0 ± 2.0	173.5	70.8 ± 1.5*
80	12.4 ± 2.1	176	75.2 ± 3.1*
97.1	20.9 ± 0.3	177	75.1 ± 3.1*
100	21.7 ± 1.2	183.5	76.1 ± 2.5*

Above 190 MeV there is a one-sided deviation of cot α_{33} from the Noyes–Edwards curve (5). All the experimental data on α_{33} (from phase-shift analysis and from σ_+) in the range 190–350 MeV was collected, and it turned out that a smooth curve could be drawn through the standard error limits on nearly all the data. The 310-MeV value[78] $\alpha_{33} = 134.8° \pm 0.6°$ has a very small error, and this helps considerably to pin down the curve at the high-energy end. Essentially in this energy range Im B_+ is known about as accurately as σ_+.

For Im B_- we use the formula

$$\text{Im } B_-(\omega_L,0) = \tfrac{2}{3}\,\text{Im } B^{(\frac{1}{2})}(\omega_L,0) + \tfrac{1}{3}\,\text{Im } B^{(\frac{3}{2})}(\omega_L,0) . \quad (4.6)$$

Up to 250 MeV reasonably accurate values of the $T = \frac{1}{2}$ phase shifts are known and it is clear that the $T = \frac{3}{2}$ term in (4.6) is predominant. For 250–350 MeV the phase shift set a_{SPD} of Zinov *et al.*[82] was used.

[79] We are indebted to Dr. T. Massam for information on this point.

[80] Inelastic processes are negligible at 185 MeV.

[81] H. P. Noyes and D. N. Edwards, Phys. Rev. **118**, 1409 (1960).

[82] V. G. Zinov, S. M. Korenchenko, N. L. Polumordvinova, and G. N. Tentyukova, Soviet Phys.–JETP **11**, 1016 (1960).

In fact, using the b_{SPD} set causes little change as the main contribution is from α_{11}, and $|\alpha_{11}|$ is about the same in both sets. Near 350 MeV, Im $B^{(\frac{1}{2})}$ begins to increase rapidly because the δ_{13} d-wave phase shift starts to rise towards the 600-MeV resonance. This will be discussed below.

(c) *Charge Independence*

In writing (4.6) we assume charge independence, and it is relevant to consider the possible effect of small violations of charge independence in a calculation which aims to find the value of f^2 accurate to a few percent. A good test of charge independence in the elastic region is given by the relation between charge exchange scattering $\pi^- + p \to \pi^\circ + n$ and elastic scattering $\pi^\pm + p \to \pi^\pm + p$. At threshold[83] and at low energies (up to 225 MeV[84]) the relation appears to be well satisfied. At higher energies accurate charge-exchange data are not available, but up to around 350 MeV the $\pi^\pm - p$ scattering data have been analyzed with considerable accuracy using charge independence (the point here is that the $T = \frac{1}{2}$ phase shifts can be assigned real values).

Above 350 MeV the higher resonances (600 MeV, 900 MeV, 1.35 BeV) appear either in the $T = \frac{1}{2}$ or $T = \frac{3}{2}$ states. Also the analyses[85] of charge-exchange data ($\pi^- + p \to \pi^\circ + n$) near 600 MeV and 900 MeV are consistent with charge independence. Nevertheless, for all we know there may be some departure from charge independence at energies above 250 MeV. It can be seen that even if this is so it should have very little effect on our results.

The dispersion relations (2) relate to elastic $\pi^\pm + p$ scattering, and their derivation does not require charge independence.[86] The experimental data which are inserted in (2) come from the differential cross sections for elastic $\pi^\pm + p$ scattering and the total cross sections $\sigma_\pm$ (which are related to elastic scattering through the optical theorem). In analyzing the $\pi^\pm + p$ scattering data the relation

$$T_- = \tfrac{2}{3} T^{(\frac{1}{2})} + \tfrac{1}{3} T^{(\frac{3}{2})}$$

is used for the $\pi^- + p$ elastic-scattering amplitude T_-, and the same combination of isospin amplitudes is again used to give the values of B_- which are inserted in (4.2). Thus if charge independence is not exactly valid above 250 MeV, no error is produced in our calculation (the phase shifts for the $T^{(\frac{1}{2})}$ amplitude need not be real[87] at these energies). Of course, the amplitude $T^{(\frac{1}{2})}$ is then no longer an isospin amplitude. Finally, we note that at very high energies ($\omega_L \gtrsim 2$ BeV) we find Im B_- directly from the total cross section σ_- (see below).

(d) *Evaluation of Im* $B_+(\omega_L,0)$ *for* 350 *MeV–2 BeV*

There is an accurate phase shift analysis of $\pi^+ + p$, scattering at 500 MeV,[88] and other analyses[89] at relevant energies, so there is no difficulty in obtaining Im B_+ sufficiently accurately up to 500 MeV. From Sec. 3, Table I or II, we see that the radius of convergence of the Legendre expansion of Im B is 1.3, so we expect the series in Eq. (4.3) to converge slowly at 500 MeV and higher energies. Therefore other methods must be used to find Im $B_\pm$ at such energies. The method used is to estimate Im $B_\pm(\omega_L,0)$ at 2 BeV from an optical model. Between 350 MeV and 2 BeV there are resonances in both the $\pi^+ - p$ and $\pi^- - p$ cases, and the contributions to Im $B_\pm$ from the resonant partial wave amplitudes are determined by a method given below. The remaining (nonresonant) parts of Im $B_\pm$ are obtained by drawing smooth curves to join the calculated values of Im $B_\pm$ at 350 or 500 MeV onto the 2-BeV values (making any possible use of any phase-shift analyses which are available between these energies). This procedure for getting the nonresonant parts of Im $B_\pm$ in this energy range is not particularly accurate, but it is seen from Table IV below that their total contribution to the integral in (4.2a) is very small, so even large percentage errors are unimportant. (The values of Im $B_\pm$ are shown in Fig. 7.)

Woolcock[73] estimates the value of Im B_+ around 2 BeV by using a partially opaque disk optical model.[90] The spin-flip amplitude $g(\theta)$ [Eq. (1.28)] is assumed to be unimportant[91] and the no-flip ampli-

[83] See J. Hamilton and W. S. Woolcock, Phys. Rev. **118**, 291 (1960) for the situation at threshold.

[84] J. Deahl, M. Derrick, J. Fetkovich, T. Fields, and G. B. Yodh, Phys. Rev. **124**, 1987 (1961).

[85] J. C. Brisson, R. Omnes, and G. Valladas, Nuovo Cimento **19**, 210 (1961); *Proceedings of the International Conference on Elementary Particles, Aix-en-Provence, 1961* (C.E.N. Saclay, France, 1961), Vol. I, p. 467.

[86] See, for example, J. Hamilton, Phys. Rev. **110**, 1134 (1958).

[87] If the charge exchange ($\pi^- + p \to \pi^\circ + n$) rate were much smaller than that given by charge independence, the real parts of the $T^{(\frac{1}{2})}$ phase shifts might have to take impossible values. However reference 85 shows that the charge-exchange rate is about what we would expect by charge independence.

[88] W. J. Willis, Phys. Rev. **116**, 753 (1959).

[89] M. E. Blevins, M. M. Block, and J. Leitner, Phys. Rev. **112**, 1287 (1958); W. D. Walker, Phys. Rev. **118**, 1612 (1960).

[90] Inside the first diffraction zero, an optical model can be consistent with the Regge pole results provided the parameters of the model vary slowly (logarithmically) with energy.

[91] As was seen in Sec. 2(viii) above, it is by no means obvious that the spin-flip amplitude $g(\theta)$ can be neglected. However, any error here should not change the estimates of Im B by more than a small factor.

tude $f(\theta)$ [Eq. (1.28)] is given by

$$f(\theta) = i(1-a)q\int_0^R J_0(q\rho\sin\theta)\rho d\rho$$
$$= i(1-a)RJ_1(qR\sin\theta)/\sin\theta\,, \quad (4.7)$$

where R is the "radius" of the nucleon and a the opacity parameter. From experiments in the region of 2 BeV it is estimated that $R = 1.04\times10^{-13}$ cm $= 0.74$ units and a is real with $1-a = 0.43$. Neglecting for the moment any difference between the π^+–p and π^-–p amplitudes, for energies near 2 BeV this gives, using Eq. (2.45),

$$\frac{1}{4\pi}\,\mathrm{Im}\,A_\pm(\omega_L,0) = q\frac{W+M}{E+M}\times 0.116$$
$$\frac{1}{4\pi}\,\mathrm{Im}\,B_\pm(\omega_L,0) = \frac{q}{E+M}\times 0.116\,. \quad (4.8)$$

The real difficulty about Im B_+ in the range 350 MeV–2 BeV is the nature of the hump in the σ_+ cross section at 1.35 BeV (Fig. 6). If this is due to one or several resonances, then one or several of the terms on the right of (4.3) will be comparatively large. Several authors[92] suggest that there is a $(T=\frac{3}{2})$ $p_{\frac{3}{2}}$ resonance at 1.35 BeV. Others[93] suggest that there is a $d_{\frac{5}{2}}$ resonance at 1.2 BeV and a $f_{\frac{7}{2}}$ resonance at 1.4 BeV.

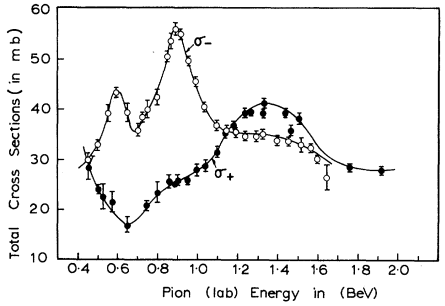

FIG. 6. Experimental values of the $\pi^+ + p$ and $\pi^- + p$ total cross sections σ_+ and σ_- in the range 0.4 BeV to 2.0 BeV. The curves are possible smooth fits to the experimental values.

The contributions to Im B from such resonances are found as follows. Let $\sigma_{l\pm}$ be the resonant part of the total cross section (it is found by estimating how much of the cross section is merely background, bearing in mind the limits set by unitarity and the elasticity parameter). The optical theorem gives

$$(j+\tfrac{1}{2})\,\mathrm{Im}\,f_{l\pm} = (q/4\pi)\sigma_{l\pm}\,(j = l\pm\tfrac{1}{2})\,, \quad (4.9)$$

where $f_{l\pm}$ is the resonant amplitude. From the estimated width and height of the resonance we can now obtain the contribution to the integral in (4.2a).

As an example we shall give a rough estimate of the contribution from the 1.35-BeV hump in σ_+ From Fig. 6 we estimate that, if this is a $p_{\frac{3}{2}}$ resonance, then the resonant part σ_{1+} is 15 mb at the maximum, and the width at half-height is around 400 MeV. Using Eqs. (4.9) and (4.3) we find that this resonance contributes -1×10^{-3} to the integral in (4.2a). Alternatively if the hump consists of $d_{\frac{5}{2}}$ and $f_{\frac{7}{2}}$ resonances at 1.2 BeV and 1.4 BeV, respectively, each being 10 mb high and 250 MeV wide (at half-height), they will contribute -1×10^{-3} and -1.7×10^{-3}, respectively, to the integral in (4.2a).

In the values given in Table V below, the hump was assumed to be a $p_{\frac{3}{2}}$ resonance. The estimates just given show that this will lead to a value of f^2 which is: (a) too small by 0.0004 if there is no resonance, and (b) too large by 0.0006 if there are actually $d_{\frac{5}{2}}$ and $f_{\frac{7}{2}}$ resonances. These uncertainties are included in the final error quoted for f^2 [Eq. (4.15)].

(e) *Evaluation of Im $B_-(\omega_L,0)$ from 350 MeV–2 BeV*

The procedure here is almost the same as in the case of Im B_+. The only difference is that the $d_{\frac{3}{2}}$ and $f_{\frac{5}{2}}$ resonances at 600 MeV and 900 MeV have to be treated somewhat more carefully as they give larger contributions than the π^+–p resonances mentioned in the previous paragraph. Using a Breit–Wigner shape Woolcock[73] estimated that the resonant part of σ_- at 600 MeV was 27 mb at maximum, and that at 900 MeV the corresponding figure was 26 mb. Then using Eq. (4.9) the contribution of the resonances to the integral in (4.2a) was evaluated. The value used for the resonant part of the cross section at 600 MeV is perhaps a little too large. A recent analysis[94] suggests 23 mb, and this correction is included in the final values for the integral given in Tables IV and V. (The correction is in fact very small as can be seen from Table IV.)

(f) *The Very High-Energy Contribution*

In the original calculation[73,74] of the integral in (4.2a) Im $B_+(\omega',0)$ and Im $B_-(\omega',0)$ were taken equal above 2.5 BeV. Recent experimental results[95] and the Regge pole methods make it possible to estimate

[92] N. P. Klepikov, Dubna preprint (1960); W. N. Wong and M. Ross, Phys. Rev. Letters **3**, 398 (1959).

[93] R. Blanckenbeckler and M. L. Goldberger, Phys. Rev. **126**, 766 (1962), footnote 24; W. M. Layson, CERN preprint (1961).

[94] R. Omnes and G. Valladas (reference 85). These authors suggest that there are also moderate amounts of amplitudes other than $D_{3/2}$ and $F_{5/2}$ at 600 MeV and 900 MeV, respectively. These give corrections which can be ignored here [cf. Sec. 5(ii) for further discussion].

[95] See Fig. 3.

more accurately the contribution from above 2 BeV. By Eq. (1.35)

$$f_L(\omega_L,0) = (1/4\pi)(A + \omega_L B)\,, \qquad (4.10)$$

where $f_L(\omega_L,0)$ is the forward scattering amplitude in the lab system. In Sec. 2(viii) we gave reasons for believing that $A(\nu,t)$ does not attain its unitary limit as $\nu \to \infty$. Thus, for very high energies Eq. (4.10) gives

$$\begin{aligned} \text{Im}\, B^{(-)}(\omega_L,0) &\simeq (4\pi/\omega_L)\, \text{Im}\, f_L^{(-)}(\omega_L,0) \\ &\simeq \tfrac{1}{2}(\sigma_- - \sigma_+)\,. \end{aligned} \qquad (4.11)$$

Also $B^{(-)} = \frac{1}{2}(B_- - B_+)$, and (4.11) can be used to find the high-energy contribution to (4.2a).

Using the Regge pole approximation and the high-energy data (Fig. 2), Udgaonkar[96] estimates that, for large ω_L,

$$\sigma_-(\omega_L) - \sigma_+(\omega_L) \backsim \omega_L^{-[1-\alpha_\rho(0)]}\,, \qquad (4.12)$$

where $\alpha_\rho(0) \simeq 0.5$. It is clear from the data that σ_- must equal σ_+ at some energy near 2 BeV (see Figs. 2 and 6). Also $\sigma_- - \sigma_+ = 2.5$ mb at 4 BeV. To be conservative we shall assume $\sigma_- - \sigma_+ = 2.5$ mb over the range 2–4 BeV. Above 4 BeV we use

$$\sigma_-(\omega_L) - \sigma_+(\omega_L) = (2.5\text{ mb})(4\text{ BeV}/\omega_L)^{1-\alpha_\rho(0)}\,.$$

This gives[97]

$$\int_{2\text{ BeV}}^{\infty} \frac{\sigma_-(\omega') - \sigma_+(\omega')}{\omega'}\, d\omega' = 0.32 \qquad (4.13)$$

on using $\alpha_\rho(0) = 0.5$.

Substituting (4.11) and (4.13) the integral in (4.2a) gives the contribution -1.2×10^{-3} from energies $\omega' \geqslant 2$ BeV. From Table IV it is seen that this is not negligible. However this is an overestimate of the high-energy contribution. From Eq. (4.8) we see that[98] Im $A^{(-)}$ will also contribute to Im $f_L(\omega_L,0)$ [Eq. (4.8)] at the lower end of the range 2 BeV $\leq \omega_L \leq \infty$. To correct for this, we estimate[99] that it is necessary to multiply the above result by 0.4, so that the contribution to the integral in (4.2a) from $\omega' \geqslant 2$ BeV is -5×10^{-4}. Ignoring this term would change f^2 by no more than 2×10^{-4}.

[96] B. Udgaonkar, Phys. Rev. Letters **8**, 142 (1962). *Note added in proof.* Even if the Regge pole ideas do not apply in any simple way to high-energy scattering, we still regard Eq. (4.12) as a useful parametrization of $\sigma_- - \sigma_+$ at high energies.

[97] The unit of area is 20 mb.

[98] To allow for the difference between σ_- and σ_+ the numerical factors in Eq. (4.8) have to be different by about 8% in the $\pm$ cases.

[99] This is obtained by comparing the incorrect value Im $B_\pm$ = $\sigma_\pm$ given by ignoring $A_\pm$ with the value predicted by Eq. (4.8) near 2 BeV. This correction is consistent with the value of Im A_+ given in Eq. (4.8).

(g) *Summary and Result*

In Table IV we give the contributions to the integral

$$I = \frac{1}{4\pi M} P \int_\mu^\infty d\omega' \left[\frac{\text{Im}\, B_+(\omega',0)}{\omega' - \omega_L} - \frac{\text{Im}\, B_-(\omega',0)}{\omega' + \omega_L} \right] \qquad (4.14)$$

for $\omega_L = 1.286$ (40 MeV). This shows how the contribution to I from the $(\frac{3}{2}, \frac{3}{2})$ resonance dominates. Even the next largest contributions, which come from the $d_{\frac{3}{2}}$ and $f_{\frac{5}{2}}$ $\pi^- p$ resonances, are very much smaller.

In Table V we give the values and errors of Re $B_+(\omega_L,0)/4\pi M$ and the integral I/π for the 24 values of ω_L, for which we have determinations of α_{33} (Table III). The last column gives the value of f^2 deduced from Eq. (4.2a). The errors quoted for I are standard errors derived from the errors in the experimental data and various uncertainties which were discussed above. [The possible systematic error mentioned in footnote 100 is not included in Table V but is included in the final value of f^2 in Eq. (4.15).]

The values of f^2 in the last column of Table V are remarkably consistent. Incidentally they provide a good proof of the validity of the B_+ dispersion relation (4.2a) up to 185 MeV. The errors in the values of f^2 cannot be treated as independent for various reasons. For example, the 135-, 143-, and 144-MeV data are undoubtedly correlated. There are various ways of getting uncorrelated values of f^2. We could select the value of f^2 with the smallest error in each of the five sections of Table V. These relate to well-separated energies and they will be uncorrelated. Their weighted average is $f^2 = 0.0825 \pm 0.003$. More data can be used by selecting the value of f^2 with least error in each (nonoverlapping) 20-MeV energy interval. Again, correlation of errors should be un-

TABLE IV. Contributions to the integral $(I/\pi) \times 10^3$ [Eq. (4.14)] from various energy ranges for $\omega_L = 1.286$ (40 MeV).

Energy region (MeV)	Integral over Im B_+	Integral over Im B_-
0– 300	−203.8	+14.2
300– 500	−10.9	−2.1
500–1200	−2.8 (100)	−14.8
1200–2000	−0.1 (100)	−0.4
2000–∞	−0.1	

[100] The sum of these terms is to be replaced by approx −1.9 if there is no resonance at 1.35 BeV, and by −4.6 if there are $d_{5/2}$ and $f_{7/2}$ resonances at 1.2 and 1.4 BeV.

important. The weighted average is $f^2 = 0.081 \pm 0.002$. Finally we have to allow for the possible systematic error due to lack of knowledge about the 1.35-BeV hump in $\pi^+ - p$ scattering. We are certain to include this if we write[101]

$$f^2 = 0.081 \pm 0.003 . \quad (4.15)$$

In Sec. 4(vii) below the result of another determination of f^2 is given.

TABLE V. Values of $-\mathrm{Re}\, B_+(\omega_L,0)/4\pi M$ and the integral I/π [Eq. (4.14)] for 24 values of ω_L. The last column gives f^2 determined by Eq. (4.2a).

Lab pion energy (MeV)	$-\mathrm{Re}\, B_+(\omega_L,0)/4\pi M$	$-I/\pi$	f^2
15	0.482 ± 0.103	0.183 ± 0.003	0.097 ± 0.026
25	0.491 ± 0.087	0.198 ± 0.003	0.081 ± 0.024
35	0.442 ± 0.100	0.213 ± 0.003	0.067 ± 0.029
37	0.446 ± 0.099	0.216 ± 0.003	0.068 ± 0.029
40	0.552 ± 0.108	0.221 ± 0.003	0.100 ± 0.033
41.5	0.507 ± 0.014	0.224 ± 0.003	0.086 ± 0.005
45	0.458 ± 0.098	0.230 ± 0.003	0.071 ± 0.030
58	0.495 ± 0.028	0.252 ± 0.003	0.081 ± 0.009
78	0.506 ± 0.067	0.289 ± 0.004	0.081 ± 0.025
80	0.468 ± 0.068	0.293 ± 0.004	0.068 ± 0.025
97.1	0.522 ± 0.008	0.314 ± 0.004	0.084 ± 0.004
100	0.510 ± 0.022	0.314 ± 0.004	0.080 ± 0.009
113	0.485 ± 0.013	0.306 ± 0.003	0.078 ± 0.006
120	0.471 ± 0.018	0.293 ± 0.003	0.079 ± 0.008
120	0.474 ± 0.014	0.293 ± 0.003	0.081 ± 0.006
135	0.420 ± 0.008	0.253 ± 0.004	0.079 ± 0.005
143	0.380 ± 0.008	0.219 ± 0.004	0.078 ± 0.005
144	0.374 ± 0.008	0.214 ± 0.004	0.079 ± 0.005
150	0.327 ± 0.013	0.179 ± 0.004	0.074 ± 0.007
170	0.175 ± 0.019	0.040 ± 0.003	0.073 ± 0.010
173.5	0.158 ± 0.012	0.011 ± 0.003	0.080 ± 0.007
176	0.170 ± 0.024	−0.008 ± 0.003	0.070 ± 0.013
177	0.113 ± 0.024	−0.016 ± 0.003	0.071 ± 0.013
183.5	0.099 ± 0.018	−0.041 ± 0.003	0.080 ± 0.010

(ii) Parametrization of Low-Energy s-Wave Scattering

It was pointed out by Cini *et al.*[102] that the expansion

$$\alpha_i = a_i q + b_i q^3 + c_i q^5 + \cdots \quad (i = 1,3)$$

is not a good way to fit the s-wave π–N phase shifts α_1 and α_3, even for energies up to 50 MeV. The convergence of the series is poor, and, by using it, one can readily deduce incorrect values of the scattering lengths a_1 and a_3 from low-energy experimental results. Dispersion relations suggested much better expansions which we applied to the low-energy data in an earlier paper[75] and found consistent and accurate values for a_1 and a_3.

The best form of these low-energy expansions for the s-wave phase shifts can be obtained from the forward-scattering dispersion relations (2.6). We write as usual $D^{(+)} = \frac{1}{2}(D_+ + D_-)$, $D^{(-)} = \frac{1}{2}(D_- - D_+)$ where $D_\pm(\omega_L)$ are the real parts of the forward-scattering amplitude in the lab system for $\pi^\pm + p \to \pi^\pm + p$ at (lab) energy. Then Eqs. (2.6) give

$$D^{(+)}(\omega_L) = D^{(+)}(\mu) + \frac{f^2}{M}\frac{q_L^2}{\omega_L^2 - \mu^4/4M^2}\frac{1}{1-\mu^2/4M^2} + \frac{q_L^2}{4\pi^2} P\int_\mu^\infty \frac{d\omega'}{q'}\sigma^{(+)}(\omega')\left[\frac{1}{\omega'-\omega_L} + \frac{1}{\omega'+\omega_L}\right], \quad (4.16)$$

and

$$D^{(-)}(\omega_L) = \omega_L D^{(-)}(\mu) - \frac{2f^2}{\mu^2}\frac{\omega_L q_L^2}{\omega_L^2 - \mu^4/4M^2}\frac{1}{1-\mu^2/4M^2} + \frac{q_L^2}{4\pi^2} P\int_\mu^\infty \frac{d\omega'}{q'}\sigma^{(-)}(\omega')\left[\frac{1}{\omega'-\omega_L} - \frac{1}{\omega'+\omega_L}\right], \quad (4.17)$$

where $\sigma^{(\pm)} = \frac{1}{2}(\sigma_- \pm \sigma_+)$. Here, $\sigma_\pm$ are the total cross sections for $\pi^\pm + p$ scattering, and q_L, q' are lab momenta and ω_L, ω' are the corresponding lab energies.

We put $\mu = 1$ in all that follows. Using (1.33), (1.31), and the partial wave expansion (1.28) the left-hand sides of (4.16) and (4.17) can be written in terms of the phase shifts. Also by (1.37)

$$D^{(+)}(1) = (1 + 1/M)\tfrac{1}{3}(a_1 + 2a_3) ,$$
$$D^{(-)}(1) = (1 + 1/M)\tfrac{1}{3}(a_1 - a_3) .$$

Now rearranging (4.16) and (4.17) we have

$$\frac{\sin 2\alpha_1 + 2\sin 2\alpha_3}{2q}\frac{W}{M+1} = (a_1 + 2a_3) + q_L^2\left[\frac{3}{4\pi^2(1+1/M)} P\int_1^\infty \frac{d\omega'}{q'}\sigma^{(+)}(\omega') \times\left(\frac{1}{\omega'-\omega_L} + \frac{1}{\omega'+\omega_L}\right) + \frac{3f^2}{(M+1)(1-1/4M^2)(\omega_L^2 - 1/4M^2)} - \frac{M}{W(1+1/M)}\mathrm{Re}\,(p_{11} + 2p_{13} + 2p_{31} + 4p_{33}) + (d\text{-wave terms})\right] \quad (4.18)$$

[101] The reasons for the differences from the value $f^2 = 0.080 \pm 0.002$ given in reference 74 are: (a) The present analysis is more careful about possible correlation of errors in Table V; (b) a larger error is allowed for uncertainties about the 1.35-BeV hump.

[102] M. Cini, R. Gatto, E. L. Goldwasser, and M. Ruderman, Nuovo Cimento **10**, 242 (1958).

$$\frac{\sin 2\alpha_1 - \sin 2\alpha_3}{2q}\frac{W}{M+1} = (a_1 - a_3)\omega_L + q_L^2\Big[\frac{3}{4\pi^2(1+1/M)}P\int_1^\infty \frac{d\omega'}{q'}\sigma^{(-)}(\omega') \times\Big(\frac{1}{\omega'-\omega_L} - \frac{1}{\omega'+\omega_L}\Big) - \frac{6f^2\omega_L}{(1+1/M)(1-1/4M^2)(\omega_L^2 - 1/4M^2)} - \frac{M}{W(1+1/M)}\,\mathrm{Re}\,(p_{11} + 2p_{13} - p_{31} - 2p_{33}) + (d\text{-wave terms})\Big]. \quad (4.19)$$

Here,

$$p_{2T,2J} = \exp(i\alpha_{2T,2J})\,\sin\alpha_{2T,2J}/q^3\,,$$

where $\alpha_{2T,2J}$ are the p-wave π–N phase shifts and q is the momentum in the c.m. system. The d-wave terms in (4.18) and (4.19) are of the form: (d-wave scattering length) $\times q^2$, and they are very small for energies below 100 MeV.

It is convenient to write (4.18) and (4.19) in the form

$$\frac{\sin 2\alpha_1 + 2\sin 2\alpha_3}{2q}\frac{W}{M+1} = (a_1 + 2a_3) + C^{(+)}q_L^2\,, \quad (4.20)$$

$$\frac{\sin 2\alpha_1 - \sin 2\alpha_3}{2q}\frac{W}{M+1} = (a_1 - a_3)\omega_L + C^{(-)}q_L^2\,, \quad (4.21)$$

where $C^{(+)}$ and $C^{(-)}$ are given by the terms inside the square brackets in (4.18) and (4.19). Woolcock[73] roughly evaluated these expressions for $C^{(+)}$ and $C^{(-)}$ at low energies. The experimental values of $\sigma_\pm$ and α_{33} (cf. Table III), and the value (4.15) for f^2 were used to give accurate values of the integrals, the Re p_{33} terms, and the Born terms. Estimates of the remaining Re $p_{2T,2J}$ at low energies were made on the basis of the available phase-shift analyses. The results showed that these expressions for $C^{(+)}$ and $C^{(-)}$ varied only a little over the energy range $0 \le (\omega_L - \mu) \le 45$ MeV.

Next the Eqs. (4.20) and (4.21) were used to fit the experimental values[103] of α_1 and α_3 up to 45 MeV, and it was found that, to within the experimental errors, $C^{(+)}$ and $C^{(-)}$ were constant over this range of energies.

[103] The available accurate data used were 13 values of $\sin 2\alpha_3$, 4 values of $(2\sin 2\alpha_1 + \sin 2\alpha_3)$, and one value of $(\sin 2\alpha_1 - \sin 2\alpha_3)$. For details see reference 73. The appropriate inner Coulomb correction [J. Hamilton and W. S. Woolcock, Phys. Rev. **118**, 291 (1960)] was used, bearing in mind that different authors may use different values of the Coulomb cutoff radius r_0.

Why $C^{(+)}$ and $C^{(-)}$ Are Almost Constant at Low Energies

The fact that $C^{(+)}$ and $C^{(-)}$ are constant at low energies may appear somewhat surprising, since individual terms in the square brackets on the right of (4.18) and (4.19) vary considerably with energy. We begin to understand the reason for this result if we use the rough approximation for the p-wave amplitudes $p_{2T,2J}$ given by CGLN.[2] These equations are

$$\mathrm{Re}\,p_{33}(\omega^*) = \frac{4f^2}{3\omega^*} + \frac{1}{\pi}P\int_1^K d\omega^{*\prime}\,\mathrm{Im}\,p_{33}(\omega^{*\prime}) \times\Big[\frac{1}{\omega^{*\prime}-\omega^*} + \frac{1}{M} + \frac{1}{9}\frac{1}{\omega^{*\prime}+\omega^*}\Big]$$

$$\mathrm{Re}\,p_{11}(\omega^*) = -\frac{8f^2}{3\omega^*} + \frac{3f^2}{M} + \frac{16}{9\pi}\int_1^K d\omega^{*\prime}\,\frac{\mathrm{Im}\,p_{33}(\omega^{*\prime})}{\omega^{*\prime}+\omega^*}$$

$$\mathrm{Re}\,p_{13}(\omega^*) = \mathrm{Re}\,p_{31}(\omega^*) = \tfrac{1}{4}\,\mathrm{Re}\,p_{11}(\omega^*) - 3f^2/4M\,. \quad (4.22)$$

Here, $\omega^* = W - M$, where W is the total energy in the c.m. system, and K is a cutoff whose value is around M.

According to Eqs. (4.22) the chief variation in Re p_{33} at low energies is due to the Born term $4f^2/3\omega^*$, and the principal value part of the integral. The chief variation of the remaining Re $p_{2T,2J}$ at low energies is due to their Born terms. Further, the main low-energy contribution to the integrals within the brackets in (4.18) and (4.19) is due to the principal value integrals. We can approximate them as follows[104]:

$$\tfrac{1}{2}P\int_1^\infty \frac{d\omega'}{q'}\,\frac{(\sigma_+ + \sigma_-)}{\omega' - \omega_L} \simeq \tfrac{2}{3}P\int_1^\infty \frac{d\omega'}{q'}\,\frac{\sigma_+(\omega')}{\omega'-\omega_L} \simeq \frac{16\pi}{3}\,\frac{M}{W}\,P\int_1^K d\omega'\,\frac{\mathrm{Im}\,p_{33}(\omega')}{\omega'-\omega_L} \simeq \frac{16\pi}{3}\,\frac{M}{W}\,P\int_1^K d\omega^{*\prime}\,\frac{\mathrm{Im}\,p_{33}(\omega^{*\prime})}{\omega^{*\prime}-\omega^*}\,,$$

where we have used $q_L/q = W/M$, $\omega_L = (W^2 - M^2 - 1)/2M \simeq \omega^* W/M$, and

$$\sigma_+(\omega) \simeq 8\pi q\,\mathrm{Im}\,p_{33}(\omega) = 8\pi q_L(M/W)\,\mathrm{Im}\,p_{33}(\omega)\,.$$

Similarly,

$$\tfrac{1}{2}P\int_1^\infty \frac{d\omega'}{q'}\,\frac{(\sigma_- - \sigma_+)}{\omega' - \omega_L} \simeq -\frac{8\pi}{3}\,\frac{M}{W}\,P\int_1^K d\omega^{*\prime}\,\frac{\mathrm{Im}\,p_{33}(\omega^{*\prime})}{\omega^{*\prime}-\omega^*}\,.$$

[104] The approximations used are only intended to give a good account of the *variation* of the various terms with ω_L at low energies.

Now if we substitute the expression (4.22) for Re p_{33} in (4.18) and (4.19) we find that the principal value integrals cancel each other. Further the Born terms in (4.22) contribute $-6f^2/\omega^*$ and 0 to Re $(p_{11} + 2p_{13} - p_{31} - 2p_{33})$ and Re $(p_{11} + 2p_{13} + 2p_{31} + 4p_{33})$, respectively. Using $\omega_L/(\omega_L^2 - 1/4M^2) \simeq M/W\omega^*$, it is seen that the first of these cancels the Born term in (4.19). The Born term in (4.18) is less than $3f^2/M$ so it can be ignored here. [We could go further and show that the terms in (4.22) which are of the form

$$\int_1^K d\omega^{*\prime} \frac{\text{Im } p_{33}(\omega^{*\prime})}{\omega^{*\prime} + \omega^*}$$

cancel the remaining integrals in (4.18) and (4.19).]

The reason for this cancellation is obvious. CGLN[2] obtain the approximations (4.22) for the p waves from the dispersion relations for $A^{(\pm)}(\nu,t)$ and $B^{(\pm)}(\nu,t)$ [Eqs. (1.16) and (1.17)] by assuming *inter alia* that p_{33} is dominant and ignoring the coupling with other partial waves. Naturally their relations must hold for the p-wave contributions to forward scattering, so all the p-wave terms disappear from the right of (4.18) and (4.19). The correct[105] dispersion relations for the p-wave partial amplitudes are considerably more elaborate than (4.22). The unphysical region integral contains coupling with other partial waves, as well as effects of the $T = 0$ and $T = 1$ π–π interactions.[105] However, for values of ω_L between μ and $(\mu + 45$ MeV), the terms given in (4.22) still provide a rough approximation to the *energy dependence* of the p-wave amplitudes. This is because at such energies the long range Born terms are large in p-wave scattering, and they have the strongest energy dependence.

We therefore understand why $C^{(+)}$ and $C^{(-)}$ are constant up to 45 MeV. However for the purposes of this article this constancy is an empirical fact found by fitting Eqs. (4.20) and (4.21) to the low-energy experimental data.[106]

(iii) Relations for the p-Wave Scattering Lengths

The $C^{(\pm)}$ Relations

The quantities $C^{(+)}$ and $C^{(-)}$ which are determined from the low-energy s-wave experimental data can also be used to give relations for the p-wave scattering lengths. These are defined by $a_{2T,2J} = \lim_{\omega \to \mu} p_{2T,2J}(\omega)$. Letting $\omega_L \to 1$ in the terms inside the square brackets in (4.18) and (4.19), we get

$$C^{(+)} = \frac{3}{2\pi^2\zeta}\int_1^\infty d\omega' \frac{\omega'}{q'} \frac{\sigma^{(+)}(\omega')}{\omega'^2 - 1} + \frac{3f^2}{M\zeta(1 - 1/4M^2)^2} - \frac{1}{\zeta^2}(a_{11} + 2a_{13} + 2a_{31} + 4a_{33}) \tag{4.23}$$

$$C^{(-)} = \frac{3}{2\pi^2\zeta}\int_1^\infty \frac{d\omega'}{q'} \frac{\sigma^{(-)}(\omega')}{\omega'^2 - 1} - \frac{6f^2}{\zeta(1 - 1/4M^2)^2} - \frac{1}{\zeta^2}(a_{11} + 2a_{13} - a_{31} - 2a_{33}), \tag{4.24}$$

where $\zeta = (1 + 1/M)$, $\sigma^{(\pm)} = \frac{1}{2}(\sigma_- \pm \sigma_+)$, and ω', q' are the lab system energy and momentum of the pion. Applying theorem B of Sec. 2(ii) it is seen that there is no divergence at the lower end of the range of integration in the integrals (this is the case $\alpha = \frac{1}{2}$ of theorem B). From the very extensive data on σ_+ and σ_- it is easy to evaluate the integrals in (4.23) and (4.24) to high accuracy. This gives[73]

$$\frac{1}{\zeta}(2a_{33} + a_{31}) - \tfrac{1}{3}\zeta(C^{(-)} - C^{(+)}) - \frac{2f^2}{(1 - 1/2M)(1 - 1/4M^2)} = 0.166 \pm 0.006, \tag{4.25}$$

$$\frac{1}{\zeta}(2a_{13} + a_{11}) + \tfrac{1}{3}\zeta(2C^{(-)} + C^{(+)}) + \frac{4f^2(1 - 1/4M)}{(1 - 1/4M^2)^2} = 0.066 \pm 0.004. \tag{4.26}$$

(iv) The B(μ,0) Relations

Letting $\omega_L \to 1$ in Eq. (4.3) gives

$$\text{Re } B(1,0)/4\pi M = \lim_{q^2 \to 0}\left[\frac{1}{2M^2} f_S + \frac{2}{-^2}(f_{P\frac{3}{2}} - f_{P\frac{1}{2}})\right].$$

Thus,

$$a_{31} - a_{33} = \frac{1}{8\pi M}\text{Re } B^{(\frac{3}{2})}(1,0) - \frac{a_3}{4M^2}$$

$$a_{11} - a_{13} = \frac{1}{8\pi M}\text{Re } B^{(\frac{1}{2})}(1,0) - \frac{a_1}{4M^2}, \tag{4.27}$$

where a_1, a_3 are the s-wave scattering lengths and the superscripts on B are the isotopic spin values. It was seen in Secs. 2(vi) and (vii) that the dispersion relations (1.17) for $B^{(\pm)}(\nu,t)$ converge, and no additive constant is required [Sec. 2(ix)]. Using

$$B^{(\frac{3}{2})}(1,0) = B_+(1,0),$$

$$B^{(\frac{1}{2})}(1,0) = \tfrac{3}{2}B_-(1,0) - \tfrac{1}{2}B_+(1,0),$$

---

[105] See for example J. Hamilton, P. Menotti, G. C. Oades, and L. L. J. Vick, Phys. Rev. **128**, 1881 (1962).

[106] The arguments used in reference 105 and related papers to find the π–π interaction from low-energy π–N scattering are based on the s-wave π–N phase shifts. The experimental data are correlated using a more general form of Eqs. (4.20) and (4.21) in which $C^{(\pm)}$ are not assumed constant (cf. reference 75).

we again relate all quantities to $\pi^{\pm}$–p elastic scattering.[107] By (1.17) and (4.27) we get

$$(a_{33} - a_{31}) - 2f^2/(1 - 1/2M) = a_3/4M^2 - \tfrac{1}{2} I_+ , \tag{4.28}$$

$$(a_{13} - a_{11}) - 2f^2(1 - 1/M)/(1 - 1/4M^2) = a_1/4M^2 - \tfrac{3}{4} I_- + \tfrac{1}{4} I_+ , \tag{4.29}$$

where

$$I_{\pm} = \frac{1}{4\pi^2 M} \int_1^{\infty} d\omega' \left[\frac{\operatorname{Im} B_{\pm}(\omega',0)}{\omega' - 1} - \frac{\operatorname{Im} B_{\mp}(\omega',0)}{\omega' + 1} \right],$$

and ω' is the pion lab energy.

The coefficient multiplying the s-wave scattering lengths in (28) and (29) is so small that these terms are very accurately known. It is quite sufficient to use our earlier values[75]

$$a_1 = 0.178 \pm 0.005 , \quad a_3 = -0.087 \pm 0.005$$

here. The integrals $I_{\pm}$ are very closely related to the integral (4.14) used in Sec. 4(i) in the determination of f^2 and the method of evaluation is the same. This gives[73]

$$(a_{33} - a_{31}) - 2f^2/(1 - 1/2M) = 0.079 \pm 0.003 \tag{4.30}$$

$$(a_{13} - a_{11}) - 2f^2(1 - 1/M)/(1 - 1/4M^2) = -0.066 \pm 0.003 . \tag{4.31}$$

(v) The $f_1'(\nu,0)$ Relation

We now examine a relation between $T = \frac{1}{2}$ and $T = \frac{3}{2}$ p-wave scattering lengths which, unlike Eqs. (25) and (26) above, does not involve the s-wave curvature coefficients $C^{(\pm)}$. This relation is obtained by differentiating $A(\nu,t)$, and $B(\nu,t)$ with respect to t at $t = 0$, and it expresses a linear combination of a_{33}, a_{13} and f^2 in terms of a dispersion integral. The disadvantage of this relation is that the dispersion integral cannot be evaluated quite as accurately as those we have previously discussed. This is due to the fact, which is pointed out in Sec. 3(iii), that the partial wave expansions for $\partial A/\partial t$ and $\partial B/\partial t$ do not converge so well as the expansions for A and B. As a result our lack of accurate knowledge of the details of the higher π–N resonances is a strong limitation on the accuracy of the derivative dispersion integrals.

Using Eqs. (2.31) and (1.30) and writing $\Delta^2 = -t/4 = \frac{1}{2} q^2(1 - \cos\theta)$, simple manipulation gives

$$\frac{1}{4\pi} \left.\frac{\partial A}{\partial \Delta^2}\right|_{\Delta^2=0} = -\frac{6M}{q^4} [(\omega_L - \omega_C) f_{P\frac{3}{2}} - (\omega_L + \omega_C) f_{D\frac{3}{2}} + 2(3\omega_L - 2\omega_C) f_{D\frac{5}{2}} - 2(3\omega_L + 2\omega_C) f_{F\frac{5}{2}} + 10(2\omega_L - \omega_C) f_{F\frac{7}{2}} - 10(2\omega_L + \omega_C) f_{G\frac{7}{2}} + 10(5\omega_L - 2\omega_C) f_{G\frac{9}{2}} - 10(5\omega_L + 2\omega_C) f_{H\frac{9}{2}} + \cdots] \tag{4.32}$$

$$\frac{1}{4\pi} \left.\frac{\partial B}{\partial \Delta^2}\right|_{\Delta^2=0} = -\frac{6}{E + M} \frac{f_{P\frac{3}{2}}}{q^2} - \frac{6}{q^4} [(E + M) f_{D\frac{3}{2}} - 2(3M - 2E) f_{D\frac{5}{2}} + 2(2E + 3M) f_{F\frac{5}{2}} - 10(2M - E) f_{F\frac{7}{2}} + 10(E + 2M) f_{G\frac{7}{2}} - 10(5M - 2E) f_{G\frac{9}{2}} + 10(2E + 5M) f_{H\frac{9}{2}} - \cdots] . \tag{4.33}$$

Here, ω_L is the total lab pion energy, and we have written ω_c for the c.m. pion energy $(1 + q^2)^{\frac{1}{2}}$.

Further, by Eq. (1.30)

$$\operatorname{Re} f_1'(\nu,t = 0) = -(2/q^2) \operatorname{Re} (3f_{1+} + 15f_{2+} - 3f_{3-} + \cdots) ,$$

where the prime denotes differentiation with respect to Δ^2, and $f_{l\pm}$ are the partial wave amplitudes. Therefore,

$$a_{33} - a_{13} = \tfrac{1}{2} \operatorname{Re} f_1^{(-)'}(1,0) , \tag{4.34}$$

where, as usual, we put $\mu = 1$. For reasons of convergence, as discussed in Sec. 2(vi), we only consider the $(-)$ charge combination. By Eq. (1.26)

$$\operatorname{Re} f_1^{(-)'}(1,0) = 1/[4\pi(1 + 1/M)] \times [\operatorname{Re} A^{(-)'}(1,0) + \operatorname{Re} B^{(-)'}(1,0)] .$$

Differentiating the $(-)$ dispersion relations (1.16) and (1.17) with respect to Δ^2, and using Eq. (1.34), we get

$$(a_{33} - a_{13}) - 2f^2/[(1 + 1/M)(1 - 1/2M)^2] = \bar{I} , \tag{4.35}$$

where

$$\bar{I} = \frac{1}{\pi(1 + 1/M)} \times \left\{ \int_1^{\infty} \frac{d\omega'}{4\pi} \frac{\operatorname{Im} [A^{(-)'}(\omega',0) + \omega' B^{(-)'}(\omega',0)]}{\omega'^2 - 1} + \frac{1}{M} \int_1^{\infty} \frac{d\omega'}{4\pi} \frac{\operatorname{Im} B^{(-)}(\omega',0)}{\omega' + 1} - \frac{1}{2M} \int_1^{\infty} \frac{d\omega'}{4\pi} \frac{q'}{(\omega' + 1)^2} (\sigma_- - \sigma_+) \right\} . \tag{4.36}$$

Here, ω' and q' are lab values and $\sigma_{\pm}$ are the total $\pi^{\pm}$–p cross sections. We now examine the accuracy with which $\bar{I}$ can be evaluated.

[107] The *subscripts* $\pm$ always refer to $\pi^{\pm} - p$ scattering.

Very High Energies

In the original evaluation of $\bar{I}$ Woolcock[73] assumed that $A^{(-)}$ and $B^{(-)}$ were zero above 2.5 BeV. It is now known that this is not so, and we have to estimate the contributions to $\bar{I}$ from energies above 2 BeV. For this purpose we use the high-energy behavior suggested by the Regge pole method[108,108a] [cf. Sec. 4(i) (f)]. For $\nu > 2$ BeV and small $|t|$ we assume that

$$A^{(-)}(\nu,t) + \nu B^{(-)}(\nu,t) \simeq iF^{(-)}(t)(\nu/\nu_0)^{\alpha_\rho(t)} . \quad (4.37)$$

ν_0 is a constant which is probably of the order of 2 BeV, and $\alpha_\rho(t)$ is the Regge trajectory of the ρ isobar. $F^{(-)}(t)$ can be determined from the shape of the diffraction peak at 2 BeV, which we assume is approximated by Eq. (4.7) above.

First we consider the derivative terms in (4.36). By (4.37)

$$A^{(-)\prime}(\nu,0) + \nu B^{(-)\prime}(\nu,0) = -4i\left(\frac{\nu}{\nu_0}\right)^{\alpha_\rho(0)}\left[\left.\frac{\partial F^{(-)}}{\partial t}\right|_{t=0} + F^{(-)}(0)\left.\frac{\partial \alpha_\rho}{\partial t}\right|_{t=0}\ln\left(\frac{\nu}{\nu_0}\right)\right]. \quad (4.38)$$

For small $|t|$ Eq. (4.7) gives

$$\mathrm{Im}\, f(\theta) \simeq (1 - a)\,\tfrac{1}{2}\,qR^2(1 + \tfrac{1}{8}R^2t) .$$

Hence,

$$\left.\frac{\partial F^{(-)}}{\partial t}\right|_{t=0} \Big/ F^{(-)}(0) = R^2/8 \simeq 0.07 , \quad (4.39)$$

where we use $R = 0.74$ as in Sec. 4(i)(d). Taking the usual estimate[108]

$$\partial\alpha_\rho/\partial t|_{t=0} \simeq 1/50\mu^2 = 0.02 ,$$

it is clear that the term in $\partial\alpha_\rho/\partial t$ in (4.38) is only important for large values of (ν/ν_0). Since the whole contribution to $\bar{I}$ from $\nu > 2$ BeV is small, we can ignore the $\partial\alpha_\rho/\partial t$ term in (4.38) without appreciable error (i.e., the sharpening of the diffraction peak is not important here).

From (4.37) and (1.34)

$$\mathrm{Im}\, f^{(-)}(\omega_L,0) = (M/4\pi W)F^{(-)}(0)(\nu/\nu_0)^{\alpha_\rho(0)} , \quad (4.40)$$

where $f^{(-)}$ is the (c.m. system) forward scattering amplitude for the $(-)$ charge combination. By the optical theorem and (1.31) this gives

$$F^{(-)}(0) = (q_L\sigma^{(-)})|_{2\ \mathrm{BeV}} , \quad (4.41)$$

where q_L is the lab momentum and $\sigma^{(-)} = \frac{1}{2}(\sigma_- - \sigma_+)$. Using $\sigma^{(-)}(2\ \mathrm{BeV}) = 1.3$ mb [cf. Sec. 4(i)(f) and Fig. 2] we get $F^{(-)}(0) = 1.0$. Finally, using $\alpha_\rho(0) \simeq 0.5$ in (4.38), we get

$$\frac{1}{\pi}\int_{2\ \mathrm{BeV}}^{\infty}\frac{d\omega'}{4\pi}\,\frac{\mathrm{Im}\,[A^{(-)\prime}(\omega',0) + \omega' B^{(-)\prime}(\omega',0)]}{\omega'^2 - 1} \simeq -0.001 . \quad (4.42)$$

The errors in this result could be as large as 40%.

The other high-energy contributions to $\bar{I}$ are easily examined. By (4.13)

$$\int_{2\ \mathrm{BeV}}^{\infty}\frac{\sigma^{(-)}(\omega')}{\omega'}\,d\omega' \simeq 0.16 ,$$

so the last term in (4.36) contributes -0.0006 to $\bar{I}$. In Sec. 2(viii), we saw that it is likely that $A(\nu,t)$ does not attain the unitary limit for large ν. If that is so,

$$\mathrm{Im}\, B^{(-)}(\omega',0) \simeq \sigma^{(-)}(\omega') .$$

Thus,

$$\frac{1}{4\pi^2 M}\int_{2\ \mathrm{BeV}}^{\infty}d\omega'\,\frac{\mathrm{Im}\, B^{(-)}(\omega',0)}{\omega' + 1} \simeq \frac{1}{4\pi^2 M}\int_{2\ \mathrm{BeV}}^{\infty}\frac{\sigma^{(-)}(\omega')}{\omega'}\,d\omega .$$

Hence, the Im $B^{(-)}(\omega',0)$ and $\sigma^{(-)}(\omega')$ terms in (4.36) almost cancel each other. Even if this conjecture about $A^{(-)}(\nu,t)$ is not strictly valid, the two integrals will be of the same order of magnitude and tend to cancel. We estimate their sum to be 0 ± 0.0003.

The Higher $\pi - N$ Resonances

Woolcock[73] evaluated Im $A^{(-)\prime}(\omega',0)$ and Im $B^{(-)\prime}(\omega',0)$ up to 2 BeV by Eqs. (4.32) and (4.33), using the methods already discussed in Sec. 4(i). The predominant contributions come from the π–N resonances, and the nonresonant amplitudes or background, was fitted by a smooth curve in the manner indicated in Sec. 4(i). The results are shown in Fig. 8. From Fig. 7 we see that Im $B^{(-)}(\omega',0)$ is much larger near the $(\frac{3}{2}, \frac{3}{2})$ resonance at 180 MeV than it is near the π^-–p $D_{\frac{3}{2}}$ and $F_{\frac{5}{2}}$ resonances at 600 MeV and 900 MeV, respectively. However Fig. 8 shows that Im $B^{(-)\prime}(\omega',0)$ is much larger near the 600-MeV and 900-MeV resonances than it is near 180 MeV, while Im $A^{(-)\prime}(\omega',0)$ has roughly the same magnitude near all three resonances.

This might suggest that the quantity $\bar{I}$ [Eq. (4.36)] can only be evaluated very roughly because of our somewhat poor knowledge of the 600-MeV and 900-MeV resonances. In fact, the situation is not too bad because: (a) the denominator $(\omega'^2 - 1)$ in the first

[108] G. F. Chew and S. C. Frautschi, Phys. Rev. Letters **7**, 394 (1961) and **8**, 41 (1962).

[108a] *Note added in proof.* If the diffraction peak does not shrink, then possibly $\alpha_\rho'(0) \simeq 0$, and the argument in the paragraph containing Eq. (4.38) is even stronger. The remainder of the argument is similar to the use of Eq. (4.12) as a convenient parametrization.

integral in (4.36) damps down the effect of the higher resonances; and (b) Eqs. (4.32) and (4.33) show that in the range 600 MeV–1.5 BeV there is considerable cancellation between the contribution to Im $A^{(-)\prime}$ and Im $B^{(-)\prime}$ from any partial wave. (The 900-MeV resonance contributes of the order of 0.005 to $\bar{I}$, whereas the value of $\bar{I}$ is about 0.08.)

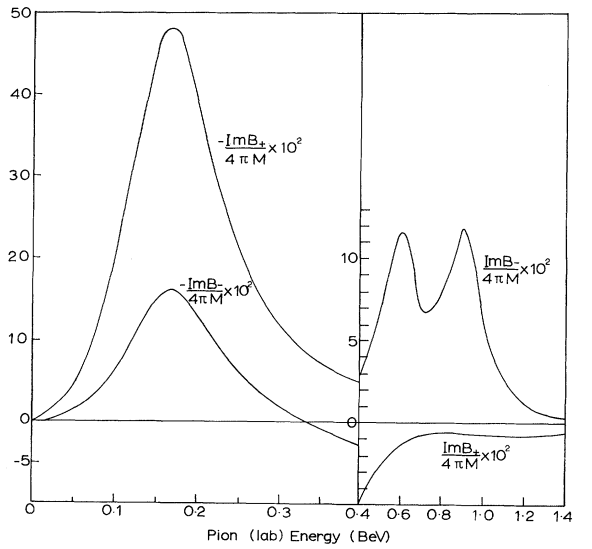

FIG. 7. The values of Im $B_+(\omega_L,0)$ and Im $B_-(\omega_L,0)$ up to 1.4 BeV. The vertical scales are in natural units ($\hbar = c = \mu = 1$).

There are of course appreciable uncertainties in the moderately high-energy contributions to $\bar{I}$. We must remember that: (i) the partial wave expansions for Im $A^{(-)\prime}$ and Im $B^{(-)\prime}$ converge very slowly above 500 MeV [cf. Sec. 3(iii) for estimates of the rate of convergence]; and (ii) there is no adequate phase-shift analysis of the experimental data at 600 MeV or above.[109] Thus it is quite possible that a number of nonresonant partial waves with high angular momentum contribute to Im $A^{(-)\prime}$ and Im $B^{(-)\prime}$ in a way which is noticeably different from the smooth curve Woolcock used to fit the nonresonant parts. For example, suppose that in an energy range of 100 MeV around 1.3 BeV, Im $f_{H\frac{3}{2}}^{(-)} = 0.1/2q$. From (4.32) and (4.33) we see that this contributes 0.0004 to $\bar{I}$. Lack of knowledge of these higher partial waves, together with the uncertainty about the π^+–p system in the 1.2–1.4 BeV range [cf. Sec. 4(ii)(d)] could give rise to an error in $\bar{I}$ which we estimate to be ± 0.003.

[109] See R. Omnes and G. Valladas (reference 85) for some discussion of the difficulties and uncertainties in such an analysis.

The Result

Using the values in Figs. 7 and 8 and the very high-energy estimates given above, $\bar{I}$ can be evaluated. Errors, in addition to those mentioned, can also arise from the uncertainties in the predominant partial wave amplitudes. We get the result

$$\bar{I} = +0.078 \pm 0.006 .$$

Inserting in (4.35), we get

$$(a_{33} - a_{13}) - 2f^2/[(1 + 1/M)(1 - 1/2M)^2] = 0.078 \pm 0.006 . \quad (4.43)$$

It should be emphasized that we believe that the error $\pm$ 0.006 includes the various uncertainties in the values of Im $A^{(-)\prime}$ and Im $B^{(-)\prime}$ at moderately high energies due to the unknown role of higher partial wave amplitudes.

(vi) Rough Estimate of the p-Wave Scattering Lengths

We now derive rough estimates of the p-wave scattering lengths by using Eqs. (4.15), (4.30), (4.31), and (4.43). First it is necessary to have a value for a_{33}, and for the present purpose we use the value obtained by fitting Eq. (4.5) to the experimental values of α_{33}, given in Table V, and extrapolating to threshold. This gives[73]

$$a_{33} = 0.220 \pm 0.008 . \quad (4.44)$$

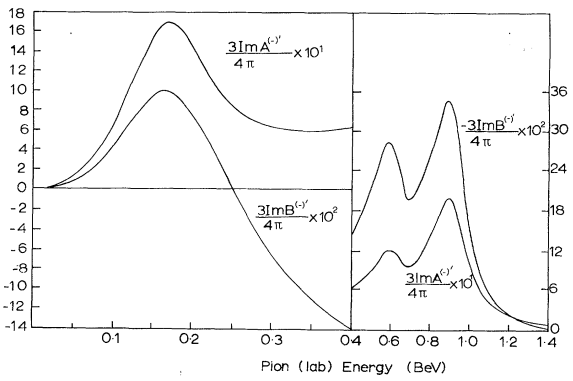

FIG. 8. The values of Im $A^{(-)\prime}$ and Im $B^{(-)\prime}$ up to 1.4 BeV. The vertical scales are in natural units.

The error here allows for some deviation from the form (4.5) at very low energies (no deviation from (4.5) is detected between 40 MeV and 190 MeV).

Using $f^2 = 0.081 \pm 0.003$ [Eq. (4.15)] and Eqs. (4.30) and (4.44) we get

$$a_{31} = -0.034 \pm 0.011 . \quad (4.45)$$

Similarly Eq. (4.43) gives

$$a_{13} = -0.022 \pm 0.012 . \quad (4.46)$$

Finally, Eqs. (4.31) and (4.43) give

$$a_{11} = -0.095 \pm 0.016 . \quad (4.47)$$

These results for a_{31}, a_{13}, and a_{11} depend very little on the s-wave π–N data [we have not used Eqs. (4.25) and (4.26) in deriving them]. They are obtained from dispersion relations whose predominant contributions are given by the total cross sections $\sigma_{\pm}$ and the resonant amplitudes. In all cases the contribution of the $(\frac{3}{2}, \frac{3}{2})$ resonance is much the most important.

The errors quoted in (4.45), (4.46), and (4.47) are obtained by assuming that the errors in (4.15), (4.30), (4.31), and (4.43) are independent. This is not strictly true, but it should be a good approximation. This is because the largest errors arise from f^2, a_{33}, and Eq. (4.43). The procedure [Sec. 4(i)] for finding f^2 is such that errors in f^2 are largely independent of errors in evaluating (4.43), and the same holds for a_{33}.

It is worth noting that if we were to change the value of f^2 by Δf^2, this would alter the values of a_{31} and a_{13} by $-2\Delta f^2$, and a_{11} by $-4\Delta f^2$.

Comparison with Experiment

Little experimental evidence about the small p-wave phase shifts at low energy is available. Barnes *et al.*[110] have examined π^+–p scattering at 24.8, 31.5, and 41.5 MeV. Assuming $\alpha_{31} = a_{31}q^3$, their results give $a_{31} = -0.042 \pm 0.004$. In fact the q^3 dependence will not be quite correct, and we suggest that these experiments give $a_{31} = -0.042 \pm 0.008$.

Knapp and Kinsey[111] have investigated π–N scattering at 30.0 and 31.5 MeV. Again assuming $\alpha_{31} = a_{31}q^3$ their results give $a_{31} = -0.038 \pm 0.008$ (solutions I and II). Clearly these values of a_{31} are in good agreement with our result (4.45).

Now we look at the experimental results for α_{31} and α_{11}. Barnes *et al.*[110] results at 35.75 MeV give (assuming q^3 dependence),[112]

$$a_{13} = -0.06 \pm 0.04 , \quad a_{11} = -0.02 \pm 0.09 .$$

These mean values disagree with Eq. (4.31) which gives

$$a_{13} - a_{11} = +0.073 \pm 0.010 . \quad (4.48)$$

Knapp and Kinsey[111] (again assuming q^3 dependence)[112] get

$$a_{13} = +0.010 \pm 0.019 , \quad a_{11} = -0.169 \pm 0.037 \quad \text{(solution I)} ,$$

$$a_{13} = -0.196 \pm 0.020 , \quad a_{11} = +0.235 \pm 0.036 \quad \text{(solution II)} .$$

Knapp and Kinsey suggest that solution II is preferable, because it gives the best agreement with their charge-exchange ($\pi^- + p \rightarrow \pi^0 + n$) data[113] at 31 MeV. Our result (48) rules out solution II. Also (4.48) is not in particularly good agreement with solution I, but we note that even for solution I, a_{11} is surprisingly large.

The Liverpool experiments at 97 and 98 MeV give[114]

$$\alpha_{31}/q^3 = -0.029 \pm 0.002 ,$$

$$\alpha_{13}/q^3 = -0.007 \pm 0.004 ,$$

$$\alpha_{11}/q^3 = -0.024 \pm 0.002.$$

These results for α_{31} and α_{13} could be in good agreement with our results (4.45) and (4.46) if we assume there is a small departure from the q^3 dependence by 95 MeV. The α_{11} result is only consistent with (4.47) if there is an appreciable departure from q^3 dependence. We shall see in Sec. 5(iv) below that the improved CGLN calculations do indeed predict the correct departures from q^3 dependence to give good agreement between these Liverpool results and our values of a_{31}, a_{13}, and a_{11} [Eqs. (4.45), (4.46), and (4.47)].

(vii) Woolcock's Evaluation of the Parameters

Woolcock[73] used further relations and a more sophisticated method to find the best values of the 9 parameters: f^2, the s-wave parameters a_1, a_3, $C^{(+)}$, $C^{(-)}$, and the p-wave scattering lengths $a_{2T,2J}$. We briefly describe the method and give the results (where necessary the input data have been improved, and the results in Eq. (4.49) are slightly different from the original results[115]).

The following input data were used:

(1) The value $f^2 = 0.081 \pm 0.003$ determined by the method of Sec. 4(i) [Eq. (15)].

[110] S. W. Barnes *et al.* (cf. reference 76).

[111] D. E. Knapp and K. F. Kinsey, Bull. Am. Phys. Soc. **6**, 435 (1961). We are indebted to Dr. Barnes and Dr. Kinsey for further information about these experiments.

[112] It is unlikely that the assumption of q^3 dependence introduces any large error at 30 MeV. The deviation from q^3 dependence is discussed in Sec. 5(iv) below.

[113] The charge-exchange data were not used in deriving their phase shifts. Its only use was in choosing between solutions I and II.

[114] D. N. Edwards, S. G. F. Frank, and J. R. Holt, Proc. Phys. Soc. (London) **73**, 856 (1959). Also D. N. Edwards and T. Massam, private communications. We are indebted to these authors for communicating their results.

[115] W. S. Woolcock, *Proceedings of the International Conference on High-Energy Physics, Aix-en-Provence, 1961* (C.E.N. Saclay, France, 1961), Vol. I, pp. 459 and 461.

(2) The value $a_1 - a_3 = 0.254 \pm 0.012$ from the Panofsky ratio.[116]

(3) The forward dispersion relations (2.6) fitted to 18 accurate experimental values of $D_+(\omega)$ or $D_-(\omega)$ up to 220 MeV. These relations involve f^2, a_1 and a_3 as parameters to be determined. The dispersion integrals are evaluated using the known data for $\sigma_\pm$.

(4) The sum rule (2.27). This involves f^2 and $(a_1 - a_3)$ as parameters. The errors in evaluating the integral are of course much larger here than in the forward dispersion relations.

(5) 18 accurate experimental determinations of the s-wave phase shifts α_1 or α_3 (up to 45 MeV) are fitted to the Eqs. (4.20) and (4.21) of Sec. 4(ii). Here a_1, a_3, $C^{(+)}$, $C^{(-)}$ are the parameters which are determined.

(6) Equations (4.25) and (4.26) which relate $a_{2T,2J}$, $C^{(+)}$, $C^{(-)}$ and f^2.

(7) The $B(\mu,0)$ relations, Eqs. (4.30) and (4.31) involving $(a_{2T,3} - a_{2T,1})$ and f^2. ($T = \frac{1}{2}, \frac{3}{2}$.)

(8) The $f_1'(\mu,0)$ relation (4.43) involving $(a_{33} - a_{13})$ and f^2.

(9) The value $a_{33} = 0.220 \pm 0.008$ [Eq. (4.44)] obtained by fitting Eq. (4.5) to the low-energy values of α_{33} given in Table III [Sec. 4(i)].

(10) The value $a_{31} = -0.038 \pm 0.008$ from the analysis of Knapp and Kinsey.[111]

Each piece of the data was given the weight $p = 1/\sigma^2$ where σ is the appropriate standard error. Using an error-matrix method the values obtained for the 9 parameters are

$$\begin{gathered} f^2 = 0.081 \pm 0.002\ ; \\ a_1 = 0.171 \pm 0.005\ , \quad a_3 = -0.088 \pm 0.004\ , \\ C^{(-)} = -0.094 \pm 0.013\ , \quad C^{(+)} = -0.096 \pm 0.026\ ; \\ a_{31} = -0.038 \pm 0.005\ , \quad a_{33} = 0.215 \pm 0.005\ , \\ a_{11} = -0.101 \pm 0.007\ , \quad a_{13} = -0.029 \pm 0.005\ . \end{gathered} \tag{4.49}$$

Comments

The errors quoted for f^2 and $a_{2T,2J}$ are smaller than those given in Secs. 4 (i) and 4 (vi) because of the extra independent data which have been used here (in particular the s-wave data and the forward-scattering data).

There are some small changes in the p-wave scattering lengths $a_{2T,2J}$ compared with the values given in Eqs. (4.44), (4.45), (4.46), and (4.47). These changes are however well within the errors given in Eqs. (4.44)–(4.47). The main reason for these changes is Eqs. (4.25) and (4.26) which relate the s-wave and p-wave parameters. $C^{(+)}$ and $C^{(-)}$ are determined from the s-wave experimental data, and using these values given in (4.49) and $f^2 = 0.081$, Eq. (4.25) yields $2a_{33} + a_{31} = 0.392$. On the other hand Eqs. (4.44) and (4.45) yield $2a_{33} + a_{31} = 0.405$. Thus (4.25) requires that both a_{33} and a_{31} are reduced somewhat from the values given in (4.44) and (4.45). Similarly, inserting $C^{(+)}$, $C^{(-)}$ and f^2 in (4.26) we get $2a_{13} + a_{11} = -0.159$. On the other hand, Eqs. (4.46) and (4.47) give $2a_{13} + a_{11} = -0.140$. So (4.26) requires that a_{13} and a_{11} become a little more negative than the values given by (4.46) and (4.47).

The error in the experimental value of a_{33} in Eq. (4.44) is large (± 0.008) and we might start the arguments in Sec. 4(vi) above from $a_{33} = 0.215$. This would give $a_{31} = -0.039$, $a_{13} = -0.027$, $a_{11} = -0.100$ instead of the values in Eqs. (4.45), (4.46), and (4.47). These values are close to those in (4.49). It is therefore clear that in Woolcock's method of determining the parameters the experimental value of a_{33} [item (9)] plays a small role. He is in effect determining a_{33} from the dispersion relation (4.25) and the experimental low energy s-wave data.

It might be thought better to omit item (10) (i.e., the experimental estimate of a_{31}). In fact omitting it causes hardly any change in the results (4.49).

Woolcock[73] points out that the consistency of the data is strong support for the assumption that there is no arbitrary additive constant in the sum rule or in the $B_\pm$, $A^{(-)\prime}$, and $B^{(-)\prime}$ dispersion relations [cf. Secs. 2(iv) and 2(ix) above].

The low-energy behavior of the s-wave phase shifts, obtained by inserting the values for a_1, a_3, $C^{(+)}$, and $C^{(-)}$ given by (4.49), in Eqs. (4.20) and (4.21) is in good agreement with our earlier parametric fit.[117] Here of course we deal with the phase shifts after the appropriate inner Coulomb correction[117] has been made. For very low energies (up to 0.15 MeV) the s-wave phase shifts have the form

$$\begin{gathered} (\sin 2\alpha_1)/2q = 0.171 - 0.024q^2 \\ \text{or} \quad \alpha_1/q = 0.171 - 0.021q^2 \\ (\sin 2\alpha_3)/2q = -0.088 - 0.051q^2 \\ \text{or} \quad \alpha_3/q = -0.088 - 0.052q^2\ . \end{gathered} \tag{4.50}$$

These are in reasonable agreement with Eqs. (27) of reference 117, but (4.50) is an improved result and its derivation included some extra accurate experimental results.

[116] This is a refinement of the work in reference 75 using more recent experimental data on photoproduction and the Panofsky ratio.

[117] J. Hamilton and W. S. Woolcock. Phys. Rev. **118**, 291 (1960). See especially Eqs. (25) and the broken curves in Fig. 3 of that paper.

(iii) Another Determination of the p-Wave Scattering Lengths

Another way of obtaining information about the p-wave scattering lengths is provided by the analysis of the π–N partial wave amplitudes based on the Mandelstam representation.[118] The argument runs as follows. The s-wave π–N amplitudes can be analyzed using the accurate information we have for the s-wave π–N scattering up to 120 MeV, together with: (a) *rough* information on the s-wave π–N scattering at higher energies; (b) information on the $T = \frac{3}{2}$, $J = \frac{3}{2}$, amplitude [as in Sec. 4(i)(a)]; and (c) *rough* information on the small p-wave amplitudes and the higher π–N resonances.

Inserting these data in the dispersion relations for the s-wave π–N amplitudes we can deduce the contribution of the $T = 0$ and $T = 1$ π–π scattering to s-wave π–N scattering, and ultimately, obtain considerable information about the $T = 0$ and $T = 1$ π–π scattering.

Next it is *assumed* that the $T = 0$ π–π scattering obeys a simple (relativistic) effective-range formula at low energies. This is merely done to exclude any strange behavior of the $T = 0$ π–π phase shift, δ_0^0 at low energies (such as δ_0^0 changing sign at a low energy). Also it is assumed that the $T = 1$ π–π scattering is dominated by a resonance in the region $24 \leqslant t \leqslant 30$).

Now the information about the π–π interactions which was obtained from the s-wave π–N dispersion relations is fed into the dispersion relations for the p-wave π–N amplitudes. Then it appears that, in effect,[119] we can predict[120] the p-wave π–N phase shifts at low energies provided we know their experimental values accurately at one energy. For the latter purpose the Liverpool results[110] at 97–98 MeV are used.

The results of this procedure are

$$a_{31} = -0.032\,, \quad a_{33} = 0.219\,, \quad a_{11} = -0.090\,, \quad a_{13} = -0.016\,. \quad (4.51)$$

The errors in each case are of the order of ± 0.008. These values are somewhat in disagreement with those in (4.49) but only in the case of a_{13} is the difference very marked. It should be emphasized that these values in Eq. (4.51) are obtained by a more complicated and less direct method than are the values in Eq. (4.49).

[118] J. Hamilton, P. Menotti, G. C. Oades, and L. L. J. Vick, Phys. Rev. **128**, 1881 (1962).

[119] For details see Sec. 3(xi) of reference (118).

[120] In practice, the low-energy p-wave phase shifts deduced in Sec. 5(iv) below are used, and the partial wave method suggests corrections to these values at low energies.

(ix) Conclusions

The best values of f^2 and the s-wave π–N parameters are given in Eq. (4.49). Concerning the p-wave scattering lengths we must provisionally accept the values given in Eq. (4.49) as being the best given at present by using the experimental results and simple direct theoretical techniques. There is, however, a possibility, as indicated in the preceding section, that with improved information these values will move in the direction of those given in Eq. (4.51).

The fact that such consistent results can be obtained by using a variety of dispersion relations derived from (1.16) and (1.17) is very strong evidence for the validity of the fixed-momentum transfer-dispersion relations in π–N scattering. The fact that the results (4.51) are so close to those in (4.49) is evidence for the validity of the Mandelstam relations as applied to π–N partial wave amplitudes, at least for the values of the complex variable s [Eq. (1.5)] lying within about 30 units from the physical threshold $s = 60$, or from the crossed threshold $s = 33$.

5. CALCULATION OF THE PARTIAL WAVE AMPLITUDES

The partial wave π–N amplitudes have been calculated by Woolcock[73,115] at energies up to a few hundred MeV. The calculations use the (fixed-momentum transfer) dispersion relations for $A(\nu,t)$ and $B(\nu,t)$ given by Eqs. (1.16), (1.17), and (2.36). In the case of $A^{(+)}(\nu,t)$ a subtraction is necessary [cf. Secs. 2(vi) and 2(viii)]. The pion–nucleon parameters which have been determined in Sec. 4 are essential for these calculations. As in Sec. 4 the dispersion integrals are approximated by a careful evaluation of the contributions from the various π–N resonances plus a rough idea of the background, or nonresonant, parts of the absorptive terms.

Here, we give a brief account of the method and discuss the results. We also study the accuracy which can be achieved and we examine the practical limitations of the method.

(i) The Method

In Sec. 3(v) we discussed the expansion of the partial wave amplitudes $f_{l\pm}$ in terms of the amplitudes $f_1(\theta = 0)$ and $f_2(\theta = 0)$ and their derivatives with respect to $\Delta^2 = \frac{1}{2} q^2(1 - \cos\theta)$. Using Eqs. (1.26), f_1 and f_2 are expressed in terms of $A(\nu,t)$ and $B(\nu,t)$, and these amplitudes satisfy the dispersion relations (1.16), (1.17), and (2.36) [in the case of $A^{(+)}(\nu,t)$]. This is the CGLN method,[2] but with considerable improvement in execution. CGLN make the approximations: (a) there is no subtraction in the $A^{(+)}$

relation; (b) in calculating s-wave amplitudes the d-wave corrections are ignored; (c) the dispersion integrals are given by the $(\frac{3}{2}, \frac{3}{2})$ resonance alone, except in the case of the s-wave amplitudes where Im f_{0+} is also included; and (d) kinematical factors are expanded in powers of (μ/M), and only terms up to order (μ/M) are retained. [The CGLN results for p waves are given in Eq. (4.22).] Woolcock does not make the approximations (a), (c), and (d). In all cases he only ignores f waves and higher. It will become clear that these improvements are essential if reasonable accuracy is to be achieved.

Woolcock uses Eqs. (1.26), (1.35), and (1.36) to write

$$\begin{aligned}\operatorname{Re} f_1(\omega_L,0) &= \frac{E+M}{2W}\left\{D(\omega_L) - [\omega_L - (W-M)]\frac{\operatorname{Re} B(\omega_L,0)}{4\pi}\right\},\\ \operatorname{Re} f_2(\omega_L,0) &= \frac{E-M}{2W}\left\{-D(\omega_L) + [\omega_L + (W+M)]\frac{\operatorname{Re} B(\omega_L,0)}{4\pi}\right\},\end{aligned} \tag{5.1}$$

where $D(\omega_L)$ is the forward scattering amplitude (in the lab system). This form has the advantage[121] that $D_\pm(\omega_L)$ obey the dispersion relations (2.6) in which the absorptive parts are given by the total cross sections $\sigma_\pm(\omega_L)$; also the absorptive parts Im $B_\pm(\omega_L,0)$ in the relations for Re $B_\pm(\omega_L,0)$ have already been thoroughly investigated in Sec. 4(i). The first derivative functions are given by

$$\begin{aligned}\operatorname{Re} f_1'(\omega_L,0) &= \frac{E+M}{2W}\frac{1}{4\pi}[\operatorname{Re} A'(\omega_L,0) + (W-M)\operatorname{Re} B'(\omega_L,0)]\\ \operatorname{Re} f_2'(\omega_L,0) &= \frac{E-M}{2W}\frac{1}{4\pi}[-\operatorname{Re} A'(\omega_L,0) + (W+M)\operatorname{Re} B'(\omega_L,0)],\end{aligned} \tag{5.2}$$

where the dash denotes differentiation with respect to Δ^2 at $\Delta^2 = 0$. The evaluation of the first derivative dispersion relations has already been discussed in Sec. 4(v) above. The $A^{(+)\prime}(\omega_L,0)$ relation requires a subtraction [cf. Secs. 2(vi), 2(viii), and Eqs. (4.7), (4.8)]. The subtraction constant at threshold is given by the combination $(a_{13} + 2a_{33})$ of p-wave scattering lengths together with the value of $B^{(+)\prime}(\mu,0)$ (which is given by the $B^{(+)\prime}$ dispersion relation).[122]

[121] A further advantage in using Eq. (5.1) is that the subtraction required by the presence of $A^{(+)}$ is made more accurately in the case of $D_\pm$ than it would be for $A^{(+)}$ itself.

[122] Alternatively it is clear from Eq. (3.14) that the subtraction constant for $f_1{}^{(+)\prime}(\omega_L,0)$ is given by $(a_{13} + 2a_{33})$.

Finally to include d waves, it is necessary to use the second-derivative functions

$$\begin{aligned}\operatorname{Re} f_1''(\omega_L,0) &= \frac{E+M}{2W}\frac{1}{4\pi}[\operatorname{Re} A''(\omega_L,0) + (W-M)\operatorname{Re} B''(\omega_L,0)],\\ \operatorname{Re} f_2''(\omega_L,0) &= \frac{E-M}{2W}\frac{1}{4\pi}[-\operatorname{Re} A''(\omega_L,0) + (W+M)\operatorname{Re} B''(\omega_L,0)].\end{aligned} \tag{5.3}$$

Typical dispersion relations used here are (with $\mu = 1$)

$$\begin{aligned}\frac{1}{4\pi}\operatorname{Re} B^{(+)\prime\prime}(\omega_L,0) &= -\frac{16f^2}{M(\omega_L - 1/2M)^2}\\ &+ \frac{2\omega_L}{\pi}P\int_1^\infty \frac{d\omega'}{4\pi}\frac{\operatorname{Im} B^{(+)\prime\prime}(\omega',0)}{(\omega'^2 - \omega_L^2)}\\ &- \frac{4}{\pi M}\int_1^\infty \frac{d\omega'}{4\pi}\frac{\operatorname{Im} B^{(+)\prime}(\omega',0)}{(\omega' + \omega_L)^2}\\ &- \frac{2}{\pi M^2}\int_1^\infty \frac{d\omega'}{4\pi}\frac{\operatorname{Im} B^{(+)}(\omega',0)}{(\omega' + \omega_L')^3},\end{aligned} \tag{5.4}$$

$$\begin{aligned}\frac{1}{4\pi}\operatorname{Re} A^{(+)\prime\prime}(\omega_L,0) &= K +\\ \frac{2q_L^2}{\pi}P\int_1^\infty \frac{d\omega'}{4\pi}\operatorname{Im} A^{(+)\prime\prime}(\omega',0)\frac{\omega'}{q'^2(\omega'^2 - \omega_L^2)}\\ &+ \frac{4}{\pi M}\int_1^\infty \frac{d\omega'}{4\pi}\frac{\operatorname{Im} A^{(+)\prime}(\omega',0)}{(\omega' + \omega_L)^2}\\ &+ \frac{2}{\pi M^2}\int_1^\infty \frac{d\omega'}{4\pi}\frac{\operatorname{Im} A^{(+)}(\omega',0)}{(\omega' + \omega_L)^3}.\end{aligned} \tag{5.5}$$

In the $A^{(+)\prime\prime}$ relation the subtraction has only been made in the first integral. K is the subtraction constant, and it can only be evaluated from experimental knowledge of the $(+)$ combination of d-wave phase shifts. The need for subtraction in the $A^{(+)\prime\prime}$ relation means that the system of equations is not closed. Further, as we shall see, the present experimental data are not good enough to determine K with accuracy.

The absorptive parts in the first integrands in Eqs. like (5.4) and (5.5) are determined from the experimental data using

$$\begin{aligned}\frac{1}{4\pi}A''(\omega_L,0) &= \frac{60}{q^4}\frac{W+M}{E+M}f_{D_{\frac{3}{2}}} - \frac{60}{q^6}(\omega_L + \omega_C)\\ &\times Mf_{F_{\frac{5}{2}}} + \frac{120}{q^6}(4\omega_L - 3\omega_C)Mf_{F_{\frac{7}{2}}}\\ &- \frac{120}{q^6}(4\omega_L + 3\omega_C)Mf_{G_{\frac{7}{2}}}\\ &+ \frac{420}{q^6}(5\omega_L - 3\omega_C)Mf_{G_{\frac{9}{2}}} - \cdots\end{aligned} \tag{5.6}$$

$$\frac{1}{4\pi}B''(\omega_L,0) = \frac{60}{E+M}\frac{f_{D\frac{5}{2}}}{q^4} + \frac{60}{q^6}(E+M)f_{F\frac{5}{2}} - \frac{120}{q^6}(4M-3E)f_{F\frac{7}{2}} + \frac{120}{q^6}(4M+3E)f_{G\frac{7}{2}} - \frac{420}{q^6}(5M-3E)f_{G\frac{9}{2}} + \cdots, \quad (5.7)$$

where ω_C is the c.m. pion energy, and q is the c.m. pion momentum. The absorptive parts Im A'' and Im B'' are evaluated using the data on the resonances and the optical model discussed in Secs. 4(i) (d) and (c). It is obvious, by comparing Eqs. (5.6) and (5.7) with (4.3), (4.32), and (4.33), that the errors in Im A'' and Im B'' due to ignoring higher partial waves are more serious than in the case of Im B, Im A', and Im B'. At the best the determinations of Re $f_1''(\omega_L,0)$ and Re $f_2''(\omega_L,0)$ are only rough, and the information obtained about the d waves is little more than qualitative.

(ii) Errors Arising From the Evaluation of the Dispersion Relations

Wherever it is practical Woolcock subtracts the dispersion relations. For example the dispersion relations (2.6) give[73]

$$D^{(+)}(\omega_L) = D^{(+)}(\mu) \mp \frac{q_L^2}{2\pi^2}\int_1^\infty d\omega'\,\frac{\omega'}{q'}\,\frac{\sigma^{(+)}(\omega')}{\omega'^2-1} + \frac{q_L^2 f^2}{M(1-1/4M^2)(\omega_L^2-1/4M^2)} + \frac{q_L^4}{2\pi^2}\left\{\int_1^{\omega_0}\frac{d\omega'}{q'}\,\frac{1}{\omega'-1}\left[\frac{\omega'\sigma^{(+)}(\omega')}{(\omega'^2-\omega_L^2)(\omega'+1)} + \frac{\sigma^{(+)}(1)}{2q_L^2}\right] + \frac{\sigma^{(+)}(1)}{2q_L^2}\cot\left(\frac{\theta_0}{2}\right) + P\int_{\omega_0}^\infty \frac{d\omega'}{q'^3}\,\frac{\omega'\sigma^{(+)}(\omega')}{\omega'^2-\omega_L^2}\right\} \quad (5.8)$$

where ω_0 is a constant and $1 < \omega_0 < \omega_L$. Also $\omega_0 = \sec\theta_0$, and ω_L, q_L; ω', q' are lab values. The form of the first integral inside the square bracket ensures that there is no difficulty for $\omega' = 1$.

Similarly the $B^{(+)}$ relation can be written in the form

$$\frac{1}{4\pi M}\,\mathrm{Re}\,B^{(+)}(\omega_L,0) = -\frac{4f^2\omega_L}{\omega_L^2-1/4M^2} + \frac{2\omega_L}{\pi}\int_1^\infty\frac{d\omega'}{4\pi M}\,\frac{\mathrm{Im}\,B^{(+)}(\omega',0)}{q'^2} + \frac{2\omega_L q_L^2}{\pi}\int_1^\infty\frac{d\omega'}{4\pi M}\,\frac{\mathrm{Im}\,B^{(+)}(\omega',0)}{q'^2(\omega'^2-\omega_L^2)}. \quad (5.9)$$

The subtraction terms in Eqs. (5.8) and (5.9) are written in integral form. They are related to the p-wave scattering lengths and $C^{(+)}$ by Eq. (4.23) and equations similar to (4.28) and (4.29). The integral form of the subtraction term in Eq. (5.8) is the most accurate value of this term and its value deduced from (4.25) and (4.26) is used. For the subtraction term in Eq. (5.9) the p-wave scattering lengths given by (4.49) are used.

The advantage of using subtracted dispersion relations is that for low energies (up to about 100 MeV) the errors in the partial-wave amplitudes relative to the scattering lengths determined in Sec. 4 will be small. Also, any errors arising from the evaluation of the principal value integrals are reduced considerably. The disadvantage of this method is that at higher energies the errors arising from the subtracted terms themselves can become large.

The effect of subtractions in reducing errors in evaluating the dispersion integrals is important here in connection with contributions from the π–N resonances above 500 MeV. There are further factors which tend to reduce the errors in these contributions. For example, Omnes and Valladas[85] suggest that at the 900-MeV resonance there may be an appreciable amount of $D_{\frac{5}{2}}$ amplitude in addition to the resonant $F_{\frac{5}{2}}$ amplitude. From Eqs. (4.32) and (4.33) it is seen that the numerical and kinematic factors in the expansion of Im A' and Im B' already reduce the size of the $D_{\frac{5}{2}}$ contributions relative to the $F_{\frac{5}{2}}$ contributions. Equations (5.6) and (5.7) above show that the same is true for Im A'' and Im B''. At 600 MeV, Omnes and Valladas[85] suggest that in addition to the resonant $D_{\frac{3}{2}}$ amplitude there is some $P_{\frac{3}{2}}$ amplitude and only a small amount of $D_{\frac{5}{2}}$ amplitude. Again Eqs. (4.32), (4.33), (5.6), and (5.7) show that this situation is favorable for accurate calculations. [For the amplitudes D and B the absorptive parts are the total cross sections $\sigma_\pm$ and Im $B_\pm$. The values of $\sigma_\pm$ are well known and the accurate evaluation of Im $B_\pm$ is discussed in Sec. 4(i)]. The result of all this is that the dominant errors in calculating the dispersion relations, at least up to 350 MeV, will come from the subtraction terms.

We now make rough estimates of the probable errors in Woolcock's evaluation of the dispersion relations. First consider Re $f_1^{(+)}(\omega_L,0)$ and Re $f_2^{(+)}(\omega_L,0)$. The subtraction term in Eq. (5.8) for $D^{(+)}(\omega_L)$ is evaluated from (4.25) and (4.26). This gives $q_L^2(0.133 \pm 0.004)$. This leads to an error $\pm q_L^2(0.004)$ in Re $f_1^{(+)}(\omega_L,0)$ [relative to Re $f_1^{(+)}(1,0)$] and a very small error in Re $f_2^{(+)}(\omega_L,0)$.

The second term on the right of Eq. (5.9) for Re $B^{(+)}$ is approximately $\frac{2}{3}\,\omega_L(a_{11} - a_{13} + 2a_{31} - 2a_{33})$. By Eq. (4.49) this gives $-\omega_L(0.387 \pm 0.007)$. [The

values given by Eq. (4.51), or (4.44)–(4.47), differ little from this value.] By (1.31) and (1.32)

$$\omega_L - (W - M) = (E - M)W/M \simeq q_L q/M ,$$

on using $E - M \simeq q^2/2M$ (q_L and q are the lab and c.m. pion momenta). Thus, Re $B^{(+)}$ contributes an error in Re $f_1^{(+)}(\omega_L,0)$ [relative to Re $f_1^{(+)}(1,0)$] of $\pm\omega_L q_L q(0.0035)$. Similarly, the error in Re $f_2^{(+)}(\omega_L,0)$ is $\pm\omega_L q^2(0.0035)$.

The total errors in Re $f_1^{(+)}(\omega_L,0)$ (relative to Re $f_1^{(+)}(1,0)$) at 100 MeV and 200 MeV are thus estimated to be ± 0.015 and ± 0.05, respectively. In each case the error from Re $B^{(+)}$ is dominant. The errors in Re $f_2^{(+)}(\omega_L,0)$ at 100 MeV and 200 MeV are $\pm q^2(0.006)$ and $\pm q^2(0.008)$, respectively. Between 200 MeV and 350 MeV, $D^{(+)}(\omega_L)$ can be calculated more accurately from Eqs. (2.6) than from Eq. (5.8). Since the errors in Re $B^{(+)}$ are dominant this is little help. At 300 MeV the errors in Re $f_1^{(+)}(\omega_L,0)$ and Re $f_2^{(+)}(\omega_L,0)$ are ± 0.08 and $\pm q^2(0.011)$, respectively.

In the $(-)$ case the subtraction term in the equation for $D^{(-)}(\omega_L)$ is $\omega_L q_L^2(-0.033 \pm 0.003)$. The subtraction term in the dispersion relation for Re $B^{(-)}/4\pi M$ is given by (4.30) and (4.31). It is $\frac{2}{3}$ (0.145 $\pm$ 0.004). Thus, the error in Re $f_1^{(-)}(\omega_L,0)$ is $\pm\omega_L q_L^2 \times (0.003)$ and the error in Re $f_2^{(-)}(\omega_L,0)$ is $\pm q^2(0.002)$. At 100 MeV and 200 MeV the errors in Re $f_1^{(-)}(\omega_L,0)$ are thus ± 0.010 and ± 0.035, respectively. Between 200 MeV and 350 MeV we can calculate $D^{(-)}(\omega_L)$ more accurately from Eqs. (2.6), and we estimate that the error in Re $f_1^{(-)}(\omega_L,0)$ at 300 MeV is ± 0.04.

The errors in the first derivative relations are more difficult to estimate. Using the discussion in Sec. 4(v) and Eq. (5.2), we estimate that the errors in Re $f_1^{(+)\prime}(\omega_L,0)$ and Re $f_1^{(-)\prime}(\omega_L,0)$ (relative to their values at $\omega_L = 1$) are $\pm 0.003 q_L^2$ and $\pm 0.003(\omega_L - 1)$, respectively. For Re $f_2^{(+)\prime}(\omega_L,0)$ the errors are ± 0.001 q^2. The errors in the second-derivative relations are closely related to the problem of the higher partial waves, and they will be discussed below.

Errors Produced in Re s_1 and Re s_3

The effect of these errors on the calculation of the s-wave amplitudes at 100 MeV and above is serious. We write $s_{2T} = f_{0+}^{(T)}$ ($T = \frac{1}{2}, \frac{3}{2}$) and use (3.15). Consider the errors due to Re $f_1^{(\pm)}$ which are dominant. They give errors of ± 0.025 and ± 0.018 in Re s_1 and Re s_3 respectively at 100 MeV. In fact, we shall see in Sec. 5(iv) below that the difference between the predicted values of Re s_1 and Re s_3 at 100 MeV and accurate experimental values is very small [Eqs. (5.12a) and (5.12b)]. This suggests that the errors given above for Re $f^{(\pm)}(\omega_L,0)$ are too large. This could be partly due to the crude method used to estimate the errors, and the fact that we have switched back and forth between $\pi^\pm - p$, $(\pm)$ and isospin integrals and amplitudes.

In view of this and the good agreement of the s-wave predictions at 100 MeV it is realistic to reduce[123] the errors quoted for Re $f_1^{(\pm)}$ by a factor 3. Since the $B^{(\pm)}$ integrals give the largest error in Re $f_1^{(\pm)}$, we shall also reduce the errors in Re $f_2^{(\pm)}$ by a factor 3. Thus the Re $f_1^{(+)}$ errors at 100 MeV, 200 MeV, and 300 MeV become ± 0.005, ± 0.017, and ± 0.04. Corresponding Re $f_2^{(+)}$ errors are $\pm q^2(0.002)$, $\pm q^2(0.003)$, and $\pm q^2(0.004)$. For Re $f_1^{(-)}$ we have at 100 MeV, 200 MeV, and 300 MeV, ± 0.003, ± 0.012, ± 0.02, and the Re $f_2^{(-)}$ error is $\pm q^2(0.001)$. The Re $f_1^{(\pm)\prime}$ and Re $f_2^{(\pm)\prime}$ errors remain as above.

(iii) Errors **Arising from Higher Partial Waves**

(*a*) *F-Wave Corrections*

Partial waves with $l \geqslant 3$ are neglected in this treatment. The corrections due to f waves can be seen by inserting f waves in Eq. (3.14) and solving to get the corrections to (3.15). This gives the following expressions for the partial wave amplitudes,

$$\begin{aligned}
f_{2+} &= (q^4/60)f_1''(0) - 7f_{3+} ,\\
f_{2-} &= -(q^2/6)f_2'(0) + (q^4/60)f_1''(0) - 5f_{3-} - 2f_{3+} ,\\
f_{1+} &= -(q^2/6)f_1'(0) - (q^4/12)f_1''(0) + f_{3-} + 20f_{3+} ,\\
f_{1-} &= f_2(0) - (q^2/6)f_1'(0) + (q^2/2)f_2'(0)\\
&\quad - (q^4/12)f_1''(0) + 10f_{3-} + 11f_{3+} ,\\
f_{0+} &= f_1(0) + (q^2/2)f_1'(0) - (q^2/6)f_2'(0)\\
&\quad + (q^4/6)f_1''(0) - 5f_{3-} - 30f_{3+} .
\end{aligned} \tag{5.10}$$

We shall use the notation

$$s_{2T} = f_{0+}^{(T)} , \quad p_{2T,1} = f_{1-}^{(T)}/q^2 , \quad p_{2T,3} = f_{1+}^{(T)}/q^2 ,$$
$$d_{2T,3} = f_{2-}^{(T)}/q^4 , \quad d_{2T,5} = f_{2+}^{(T)}/q^4 .$$

Little is known about f-wave phase shifts, so only rough estimates can be given for the corrections they produce. The analysis by Foote *et al.*[124] of $\pi^+ - p$ scattering at 310 MeV suggests that the f-wave phase shifts could well be as large as $\pm 0.5^\circ$ at 310 MeV (solution SPDF-I). Such f waves give corrections 0.15 to Re s_{2T}; 0.025 to Re $p_{2T,2J}$; 0.002 to Re $d_{2T,2J}$ at 310 MeV. Assuming that the f-wave phase shifts vary like q^7 below 310 MeV, the corresponding corrections at 200 MeV are 0.03 (Re s_{2T}); 0.008 (Re $p_{2T,2J}$); 0.001 (Re $d_{2T,2J}$). At 100 MeV they are 0.004 (Re s_{2T}); 0.002 (Re $p_{2T,2J}$); 0.0006 (Re $d_{2T,2J}$).

[123] Certain adjustments are made above 200 MeV.
[124] J. H. Foote *et al.* (cf. reference 67).

It will be seen that this f-wave correction to the s-wave amplitudes is the same size as the estimated value of these amplitudes at 310 MeV (see below), and is about 25% of the s-wave amplitudes at 200 MeV. Also at 310 MeV the f-wave correction is larger than the estimated size of several of the p-wave amplitudes. Moreover, the f-wave phase shifts might be larger than 0.5° at 310 MeV,[124] and it is also far from certain that g waves cause no trouble [cf. Eq. (5.10)].

Clearly, unless there are special reasons for believing that in certain cases they are small, the f-wave corrections make the calculations valueless at moderate energies and above. This is merely a practical example of the considerations given in Sec. 3(v). Because of the poor convergence of the series[125] in Eq. (3.15), it is not expected that the improved CGLN method of calculating partial wave amplitudes will be accurate for energies above 120 MeV, and it may be useless above 150 MeV. We shall examine below the exceptions to this rule in the case of the $(-)$ charge combination and also for the $f_2^{(+)}$ amplitude.

(b) *D Waves*

The subtraction constant K in the dispersion relation (5.5) for $A^{(+)\prime\prime}(\omega_L,0)$ has to be determined from the experimental information on the d waves at low energy. By Eq. (5.6), if we ignore f waves,

$$\frac{1}{4\pi}\,\mathrm{Re}\,A^{(+)\prime\prime}(\omega_L,0) = \frac{60}{q^4}\,\frac{W+M}{E+M}\,\mathrm{Re}\,f_{D\frac{5}{2}}^{(+)}\,, \quad (5.11)$$

and

$$\mathrm{Re}\,f_{D\frac{5}{2}}^{(+)} = \frac{1}{6q}\left[\sin(2\delta_{15}) + 2\sin(2\delta_{35})\right].$$

Foote *et al.*[124] (SPDF-I) find $\delta_{35} = -4.9° \pm 2.2°$ at 310 MeV, and the analysis of Zinov *et al.*[126] suggests that $\delta_{15} = 1.5° \pm 2.0°$ at 310 MeV. From these values, using Eq. (5.11), the subtraction constant K in Eq. (5.5) can be determined.

Unfortunately the errors here are considerable. First, if the f-wave phase shifts at 310 MeV are of the order of 0.5° as suggested by the analysis of Foote *et al.*,[124] Eq. (5.6) shows that they could cause corrections in $\mathrm{Re}\,A^{(+)\prime\prime}$ (310 MeV, 0)/4π which are as large as the d-wave contribution given by Eq. (5.11). Further, Eq. (5.6) suggests that the g-wave contribution may also be important. This is in line with the discussion of Secs. 3(iii) and (iv) which indicates that the convergence of the series (5.6) for $\mathrm{Re}\,A^{(+)\prime\prime}$ is slow at 310 MeV.

[125] See Sec. 3(v) for further discussion of these points.
[126] V. G. Zinov *et al.* (cf. reference 82).

Next, the errors in the d-wave phase shifts at 310 MeV are large. The values quoted above give $\mathrm{Re}\,f_{2+}^{(+)}$ (310 MeV) $= -0.021 \pm 0.015$. Suppose there is an error $\pm\Delta$ in our estimate of $\mathrm{Re}\,f_{2+}^{(+)}$ at 310 MeV. By Eq. (5.10) this will give rise to an error $\pm 10\,\Delta(q/2.17)^4$ in $\mathrm{Re}\,f_{0+}^{(+)}(\omega_L)$ and an error $\pm 5\,\Delta q^2/(2.17)^4$ in $\mathrm{Re}\,f_{1\pm}^{(+)}(\omega_L)/q^2$. As usual q is the c.m. momentum and the unit is 140 MeV/c. With $\Delta = 0.015$ the errors in $\mathrm{Re}\,f_{0+}^{(+)}$ are ± 0.011, ± 0.06, and ± 0.15 at 100 MeV, 200 MeV, and 300 MeV, respectively. For $\mathrm{Re}\,f_{1\pm}^{(+)}(\omega_L)/q^2$ the errors are ± 0.004, ± 0.010, and ± 0.016 at 100 MeV, 200 MeV, and 300 MeV, respectively.

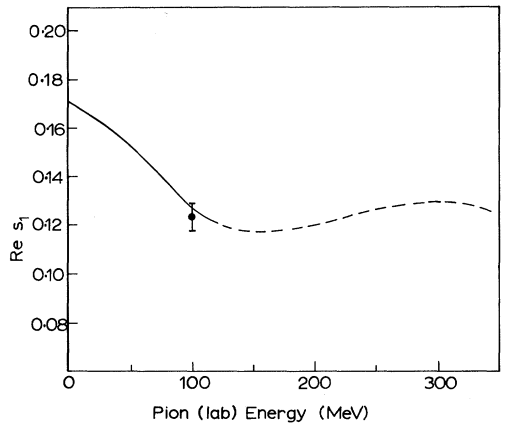

FIG. 9. The solid curve shows the predicted values of Re s_1 up to 120 MeV. The experimental point at 98 MeV is the Liverpool result (reference 114). The broken curve from 120 MeV to 350 MeV is obtained by using the predicted values of $\mathrm{Re}(s_1 - s_3)$ shown in Fig. 12 and the extrapolated values of Re s_3 given by the broken line in Fig. 10.

The other errors in the evaluation of relations (5.4) and (5.5) are far less important than the errors in K. In particular the contribution from the integrals over Im $A^{(+)\prime\prime}$ and Im $B^{(+)\prime\prime}$ are small, and moderate sized fractional errors in the evaluation of these terms can be tolerated.

It should be noted that by Eq. (5.3) the error in $\mathrm{Re}\,f_2^{(+)\prime\prime}(\omega_L,0)$ caused by an error in the subtraction constant K is much smaller than the error produced in $\mathrm{Re}\,f_1^{(+)\prime\prime}$ because of the factor $(E-M)/2W$ in the second equation of (5.3). The ratio of the error in $\mathrm{Re}\,f_2^{(+)\prime\prime}$ to that in $\mathrm{Re}\,f_1^{(+)\prime\prime}$ is $q^2/4M^2 = q^2/180$. Thus even at 300 MeV, errors in K are unimportant for $\mathrm{Re}\,f_2^{(+)\prime\prime}$, and, therefore, they are unimportant for $\mathrm{Re}\,(f_{1+}^{(+)} - f_{1-}^{(+)})$ and $\mathrm{Re}\,(f_{2+}^{(+)} - f_{2-}^{(+)})$.

(iv) Results Up to 120 MeV

The most serious of the errors we have discussed is that in Sec. 5(iii)(a). Due to the difficulty with higher partial waves and the poor convergence or

lack of convergence of Eqs. (5.10), the improved CGLN method for predicting *all* the π–N s- and p-wave phase shifts from the dispersion relations cannot be trusted at energies much above 120 MeV. On the other hand the errors appear to be reasonably small up to around 100 MeV, and in that region the results of the method should be reliable.

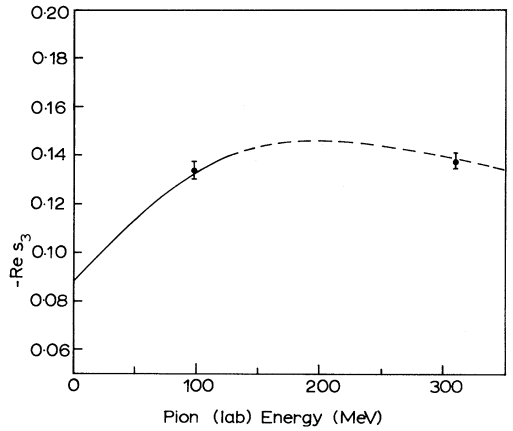

FIG. 10. The solid curve shows the predicted values of Re s_3 up to 120 MeV. The experimental values shown are the Liverpool result at 98 MeV (reference 114) and the result of Foote *et al.* at 310 MeV. The broken curve from 120 MeV up to 350 MeV is a smooth continuation of the predicted values drawn to pass through the experimental value at 310 MeV.

The calculations were made using the π–N parameters given in Eq. (4.49). The results for Re s_1, and Re s_3 and the small amplitudes Re $p_{2T,2J}$ are shown in Figs. 9, 10, and 11 (only those parts of the plots up to 120 MeV are relevant here). We shall compare the predictions with the accurate Liverpool data[77,114] at 97/98 MeV. The errors in the theoretical values are those we have estimated above in Secs. 5(ii) and (iii).

S Waves

For the s waves at 100 MeV, the theoretical values are

$$\text{Re } s_1 = 0.129 \pm 0.015\,, \quad \text{Re } s_3 = -0.133 \pm 0.014\,. \tag{5.12a}$$

The experimental values at 97/98 MeV are

$$\text{Re } s_1 = 0.123 \pm 0.006\,, \quad \text{Re } s_3 = -0.135 \pm 0.003\,. \tag{5.12b}$$

These are in good agreement, and there is also good agreement with the accurate experimental values at lower energies. The curves in Figs. 9 and 10 show that (up to 100 MeV) the dispersion relations predict the steady decrease in Re s_1 and Re s_3 from the threshold values $a_1 = 0.171 \pm 0.005$, and $a_3 = -0.088 \pm 0.004$. This decrease is of course already well-known from the semiphenomenological fits to the data which were discussed in Sec. 4(ii). The part of the total errors in these s-wave amplitudes at 100 MeV arising from neglect of the f waves [Sec. 5(iii)(a)] and the uncertainty in K [Sec. 5(iii)(b)] are ± 0.012 for Re s_1 and Re s_3.

P Waves

At 100 MeV the calculated values are

$$\text{Re } p_{11} = -0.023 \pm 0.006,\ \text{Re } p_{31} = -0.017 \pm 0.005,$$
$$\text{Re } p_{13} = -0.003 \pm 0.005,\ \text{Re } p_{33} = 0.250 \pm 0.005, \tag{5.13a}$$

and the experimental results at 97/98 MeV are[77,114]

$$\text{Re } p_{11} = -0.024 \pm 0.004,\ \text{Re } p_{31} = -0.027 \pm 0.002,$$
$$\text{Re } p_{13} = -0.008 \pm 0.004,\ \text{Re } p_{33} = 0.246 \pm 0.003. \tag{5.13b}$$

There is good agreement here between the experimental and calculated values, except in the case of Re p_{31}. A recent experiment at 120 MeV[127] gives Re $p_{31} = -0.023 \pm 0.006$, Re $p_{33} = 0.228 \pm 0.006$. From Fig. 11 it is seen that these values are in reasonably good agreement with the predicted values, but again there is a suggestion that the calculated value of Re p_{31} is a little too small. The largest part of the errors in Re p_{11} and Re p_{31} at 100 MeV is due to the error in K which was discussed in Sec. 5(ii). Probably this error actually accounts for the small discrepancy in Re p_{31} near 100 MeV.

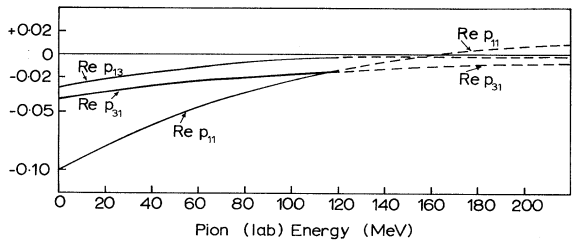

FIG. 11. Predicted values of the small p-wave scattering amplitudes Re p_{11}, Re p_{31}, Re p_{13} are shown up to 120 MeV. Between 120 MeV and 220 MeV we show conjectured values which are in agreement with the predicted values of Re $(p_{11} - p_{31})$ and Re $(p_{33} - p_{13})$ shown in Figs. 13 and 14, and with the experimental data which are discussed in Sec. 5(v) below.

[127] A. Loria *et al.*, Nuovo Cimento 22, 820 (1961). We use their final values $\alpha_{31} = -2.60° \pm 0.69°$, $\alpha_{33} = 31.67° \pm 1.01°$.

It should be emphasized that these results reconcile the experimental values of Re $p_{2T,2J}$ near 100 MeV with their threshold values $a_{2T,2J}$ as given in Sec. 4. For Re p_{11} in particular the 100 MeV and threshold values are very different. The results for the p_{33} amplitude are in good agreement with the experimental values given in Sec. 4(i)(a) above (up to 120 MeV). This is merely a further proof of the validity of the fixed momentum transfer dispersion relations.

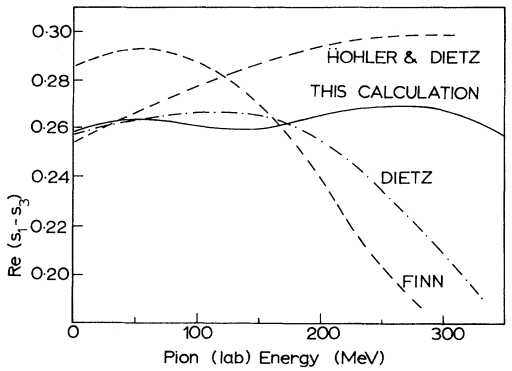

FIG. 12. The predicted values of Re$(s_1 - s_3)$. The broken lines show other predictions by the CGLN method due to Finn and Höhler and Dietz. The latter approximated the dispersion integrals by inserting only the $(\frac{3}{2}, \frac{3}{2})$ resonance, and then made a rough estimate of the necessary corrections. The curve —.—.— shows the results of Dietz [Karlsrube preprint; see also K. Dietz and G. Höhler in *International Conference on High Energy Physics*, edited by J. Prenthi (CERN, Geneva, Switzerland, 1962), p. 138], who tried to estimate these corrections by using a subtracted dispersion relation and incorporating knowledge of the $T = 1$, $\pi - \pi$ interaction.

D Waves

Because of the uncertainties in the subtraction constant K [Sec. 5(iii)(b)], no useful and reliable results can be deduced for the individual d waves. We shall see below that there are useful predictions for certain combinations of the d-wave amplitudes.

(v) The (−) Amplitudes

In Sec. 3(v) we showed that the amplitudes for the (−) charge combination are a special case. Assuming that there is no appreciable $T = 1$, π–π interaction in the range $4\mu^2 \leqslant t \lesssim 15\mu^2$ (and the experimental investigations of $T = 1$, π–π interactions appear to bear this out [65]), then in the case of the (−) amplitudes the Eqs. (3.15) should converge well up to 250 MeV, and should also give useful results up to somewhat higher energies (say 350 MeV).

This means that for the (−) amplitudes the f-wave corrections are expected to be small up to around 300 MeV. There is a further reason why the improved CGLN procedure should work much better in the (−) case than in the (+) case up to these energies. We saw in Sec. 5(iii)(b) that no subtraction constant is required in the $A^{(-)\prime\prime}$ dispersion relation, and therefore the large errors arising from uncertain experimental information about d waves are avoided.

The remaining errors in the $A^{(-)\prime\prime}$ and $B^{(-)\prime\prime}$ dispersion relations should not be very important, and it is possible to make predictions about the (−) combinations of d-wave amplitudes. Unfortunately, the results do not agree with the few experimental values which are available, and we do not reproduce them. Any error in the d-wave results will cause errors in the other (−) combination partial wave predictions, and the s-wave (−) amplitudes at the higher energies are particularly subject to this type of error (it is readily seen from Sec. 5(iii)(b) how this comes about).

The results for Re $(s_1 - s_3)$, Re $(p_{11} - p_{31})$, and Re $(p_{33} - p_{13})$ are shown in Figs. 12, 13, and 14 for energies up to 350 MeV. Except where otherwise stated the values of the parameters in Eq. (4.49) are used.[128] We shall briefly discuss the results.

Re $(s_1 - s_3)$

The predicted values are shown in Fig. 12 together with the predictions of Höhler and Dietz[129]

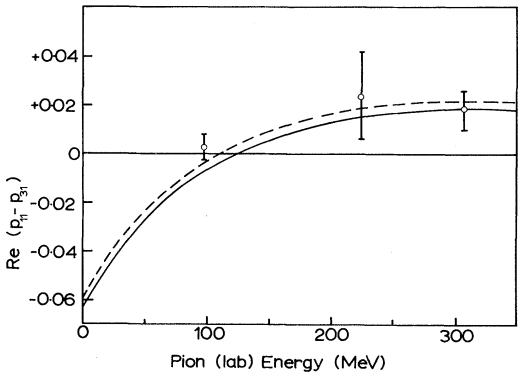

FIG. 13. The predicted values of Re $(p_{11} - p_{31})$. The solid line shows the values derived using the parameters given in Eq. (4.49). The broken line shows the values obtained using $a_{11} - a_{31} = -0.060$. The experimental values at 98 MeV, 224 MeV, and 310 MeV are those discussed in the text.

and of Finn.[69] We compare the predicted values with the experimental results at 224 MeV and 310 MeV. These appear to be reasonably accurate experimental

[128] There are some small changes from Woolcock's original values given in references 73 and 115. These are due to the fact that in preparing Sec. 4 above the parameters were critically examined and reassessed, giving the values in Eq. (4.49) above. The assessment of the errors in the phase shift predictions in Sec. 5 of the present article is quite new.

[129] G. Höhler and K. Dietz, Z. Physik **160**, 453 (1960).

results. At 224 MeV the experiments give[130] $\alpha_1 = 14.8° \pm 3.5°$, $a_3 = -15.5° \pm 3.5°$, so

$$\text{Re}\,(s_1 - s_3) = 0.282 \pm 0.039\,. \quad (5.14a)$$

The predicted result is

$$\text{Re}\,(s_1 - s_3) = 0.269 \pm 0.050\,. \quad (5.14b)$$

An estimate of the f-wave and d-wave error is included in (5.14b).[131]

At 310 MeV, Foote *et al.*[124] give $\alpha_3 = -17.2° \pm 2.6°$ (SPDFI). From the several results of Zinov *et al.*[126] we infer that, at 310 MeV, $\alpha_1 = 24.0° \pm 3°$ (Solution a_{SPD}). These give

$$\text{Re}\,(s_1 - s_3) = 0.301 \pm 0.020\,. \quad (5.15a)$$

The predicted value[131] is

$$\text{Re}\,(s_1 - s_3) = 0.27 \pm 0.07\,. \quad (5.15b)$$

The agreement between the experimental and predicted values is reasonably good, particularly at 224 MeV. In judging the accuracy of the 310-MeV prediction it is worth noting that an error of $\pm 1.0°$ in the predicted value of $(\delta_{15} - \delta_{35})$ (where δ_{15} and δ_{35} are d-wave phase shifts) would give an additional error of ± 0.08 in (5.15b).[132] The agreement in Eqs. (5.14) and Eqs. (5.15) supports the argument we gave at the beginning of this section for believing that the f-wave (and d-wave) errors are reasonably small in the $(-)$ case.

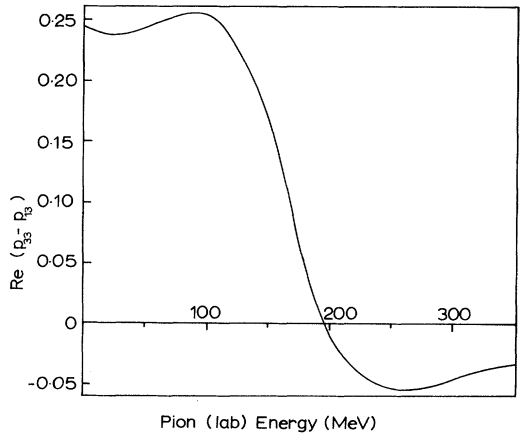

FIG. 14. The predicted values of $\text{Re}(p_{33} - p_{13})$, using the parameters given in Eq. (4.49).

[130] J. Deahl *et al.* (cf. reference 84).

[131] That is we take the error in Re $f^{(-)}(\omega_L,0)$ to be $\pm\omega_L q_L^2$ (0.001) up to 200 MeV and ± 0.013 at 300 MeV; the extra error due to d waves is discussed in the section on $d^{(-)}$ solutions following.

[132] We shall show below that ± 0.08 is the maximum extra error we would expect in (5.15b) due to errors in the d-wave calculations.

We now make two further deductions:

(a) The b_{SPD} solution of Zinov *et al.*[126] gives $\alpha_1 < 0$ between 240 MeV and 333 MeV. Since there is no doubt that $\alpha_3 < -10°$ in this region, the b_{SPD} solution is ruled out, even if we allow the full error in Re $f_1^{(-)}(\omega_L,0)$, i.e., ± 0.12 in Re $(s_1 - s_3)$ at 300 MeV as in Sec. 5(ii) above.

(b) In Fig. 10 the broken curve from 120 MeV to 350 MeV is a smooth continuation of the predicted value of Re s_3 drawn to pass through the 310-MeV experimental value.[124] Now using the values of Re $(s_1 - s_3)$ from Fig. 12, the values of Re s_1 between 120 MeV and 350 MeV are found. These are shown in Fig. 9 by the broken curve. Although these values of Re s_1 are necessarily somewhat rough, it would be valuable to test them by precision experiments in the 250 MeV–350 MeV region.

$$Re\,(p_{11} - p_{31})$$

The predicted values are shown by the solid curve in Fig. 13 together with a few accurate experimental values. There is good agreement with the experimental values. Typical results are those at 224 MeV and 310 MeV. At 224 MeV the experimental results are[130]

$$\alpha_{11} = 5.9° \pm 4.5°\,, \quad \alpha_{31} = -2.1° \pm 5.5°\,,$$

giving

$$\text{Re}\,(p_{11} - p_{31}) = 0.024 \pm 0.018\,. \quad (5.16a)$$

The predicted value is

$$\text{Re}\,(p_{11} - p_{31}) = 0.015 \pm 0.004\,. \quad (5.16b)$$

At 310 MeV Foote *et al.*[124] gave $\alpha_{31} = -2.9° \pm 4.0°$ and the results of Zinov *et al*[126] suggest $\alpha_{11} = 8.0° \pm 4.0°$ (a_{SPD} solution). This gives

$$\text{Re}\,(p_{11} - p_{31}) = 0.018 \pm 0.008\,. \quad (5.17a)$$

The predicted value is

$$\text{Re}\,(p_{11} - p_{31}) = 0.018 \pm 0.006\,. \quad (5.17b)$$

In accordance with our general assumption about the $(-)$ amplitudes, the d-wave and f-wave errors are taken to be small in (5.16b) and (5.17b).

These calculations use the parameter values in (4.49). So $a_{11} - a_{31} = -0.063$. If instead we used the value $a_{11} - a_{31} = -0.060$, which is within the errors given in (4.49), the predicted values would lie on the broken curve in Fig. 13. The latter curve gives somewhat better agreement with the 97/98 MeV result, and gives 0.018 ± 0.004 at 224 MeV, and 0.022 ± 0.006 at 310 MeV, instead of the values in Eqs. (4.16b) and (4.17b).

Again the assumption that the d-wave and f-wave corrections are unimportant for the $(-)$ amplitude, at least up to 300 MeV, appears to be justified. On the basis of the predicted values of Re $(p_{11} - p_{31})$ further conclusions can be drawn[73]:

(a) The b_{SPD} solution of Zinov *et al.*[126] gives Re $(p_{11} - p_{31}) < 0$ between 240 MeV and 330 MeV. This is definitely excluded by the predicted values. (b) The experimental results between 224 MeV and 333 MeV show that α_{31} is negative, and it appears to be between $-2°$ and $-4°$ over that range. Then Figs. 11 and 13 suggest that α_{11} changes sign below 200 MeV, and attains positive values between 5° and 8° in the range 220 MeV to 330 MeV.

Re $(p_{33} - p_{13})$

The predicted values [based on the parameters in (4.49)] are shown in Fig. 14. The errors are much the same as in the case of Re $(p_{11} - p_{31})$ with one exception. Just above the resonance (200 MeV–250 MeV) there is some uncertainty about the value of α_{33}, and this can have an appreciable effect on the dispersion integrals.

The experimental value[130] of α_{33} at 224 MeV ($\alpha_{33} = 112.3° \pm 3.0°$) combined with the predicted value of Re $(p_{33} - p_{13})$ suggests that α_{13} is positive and equals a few degrees. The experimental value[130] of α_{13} at 224 MeV is $0° \pm 2.0°$, so there is a small discrepancy here. At 310 MeV there is agreement to within the errors. The experimental value[124] of $\alpha_{33} = 135.0° \pm 0.6°$ plus the predicted value of Re $(p_{33} - p_{13})$ gives $\alpha_{13} = 2.3° \pm 2.0°$. The values of Zinov *et al.*[126] suggest that $\alpha_{13} = -2.0° \pm 2.0°$.

It is clear that again the $(-)$ relation is working well up to about 300 MeV, and it appears that the phase shift α_{13} differs from zero by no more than 2° from 200 MeV up to around 300 MeV. (Again the solution b_{SPD} of Zinov *et al.*[126] is excluded since it gives values of α_{13} between 7° and 15° over the range 240 MeV to 333 MeV).

The $d^{(-)}$ Solutions

There is not sufficient reliable experimental information to compare with the predicted values for the $(-)$ combinations of amplitudes. The good agreement of Re $(p_{11} - p_{31})$ and Re $(p_{33} - p_{13})$ with the experimental values in the 300-MeV region indicates that the extra error in the predicted value of Re $(s_1 - s_3)$ at 310 MeV [Eq. (5.15b)] arising from d-wave errors cannot exceed ± 0.08. [This is seen from Eq. (5.10), remembering that Re $(p_{11} - p_{31})$ and Re $(p_{33} - p_{13})$ are not in error by more than 0.008 at 310 MeV.] In evaluating (5.15b) we allowed ± 0.06 for this extra error and a corresponding value in (5.14b).

(vi) The $f_2^{(+)}$ Amplitudes

An additional piece of information, which is fairly reliable up to about 230 MeV, can be obtained from the $f_2^{(+)}(\omega_L,0)$ and $f_2^{(+)\prime}(\omega_L,0)$ amplitudes. By Eq. (5.10)

$$f_{1-} - f_{1+} = f_2(0) + (q^2/2)f_2'(0) + 9(f_{3-} - f_{3+}) + \cdots,$$
$$f_{2-} - f_{2+} = -(q^2/6)f_2'(0) - 5(f_{3-} - f_{3+}) + \cdots. \tag{5.18}$$

There is reason to expect that the effects of d-wave errors and of corrections due to f waves and higher amplitudes are not so important in the $(+)$ case of Eqs. (5.18) as they are in the original equations (5.10). This is seen by considering the equation. [cf. (1.26)]:

$$\operatorname{Re} f_2^{(+)}(\omega_L,0) = \frac{E-M}{2W}\frac{1}{4\pi}[-\operatorname{Re} A^{(+)}(\omega_L,0) + (W+M)\operatorname{Re} B^{(+)}(\omega_L,0)] \tag{5.18a}$$

and Eq. (5.2). Estimates show that at most energies up to 250 MeV $(W + M)$ Re $B^{(+)}$ is much larger than Re $A^{(+)}$, and $(W + M)$ Re $B^{(+)\prime}$ is much larger than Re $A^{(+)\prime}$. Thus, up to 250 MeV, the predominant contributions to Re $f_2^{(+)}$ and Re $f_2^{(+)\prime}$ come from the $B^{(+)}$ terms.

Now we look at the arguments in Sec. 3(v), concerning the convergence of series like Eqs. (3.15) and (5.18). The convergence is governed by the value of $y_0(s)$, the radius of convergence in the cos θ plane for the real parts of the amplitudes (cf. Table II). To get good convergence we required a value of $y_0(s)$ close to 3, or greater. The value of $y_0(s)$ is determined by the nearest singularity in the channel $\pi + \pi \to N + \bar{N}$.

Since the $A^{(+)}$ terms in Eqs. (5.2) and (5.18a) are small below 250 MeV, we assume that the higher partial wave corrections which they produce in Eq. (5.18) can be ignored. Now the $A^{(+)}$ amplitude is related to the $T = 0$, $J = 0, 2, \cdots \pi - \pi$ states, but the $B^{(+)}$ amplitude is related to the $T = 0$, $J = 2$, $\cdots \pi - \pi$ states.[133] It is known[118] that the $T = 0$, $J = 0$, $\pi - \pi$ interaction is strong for low values of t ($t = 5$ or $6\mu^2$), but the results of Atkinson[134] suggest that the $T = 0$, $J = 2$, $\pi - \pi$ phase shift δ_2^0 does not reach 20° until $t \simeq 12\mu^2$. If we ignore the $T = 0$, $J = 2$, $\pi - \pi$ interaction when $\delta_2^0 < 20°$,

[133] See, for example, Eq. (36) of J. Hamilton and T. D. Spearman, Ann. Phys. **12**, 172 (1961).

[134] D. Atkinson, Phys. Rev. **128**, 1908 (1962). It should be pointed out that Atkinson's results do not depend on any data derived from the $f_2^{(+)}$ amplitudes by the method of the present section.

then the nearest singularity of Re $B^{(+)}$ is given by $\cos\theta = 1 + 6/q^2$ [cf. Eq. (3.12)].

With these approximations the value of $y_0(s)$ for the Re $f_2^{(+)}$ amplitude is 4.0 for $\omega_L = 150$ MeV and 2.5 for $\omega_L = 250$ MeV. Thus up to about 250 MeV the f-wave (and higher) corrections to Eqs. (5.18) for the (+) charge combination should be small. Further advantages of Eqs. (5.18) are: (a) double derivative relations do not appear, so the main source of d-wave error is removed; (b) the factor $(E - M)/2W$ tends to suppress the errors in evaluating the dispersion relations for Re f_2 and Re f_2', as we saw in Sec. 5(ii).

Results for Re $f_2^{(+)}$

We only give some of the results for the p-wave case [i.e., the first Eq. in (5.18)]. At 200 MeV the predicted value is

$$\text{Re}\,(p_{11} + 2p_{31} - p_{13} - 2p_{33}) = -0.019 \pm 0.008\,. \tag{5.19}$$

The error here is only that discussed in Sec. 5(ii) for the evaluation of the various dispersion integrals. If it were not for the special arguments given above we would have to ascribe a much larger error to allow for f-wave effects [this can be seen from the estimates given in Sec. 5(iii) (a)]. Using experimental values[135] we have Re $p_{31} = -0.010 \pm 0.004$. Combining (5.19) with the predicted values Re$(p_{11} - p_{31}) = 0.012 \pm 0.003$, Re$(p_{33} - p_{13}) = -0.010 \pm 0.002$, we find Re $p_{33} = -0.003 \pm 0.004$, and Re $p_{13} = 0.007 \pm 0.006$. These give values of α_{33} and α_{13} which are in good agreement with the experimental data.

At 224 MeV the predicted value is

$$\text{Re}\,(p_{11} + 2p_{31} - p_{13} - 2p_{33}) = 0.025 \pm 0.008\,, \tag{5.20a}$$

and the experimental value[130] is

$$\text{Re}\,(p_{11} + 2p_{31} - p_{13} - 2p_{33}) = 0.028 \pm 0.020\,. \tag{5.20b}$$

Again the agreement is good. However at 310 MeV the predicted value is[136]

$$\text{Re}\,(p_{11} + 2p_{31} - p_{13} - 2p_{33}) = 0.063 \pm 0.012 \tag{5.21a}$$

and the experimental value is [124,126]

$$\text{Re}\,(p_{11} + 2p_{31} - p_{13} - 2p_{33}) = 0.103 \pm 0.015\,. \tag{5.21b}$$

Comparing (5.21a) and (5.21b), it appears that the $f_2^{(+)}$ method is breaking down at 310 MeV. Our general arguments at the beginning of the present section about the approximations involved in the $f_2^{(+)}$ method would lead us to expect the method to fail above 250 MeV.

Below 250 MeV we can try to use these predictions to improve our knowledge of the small p-wave amplitudes. There is no contradiction with the results discussed in Sec. 5(v) above, but unfortunately the errors on the predicted values are appreciable and they give nothing new.

(vii) Summary of the Results

The main limitation of the improved CGLN method is the failure of Eqs. (3.15) to converge at moderate or high energies. A further, and related, limitation is caused by the (d-wave) subtraction constant in the $A^{(+)\prime\prime}$ relation. The convergence problem becomes serious for the complete set of amplitudes around lab energy 150 MeV, and it can be traced to the effects of the strong low-energy $T = 0$, $J = 0$, $\pi - \pi$ interaction on the $A^{(+)}$ amplitude. We saw that the complete set of amplitudes gave good s- and p-wave predictions up to around 120 MeV [Sec. 5(iv)]. At higher energies they do in fact go wrong.

The $B^{(+)}$ amplitude is not affected by the $T = 0$, $J = 0$, $\pi - \pi$ interaction, but here the $T = 0$, $J = 2$, $\pi - \pi$ interaction determines the convergence of Eqs. like (3.15). It is estimated that the breakdown now occurs in the region 250 MeV–300 MeV lab pion energy. Using this and another approximation, the CGLN method can be applied to the $f_2^{(+)}$ amplitude, and the subtraction problem does not appear here. The results [Sec. 5(vi)] are good up to 224 MeV, but by 310 MeV they have gone badly wrong, as we would expect.

For the (−) amplitudes the situation is very favorable. There is no subtraction problem and the convergence of Eqs. (3.15) is governed by the $T = 1$, $J = 1$, $\pi - \pi$ interaction. The latter appears to be small up to comparatively high $\pi - \pi$ energies, and as a result the improved CGLN method works well for the (−) amplitudes up to about 300 MeV.

The results of applying these various cases are: (a) complete and accurate s- and p-wave predictions up to 120 MeV; (b) in the range 120 MeV–220 MeV,

[135] There is no accurate experimental value of Re p_{31} near 200 MeV. In fact there is no precision value between 120 MeV and 310 MeV. However Re p_{31} varies slowly in this range of energies, and it is safe to assert that, at 200 MeV, it has the value -0.010 ± 0.004.

[136] Here, f-wave errors have been ignored.

by combining the predictions with a limited amount of accurate experimental data, we can obtain a fairly accurate idea of the s- and p-waves; and (c) in the range 220 MeV–310 MeV we get a fair idea about the p-wave behavior but only a very rough idea about the s-wave amplitudes.

APPENDIX A

Theorem D and Related Formulas

Let

$$h(y) = P\int_1^\infty \frac{f(x)}{x^{\frac{1}{2}}(x-y)}\,dx \qquad \text{(A1)}$$

and assume $f(x)$ obeys conditions (i), (ii), and (iii) stated in Sec. 2(iii). Divide the range of integration into $(1, \Delta)$, $(\Delta, \frac{1}{2}y)$, $(\frac{1}{2}y, y-\delta)$, $(y-\delta, y+\delta)$, $(y+\delta, 2y)$, $(2y, \infty)$ where Δ is large and δ small. Call the corresponding contributions to the integral (1), $h_1, h_2, \cdots h_6$ respectively. Then,

$$|h_1| \leqslant \frac{1}{y-\Delta}\int_1^\Delta \left|\frac{f(x)}{x^{\frac{1}{2}}}\right| dx$$

$$h_2 = \int_\Delta^{\frac{1}{2}y} \frac{x^{\frac{1}{2}}}{x-y}\,\frac{f(x)}{x}\,dx = -\left(\frac{2}{y}\right)^{\frac{1}{2}}\int_\xi^{\frac{1}{2}y}\frac{f(x)}{x}\,dx\,,$$

where $\Delta < \xi < \frac{1}{2}y$ by the second mean value theorem. By taking Δ (and therefore ξ) sufficiently large, the integral on the right can be made as small as we wish [condition (i)]

$$h_3 = \int_{\frac{1}{2}y}^{y-\delta}\frac{f(x)dx}{x^{\frac{1}{2}}(x-y)} = o\left[\frac{1}{\ln y}\int_{\frac{1}{2}y}^{y-\delta}\frac{dx}{x^{\frac{1}{2}}(y-x)}\right]$$

[condition (ii)]

$$= y^{-\frac{1}{2}}o\left(\frac{\ln y - \ln\delta}{\ln y}\right)$$

$$|h_4| = \left|P\int_{-\delta}^{\delta}\frac{f(y+t)}{t(y+t)^{\frac{1}{2}}}\,dt\right|$$

$$= y^{-\frac{1}{2}}\left|\int_0^\delta \frac{f(y+t)-f(y-t)}{t}\,dt\right| + O(y^{-\frac{3}{2}})$$

$$= y^{-\frac{1}{2}}\left|\int_0^\delta \frac{2tf'(y+\Theta t)}{t}\,dt\right| \leqslant 2M\delta y^{-\frac{1}{2}}$$

[condition (iii)] $(0 < \Theta < 1)$

$$h_5 = o\left[\frac{1}{\ln y}\int_{y+\delta}^{2y}\frac{dx}{x^{\frac{1}{2}}(x-y)}\right] \qquad \text{[condition (ii)]}$$

$$= y^{-\frac{1}{2}}o\left(\frac{\ln y - \ln\delta}{\ln y}\right);$$

$$h_6 = \int_{2y}^\infty \frac{x^{\frac{1}{2}}}{x-y}\,\frac{f(x)}{x}\,dx$$

$$= \left(\frac{2}{y}\right)^{\frac{1}{2}}\int_{2y}^{\xi'}\frac{f(x)}{x}\,dx \quad \text{where } \xi' > 2y$$

by the second mean value theorem.

Choose first Δ large and δ small, and then y large enough.

Now consider the special case of Eq. (A1) when $f(x) = 1/\ln x$ and the lower limit of integration is $x = 2$. Subdivide the range of integration into $(2, \Delta)$, $(\Delta, \frac{1}{2}y)$, $(\frac{1}{2}y, y-\delta)$, $(y-\delta, y+\delta)$, $(y+\delta, 2y)$, $(2y, \infty)$, and call the corresponding contributions $h_1, \cdots h_6$.

Treat h_1 as before. For h_2 use the second mean value theorem in the form

$$h_2 = \int_\Delta^{y/2}\frac{dx}{x^{\frac{1}{2}}\ln x(x-y)}$$

$$= \frac{1}{\ln\Delta}\int_\Delta^\xi \frac{dx}{x^{\frac{1}{2}}(x-y)}\,, \quad \text{where } \Delta < \xi < y/2$$

so

$$|h_2| < \frac{1}{\ln\Delta}\int_\Delta^{y/2}\frac{dx}{x^{\frac{1}{2}}(x-y)}\,,$$

giving

$$|h_2| < \frac{2}{y^{\frac{1}{2}}\ln\Delta}\ln(\sqrt{2}+1)\,.$$

We note that

$$h_3 \backsim \frac{1}{\ln y}\int_{y/2}^{y-\delta}\frac{dx}{x^{\frac{1}{2}}(x-y)} \qquad \text{(A2)}$$

with an error of order $y^{-\frac{1}{2}}(\ln y)^{-2}$. Equation (A2) gives

$$h_3 \backsim (1/y^{\frac{1}{2}}\ln y)(-\ln y + \ln\delta + O(1))\,.$$

Similarly,

$$h_5 \backsim (1/y^{\frac{1}{2}}\ln y)(\ln y - \ln\delta + O(1))\,,$$

so

$$h_3 + h_5 \backsim O(1)/y^{\frac{1}{2}}\ln y\,.$$

Also,

$$|h_4| < 2\delta/y^{\frac{3}{2}}(\ln y)^2\,.$$

Finally,

$$h_6 = \int_{2y}^\infty \frac{dx}{x^{\frac{1}{2}}\ln x(x-y)}$$

$$< \frac{1}{\ln(2y)}\int_{2y}^\infty \frac{dx}{x^{\frac{1}{2}}(x-y)} = \frac{2\ln(\sqrt{2}+1)}{y^{\frac{1}{2}}\ln(2y)}\,.$$

Now $y^{\frac{1}{2}}h_2$ can be made arbitrarily small by choosing Δ sufficiently large. Finally, $y^{\frac{1}{2}}h_1$, $y^{\frac{1}{2}}(h_3+h_5)$, $y^{\frac{1}{2}}h_4$, and $y^{\frac{1}{2}}h_6$ tend to zero as $y \to \infty$. Hence,

$$y^{\frac{1}{2}}h(y) \to 0 \quad \text{as} \quad y \to \infty\,.$$

A similar argument is valid if $f(x) = 1/\ln\ln x$.

APPENDIX B

Convergence of Legendre Series and Cosine Series

First we discuss why Legendre series like (3.1) have elliptic regions of convergence in the complex $\cos\theta$ plane. Then we show how to deduce the ellipse of convergence for the Legendre series from the position of the singularities in the Mandelstam representation.

We define $P_n(z)$, where z may be complex, by

$$P_n(z) = \frac{(2n-1)!!}{n!}\left[z^n - \frac{n(n-1)}{2(2n-1)}z^{n-2} + \frac{n(n-1)(n-2)(n-3)}{2\cdot 4\cdot(2n-1)(2n-3)}z^{n-4} - \cdots\right]. \tag{B1}$$

Let $z = x + iy$ when x and y are real. For $z = x$ where $|x| \leqslant 1$, we write $x = \cos\theta$ where θ is real, and we have

$$P_n(x) = 2\frac{(2n-1)!!}{2^n n!}\left[\cos(n\theta) + \frac{1}{1}\frac{n}{2n-1} \times \cos((n-2)\theta) + \frac{1\cdot 3}{1\cdot 2}\frac{n(n-1)}{(2n-1)(2n-3)} \times \cos[(n-4)\theta] + \cdots\right]. \tag{B2}$$

Equation (B2) gives $P_n(z)$ for unphysical values of z if we write $\theta = \alpha + i\beta$ and

$$z = \cos(\alpha + i\beta) = \cos\alpha\cosh\beta - i\sin\alpha\sinh\beta\,, \tag{B3}$$

where α and β are real and $\beta \geqslant 0$. On the real axis $x > 1$ we have $\alpha = 0$ and $x = \cosh\beta$, while the portion $x < -1$ is given by $\alpha = \pi$, $x = -\cosh\beta$.

If n is large Stirling's theorem shows that Eq. (B2) has the asymptotic form

$$P_n(x) \simeq \frac{2}{(\pi n)^{\frac{1}{2}}}\left\{\cos(n\theta) + \tfrac{1}{2}\cos[(n-2)\theta] + \frac{1\cdot 3}{1\cdot 2}\cdot\frac{1}{2^2}\cos[(n-4)\theta] + \frac{1\cdot 3\cdot 5}{1\cdot 2\cdot 4}\frac{1}{2^3}\cos[(n-6)\theta] + \cdots\right\}. \tag{B4}$$

This is a suitable expression for examining the form of $P_n(z)$ for large n. Using (B2) and (B3) with $\beta > 0$ we get

$$P_n(z) \simeq [2/(\pi n)^{\frac{1}{2}}]\{\cos[n(\alpha + i\beta)] + \tfrac{1}{2}\cos[(n-2)(\alpha+i\beta)] + \cdots\} \simeq [1/(\pi n)^{\frac{1}{2}}]e^{n\beta}e^{-in\alpha}F(\alpha,\beta)\,, \tag{B5}$$

where

$$F(\alpha,\beta) = 1 + \frac{1}{2}e^{-2\beta}e^{2i\alpha} + \frac{1\cdot 3}{1\cdot 2}\frac{1}{2^2}e^{-4\beta}e^{4i\alpha} + \cdots. \tag{B6}$$

The approximation (B5) is only valid for $n\beta \gg 1$. Since $\beta > 0$, the series (B6) converges, and gives[137]

$$F(\alpha,\beta) = (1 - e^{-2\beta}e^{2i\alpha})^{-\frac{1}{2}}. \tag{B7}$$

From (B5) and (B7) we have the asymptotic behavior

$$|P_n(z)| \simeq [1/(\pi n)^{\frac{1}{2}}] \times e^{n\beta}(1 - 2e^{-2\beta}\cos 2\alpha + e^{-4\beta})^{-\frac{1}{4}}. \tag{B8}$$

The convergence of a Legendre series $\sum_{n=0}^{\infty}a_nP_n(z)$ is therefore determined by the convergence of the series $\sum_{n=0}^{\infty}a_ne^{n\beta}n^{-\frac{1}{2}}$. If

$$\overline{\lim_{n\to\infty}}\,|a_n|^{1/n} = e^{-\beta_0}\,, \tag{B9}$$

then by Cauchy's test, the latter series converges for $\beta < \beta_0$. The points z for which $\beta = \beta_0$ lie on the ellipse

$$\frac{x^2}{\cosh^2\beta_0} + \frac{y^2}{\sinh^2\beta_0} = 1\,.$$

If the length of the real semi-axis is $x_0 = \cosh\beta_0$, the other semi-axis has length $(x_0^2 - 1)^{\frac{1}{2}} = \sinh\beta_0$. Finally the relation $e^{\beta_0} = [x_0 + (x_0 - 1)^{\frac{1}{2}}]$ expresses Eq. (B9) in terms of x_0. These results explain the general form of Lehmann's theorems in Sec. 3(i).

When we use the Mandelstam representation to find the singularities in the $\cos\theta$ plane, we have pole terms like $(u - M^2)^{-1}$ and cuts involving $(u' - u)^{-1}$, $(t' - t)^{-1}$. We can regard a cut as a line of poles, and if we remember that u and t are linear in $\cos\theta$ when s is fixed, we see that the singularities in the $z = \cos\theta$ plane are all of the form $(x_0 - z)^{-1}$ where x_0 is real and $|x_0| > 1$. We need only consider the singularity which gives the smallest $|x_0|$. The smallest value of $|x_0|$ was called $y_0(s)$ in Sec. 3(iv).

Consider the expansion

$$\frac{1}{x_0 - z} = \frac{1}{x_0}\sum_{n=0}^{\infty}\left(\frac{z}{x_0}\right)^n. \tag{B10}$$

This gives the Taylor series in powers of $\cos\theta$, and it has radius of convergence x_0 (we take $x_0 > 0$). We wish to find the ellipse of convergence of the Legendre series for $(x_0 - z)^{-1}$. Take the point x on the real axis when $x > 1$. Then

$$x = \cos\theta = \cosh\beta = \tfrac{1}{2}(\xi + 1/\xi) \text{ where } \xi = e^{\beta}.$$

[137] The asymptotic estimate given by Eqs. (B5) and (B7) is sometimes written in the form
$P_n(z) \sim [1/(2\pi n\sin\theta)^{\frac{1}{2}}]\exp[-i(n+\frac{1}{2})\theta + i\pi/4]$, $\operatorname{Im}\theta \geq 0$.

Also

$$\frac{1}{x_0 - x} = \frac{2\xi}{2x_0\xi - \xi^2 - 1} = \frac{2\xi}{(\gamma_1 - \xi)(\xi - \gamma_2)}, \quad \text{(B11)}$$

where γ_1, γ_2 are the zeros of

$$\xi^2 - 2x_0\xi + 1 .$$

Now $x_0 > 1$, and we write $\gamma_1 = x_0 + (x_0^2 - 1)^{\frac{1}{2}}$. Also $\gamma_1\gamma_2 = 1$, so $\gamma_2 < 1$. Expand (B11) in a Laurent series in ξ,

$$\frac{2\xi}{(\gamma_1 - \xi)(\xi - \gamma_2)} = \frac{2}{\gamma_1} \sum_{r=0}^{\infty} \left(\frac{\gamma_2}{\xi}\right)^r \sum_{s=0}^{\infty} \left(\frac{\xi}{\gamma_1}\right)^s$$
$$= \frac{2}{\gamma_1 - \gamma_2} \left[\sum_{n=0}^{\infty} \left(\frac{\xi}{\gamma_1}\right)^n + \sum_{n=1}^{\infty} \left(\frac{\gamma_2}{\xi}\right)^n \right] \quad \text{(B12)}$$

after a little rearrangement.
Hence,

$$\frac{1}{x_0 - x} = \frac{2}{\gamma_1 - \gamma_2} \left[\sum_{n=0}^{\infty} \gamma_1^{-n} e^{n\beta} + \sum_{n=1}^{\infty} \gamma_2^{n} e^{-n\beta} \right]. \quad \text{(B13)}$$

Now let the Legendre expansion be

$$\frac{1}{x_0 - x} = \sum_{n=0}^{\infty} a_n P_n(x) . \quad \text{(B14)}$$

Consider the form of this for $x > 1$. Putting $\alpha = 0$ in (B5) and using (B7) gives for $\beta > 1$ and $n \to \infty$,

$$P_n(x) \simeq (\pi n)^{-\frac{1}{2}} (1 - e^{-2\beta})^{-\frac{1}{2}} e^{n\beta} .$$

Comparing with the series of positive powers of e^{β} in (B13), we see that for n large,

$$a_n \backsim n^{\frac{1}{2}} \gamma_1^{-n} . \quad \text{(B15)}$$

Also (B13) converges for $e^{\beta} < \gamma_1$, similarly the Legendre series (B14) converges for

$$x + (x^2 - 1)^{\frac{1}{2}} < x_0 + (x_0^2 - 1)^{\frac{1}{2}}$$
$$\text{i.e., for } x < x_0 . \quad \text{(B16)}$$

It follows from the above analysis that if the nearest singularity in the Mandelstam representation is $y_0(s)$, the Legendre expansion for the scattering amplitude converges in an ellipse with foci $x = \pm 1$, and semi-axes $y_0(s)$, $[(y_0(s))^2 - 1]^{\frac{1}{2}}$. Further, by (B15)

$$\lim_{n\to\infty} a_n^{1/n} = \{y_0(s) + [(y_0(s))^2 - 1]^{\frac{1}{2}}\}^{-1} . \quad \text{(B17)}$$

A rigorous derivation of the above result comes from Heine's expansion[138]

$$\frac{1}{t - z} = \sum_{n=0}^{\infty} (2n + 1) P_n(z) Q_n(t)$$

which is valid if z is in the interior of the ellipse which has foci ± 1 and passes through t.

[138] See for example Sec. 15.4 of E. T. Whittaker and G. N. Watson, *Modern Analysis* (Cambridge University Press, New York, 1952). For further details of the asymptotic expansion of $P_n(z)$ for large n see Sec. 11.3 of E. T. Copson, *Theory of Functions of a Complex Variable* (Oxford University Press, New York, 1952).